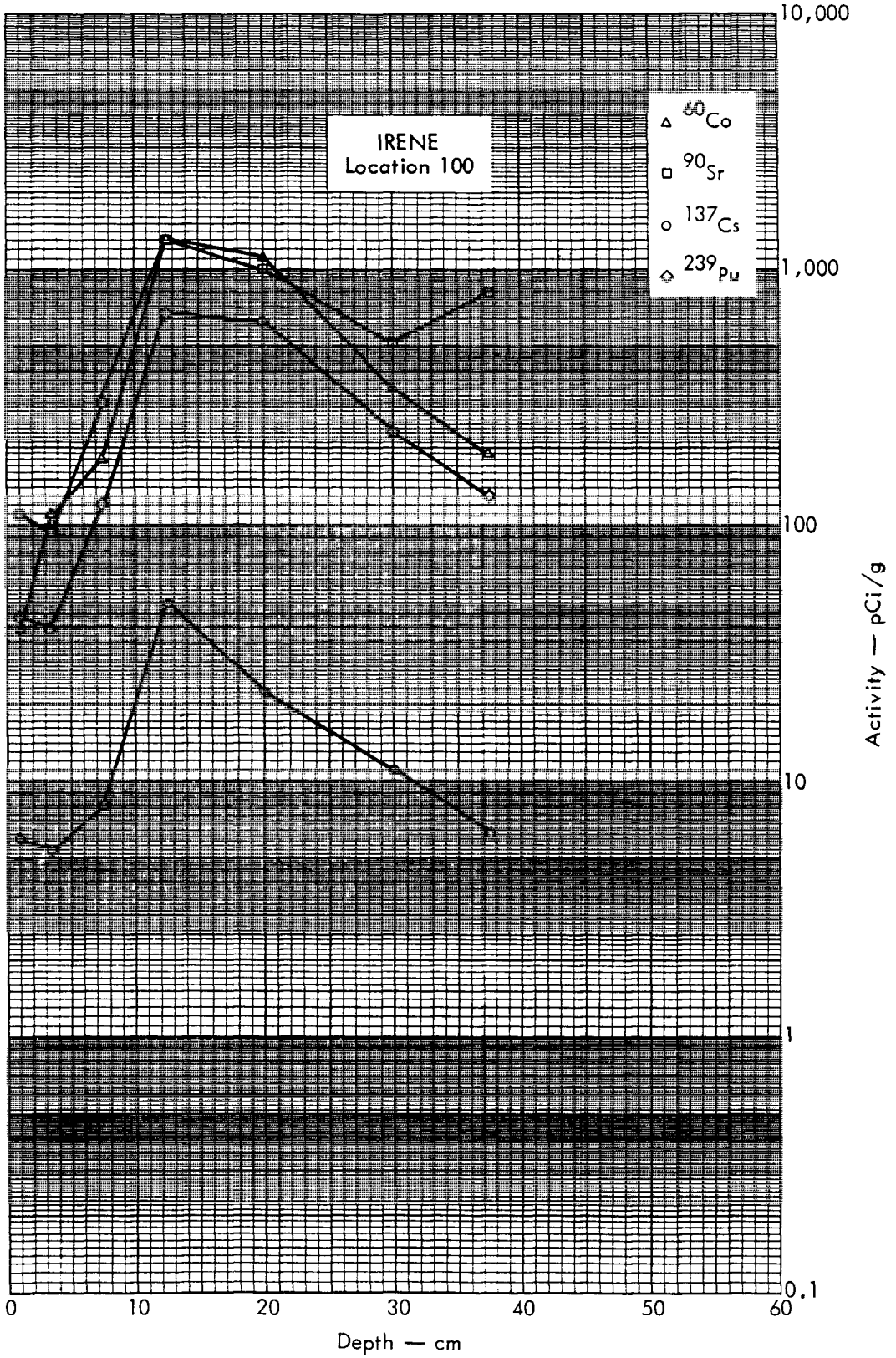

Fig. B.7.2t. Activities of selected radionuclides as a function of soil depth.

Fig. B.8.1.a.

Fig. B.8.1.b. Gross count isoexposure contours. (Refer to alphabetic symbol key in this appendix.)

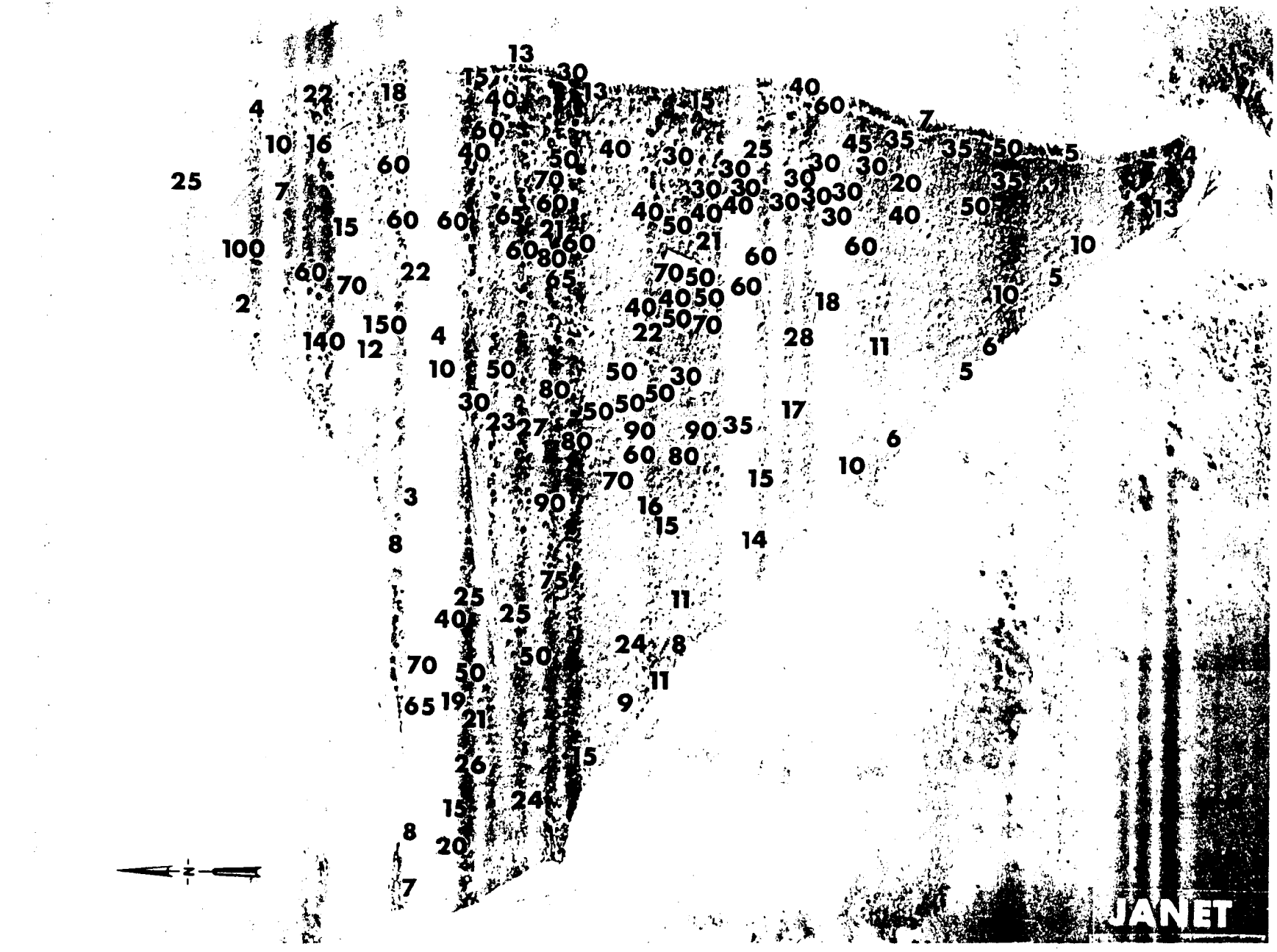

Fig. B.8.1.d. The gamma background exposure rate (μR/hr) at 1 m above the ground, measured with a portable NaI scintillation counter.

Fig. B.8.1.f. Soil-sample locations.

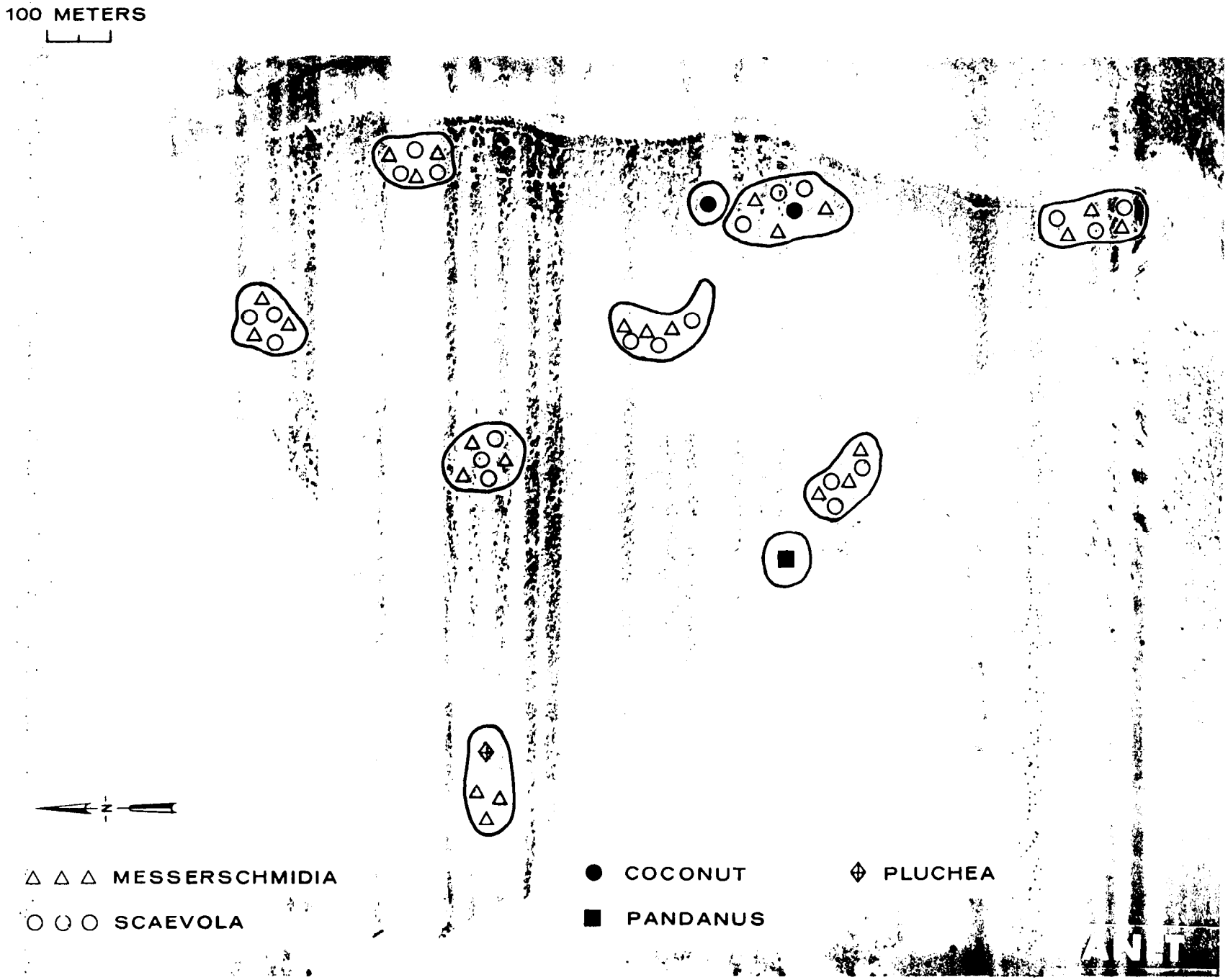

Fig. B.8.1.g. Vegetation sample locations.

Fig. B.8.1.h. The gamma-ray exposure rates (μR/hr) measured 1 m above the ground by the LiF thermoluminescent dosimeters (TLD). The numbers shown in parentheses denote the location identification numbers.

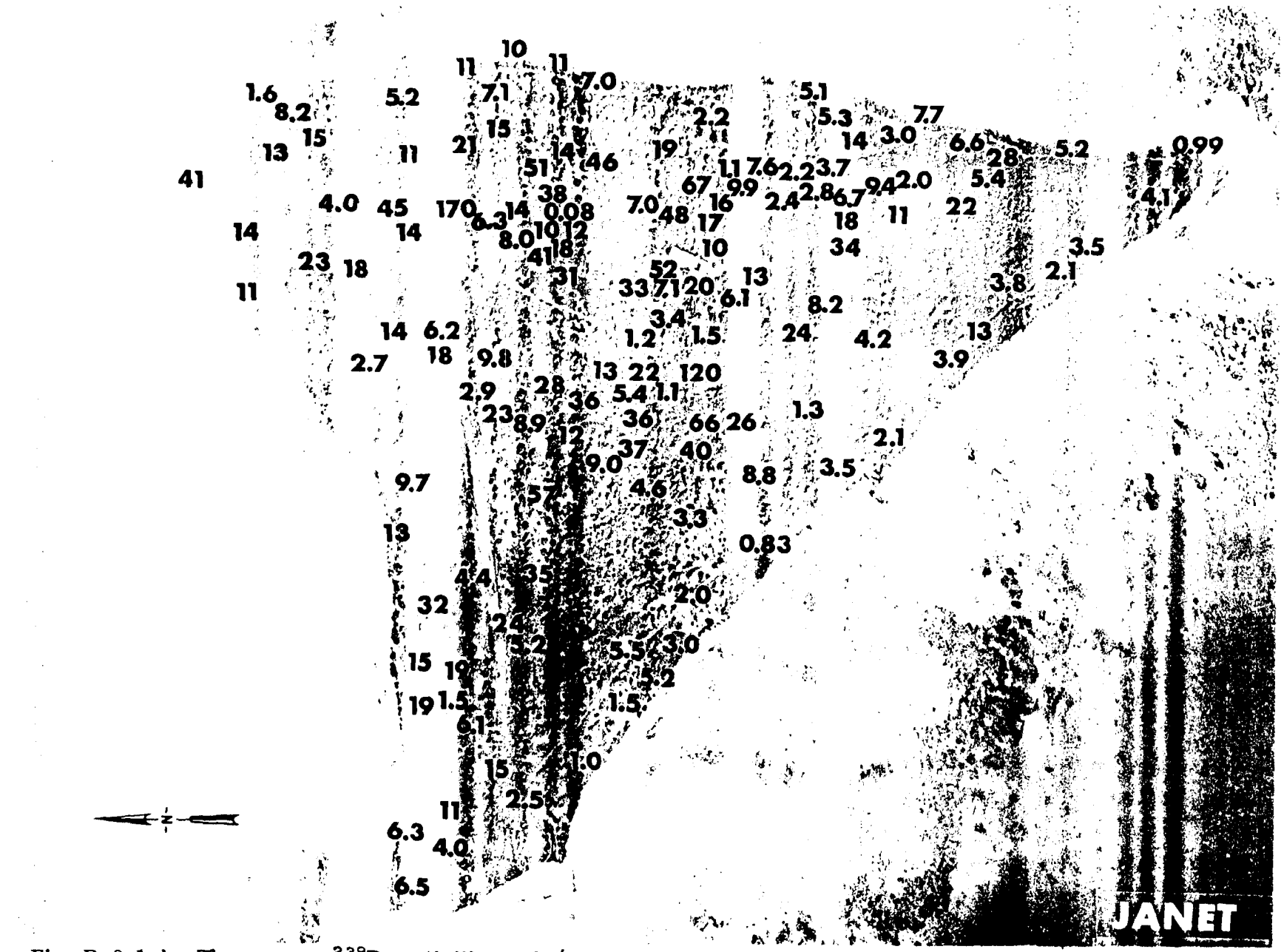

Fig. B.8.1.i. The average ^{239}Pu activities (pCi/gm) in soil samples collected to a depth of 15 cm.

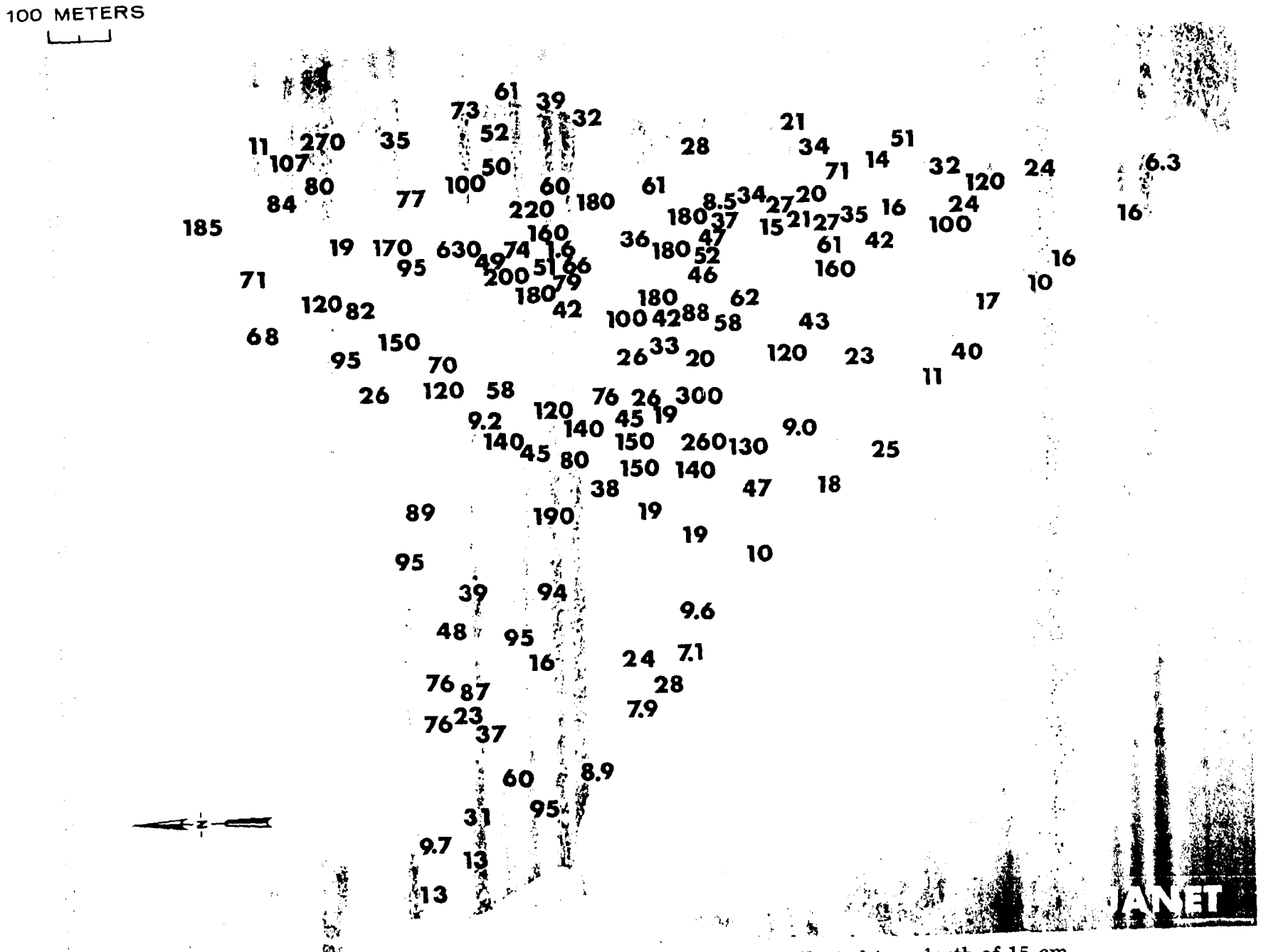

Fig. B.8.1.j. The average ^{90}Sr activities (pCi/gm) in soil samples collected to a depth of 15 cm.

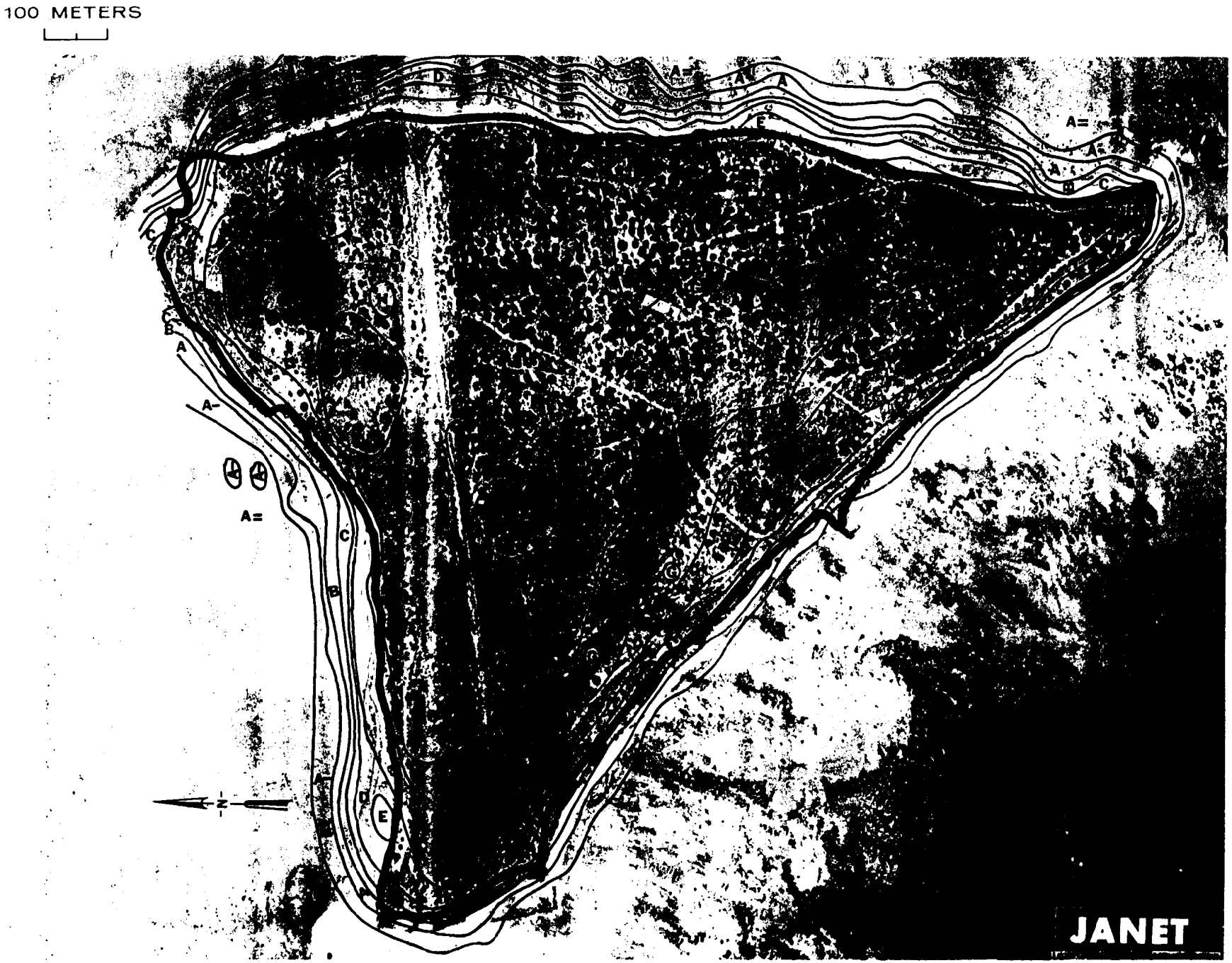

Fig. B.8.1.k. ^{137}Cs isoexposure and isoconcentration contours. (Refer to alphabetic symbol key in this appendix.)

Fig. B.8.1.1. The average ^{137}Cs activities (pCi/gm) in soil samples collected to a depth of 15 cm.

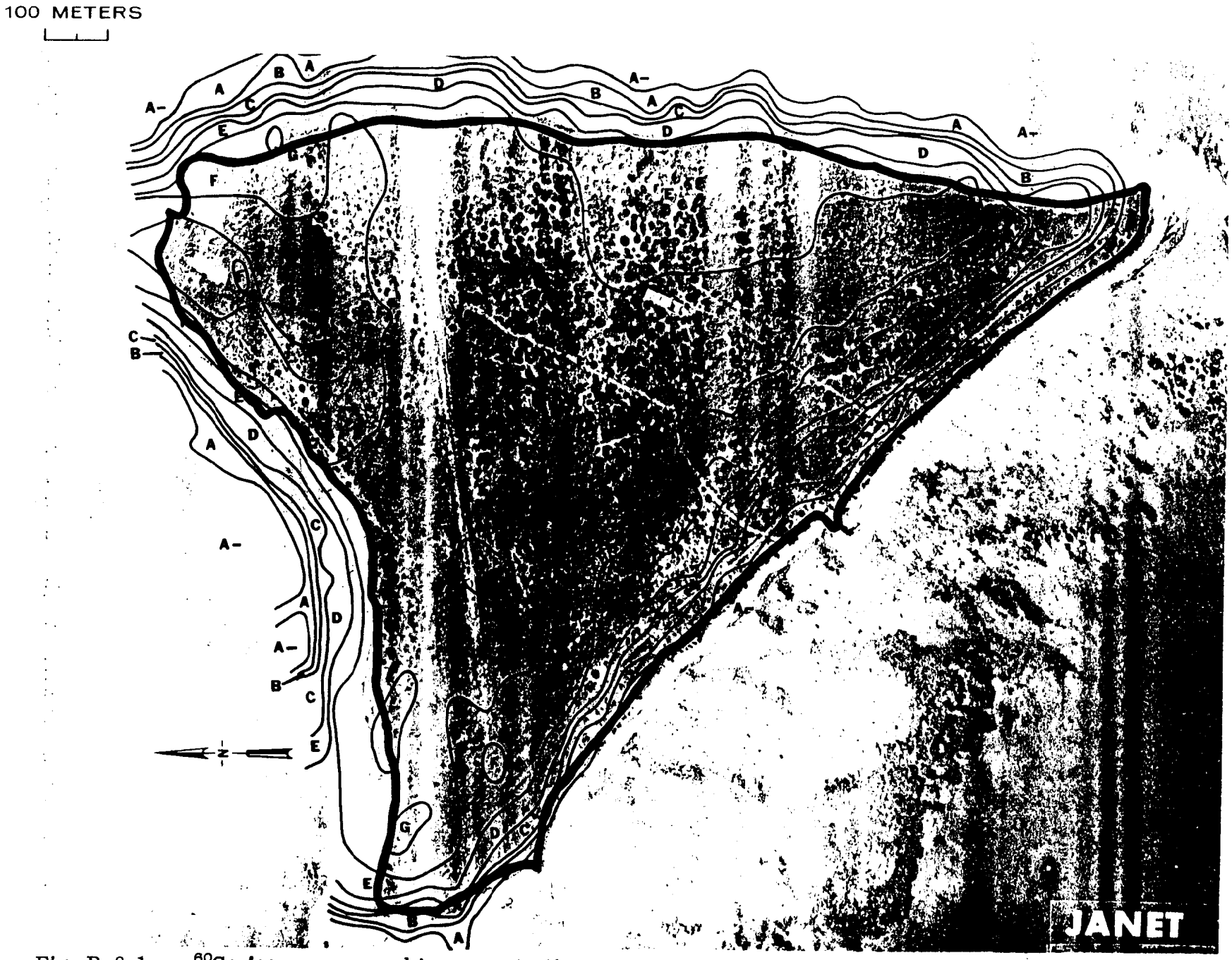

Fig. B.8.1.m. ^{60}Co isoexposure and isoconcentration contours. (Refer to alphabetic symbol key in this appendix.)

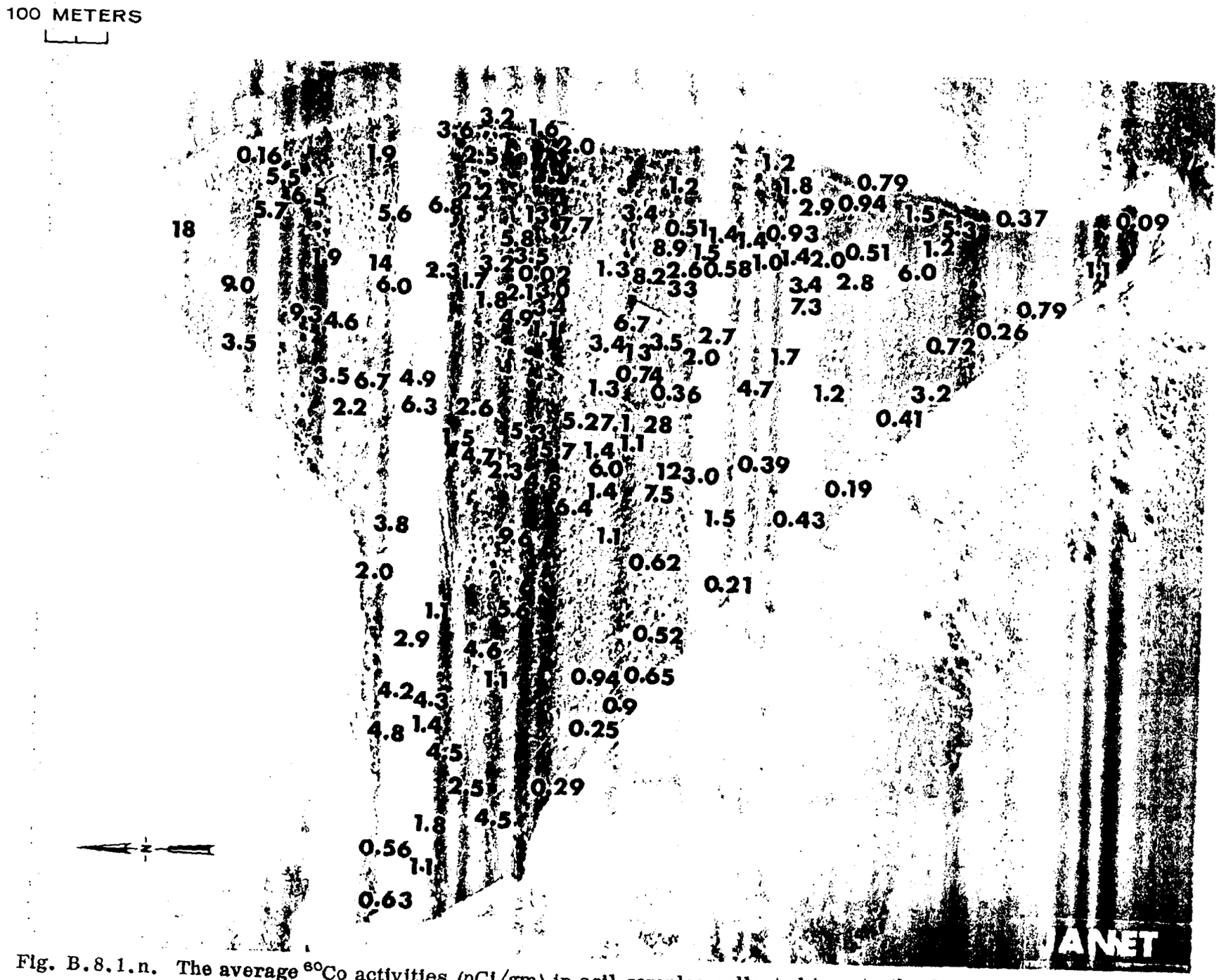

Fig. B.8.1.n. The average ^{60}Co activities (pCi/gm) in soil samples collected to a depth of 15 cm.

Fig. B.8.1.o. Terrestrial animal sample locations.

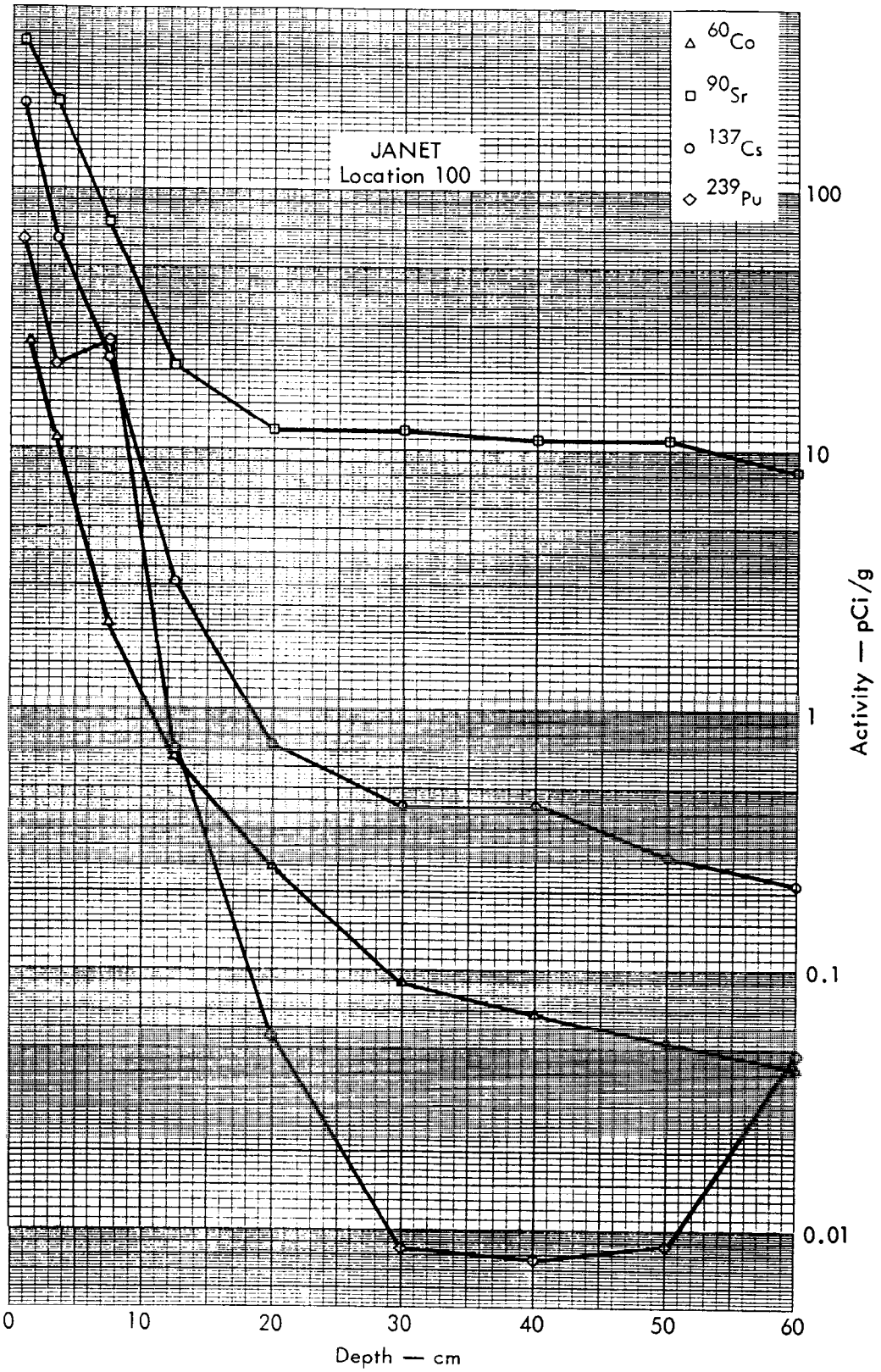

Fig. B.8.2a. Activities of selected radionuclides as a function of soil depth.

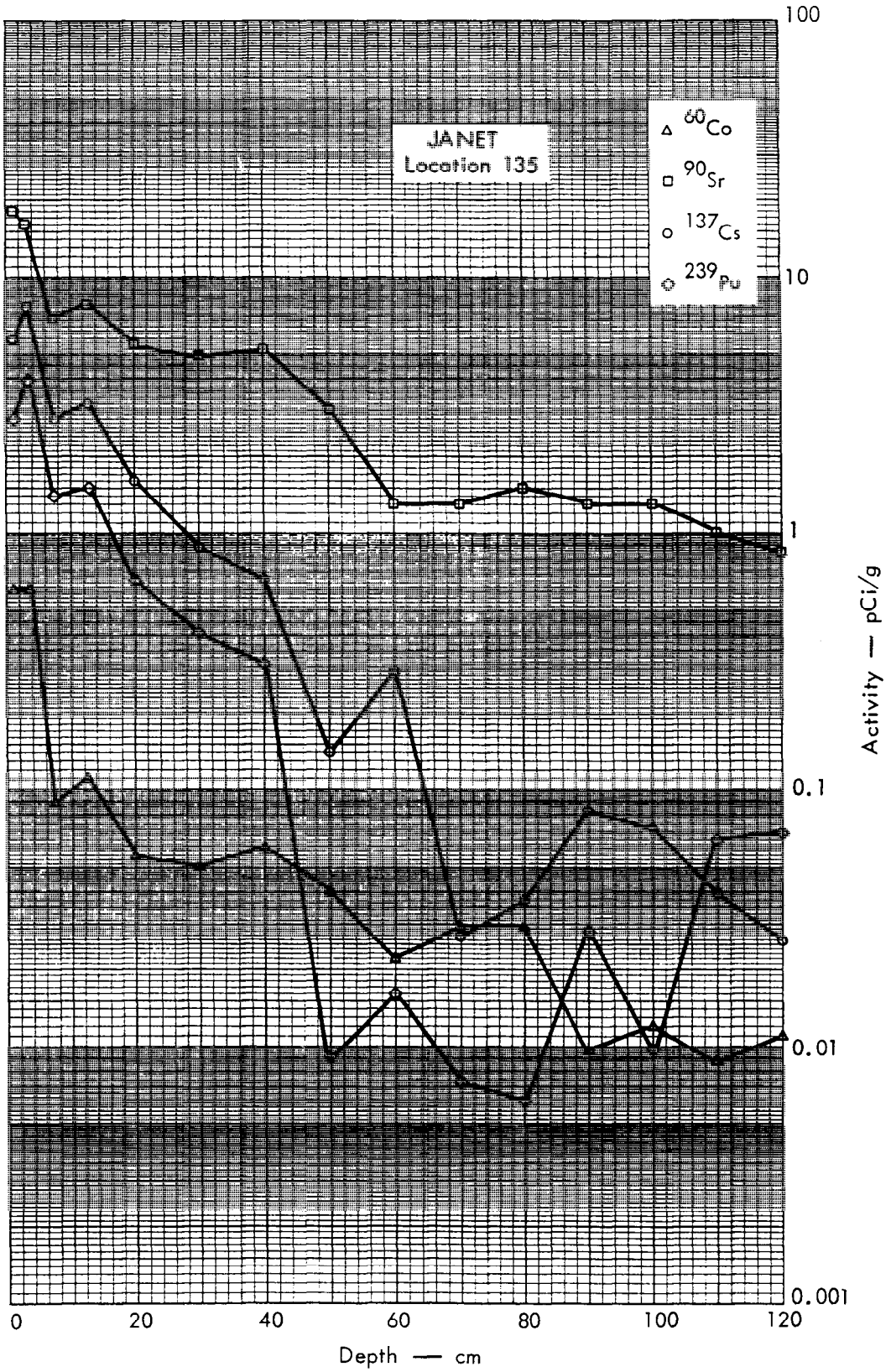

Fig. B. 8.2b. Activities of selected radionuclides as a function of soil depth.

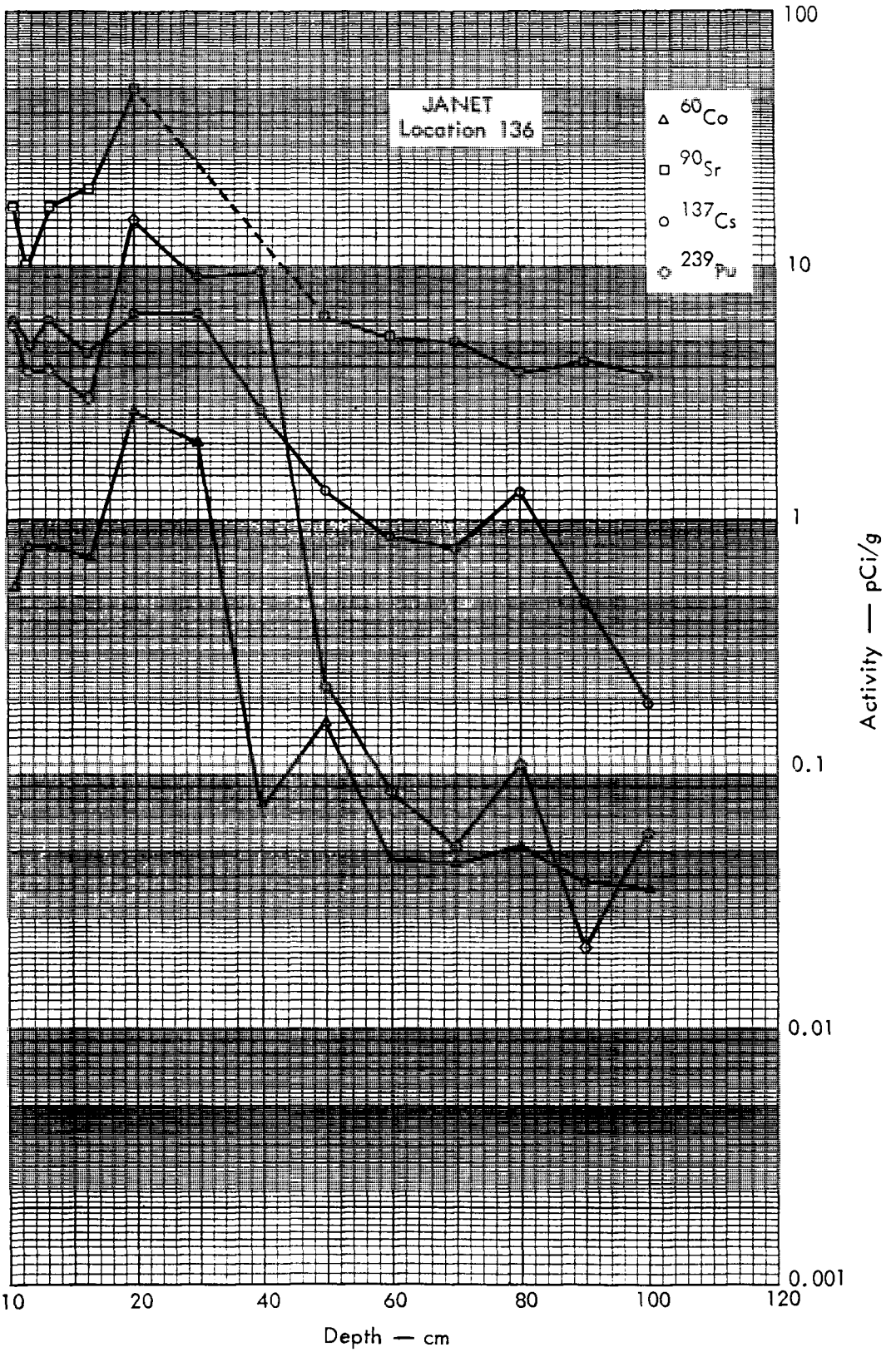

Fig. B. 8.2c. Activities of selected radionuclides as a function of soil depth.

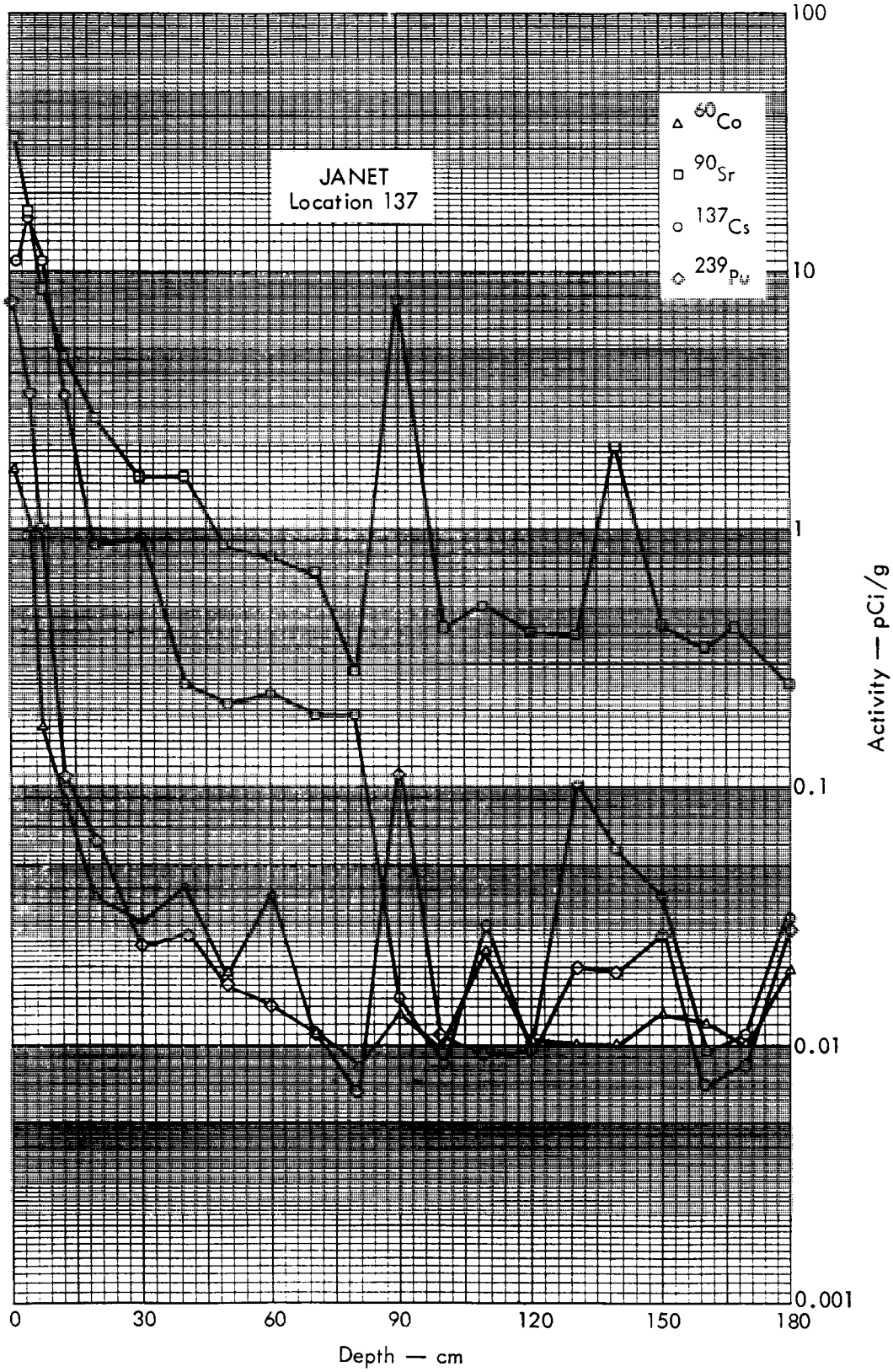

Fig. B. 8.2d. Activities of selected radionuclides as a function of soil depth.

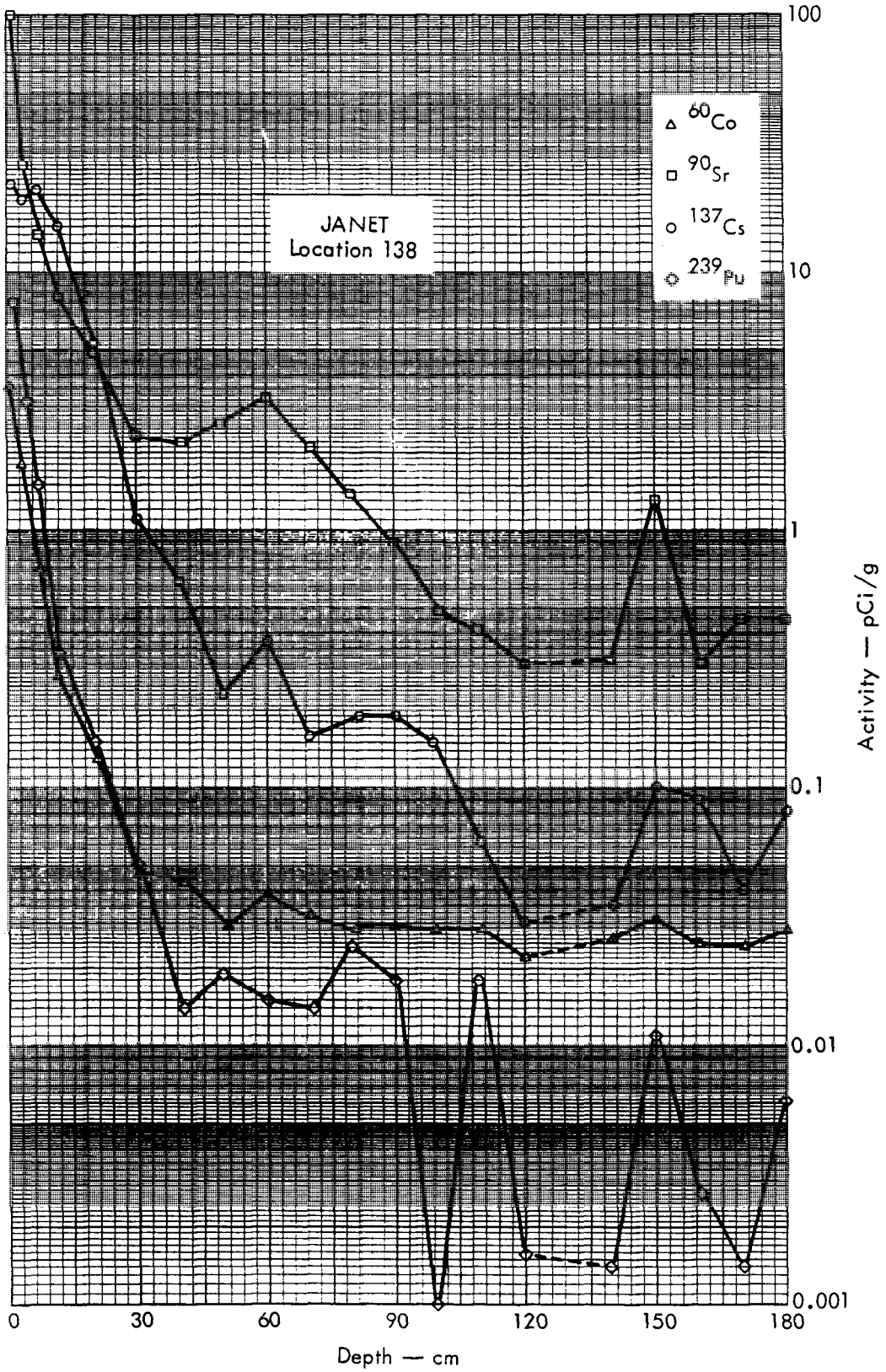

Fig. B.8.2e. Activities of selected radionuclides as a function of soil depth.

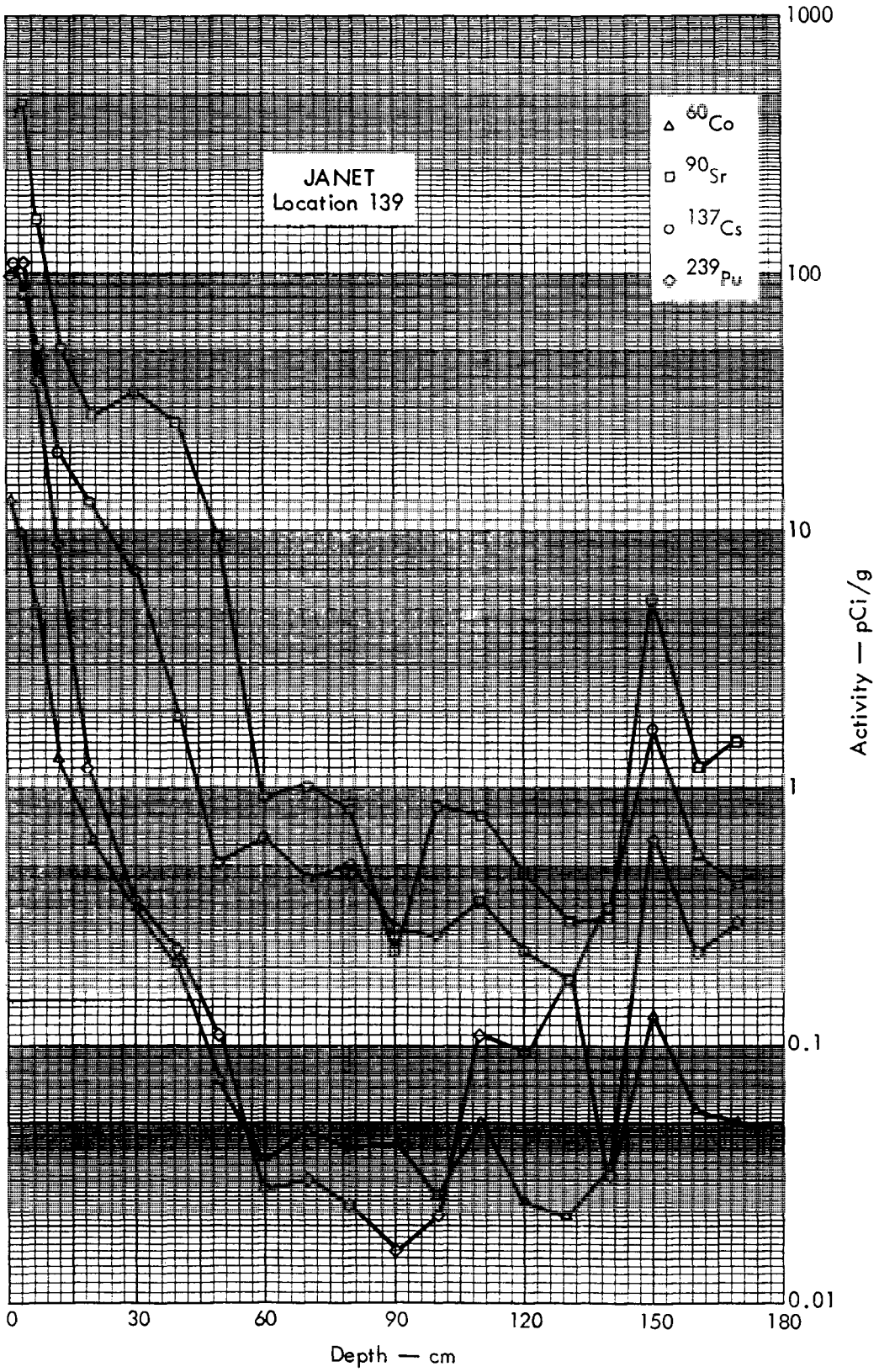

Fig. B. 8.2f. Activities of selected radionuclides as a function of soil depth.

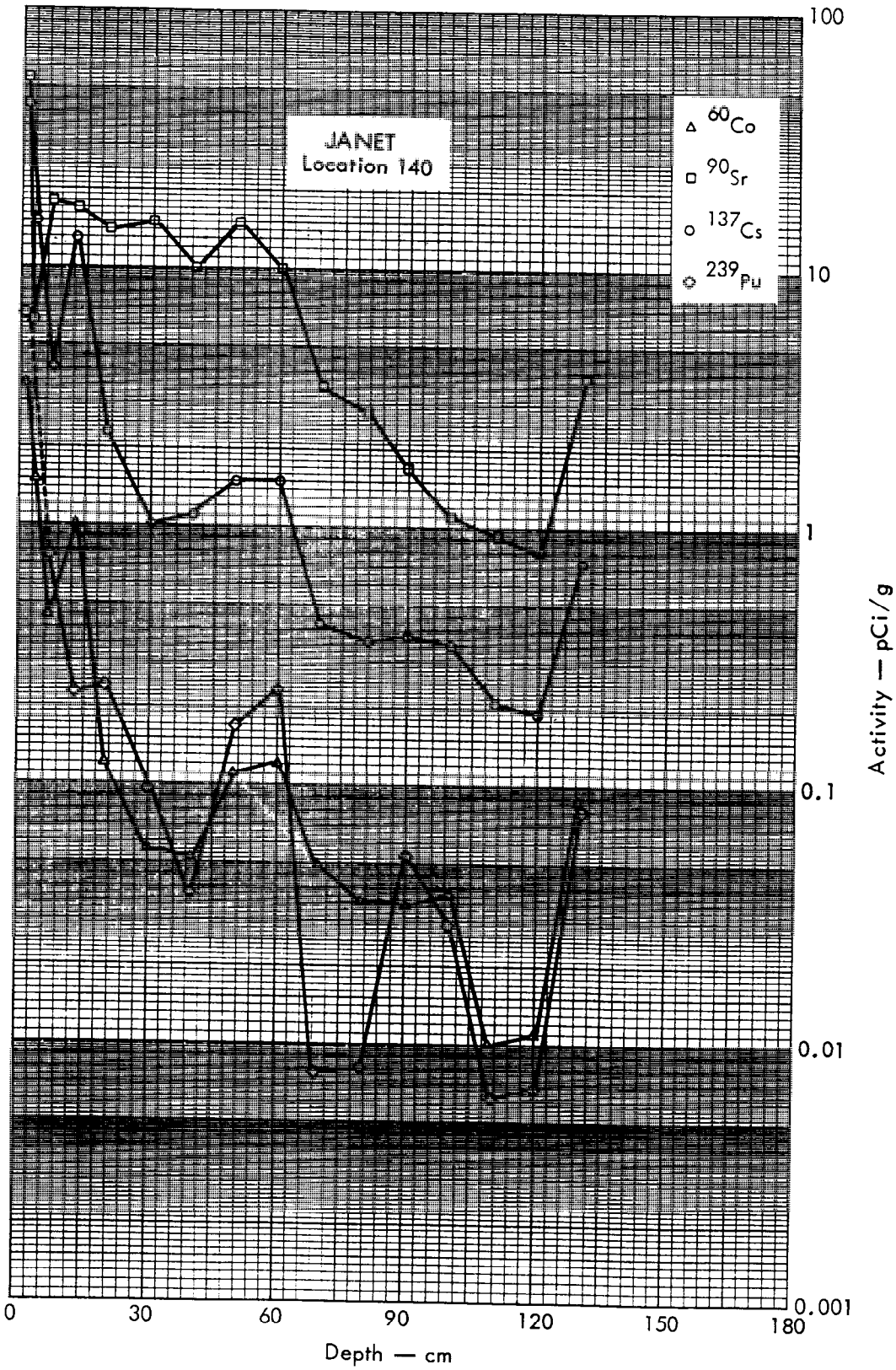

Fig. B. 8.2g. Activities of selected radionuclides as a function of soil depth.

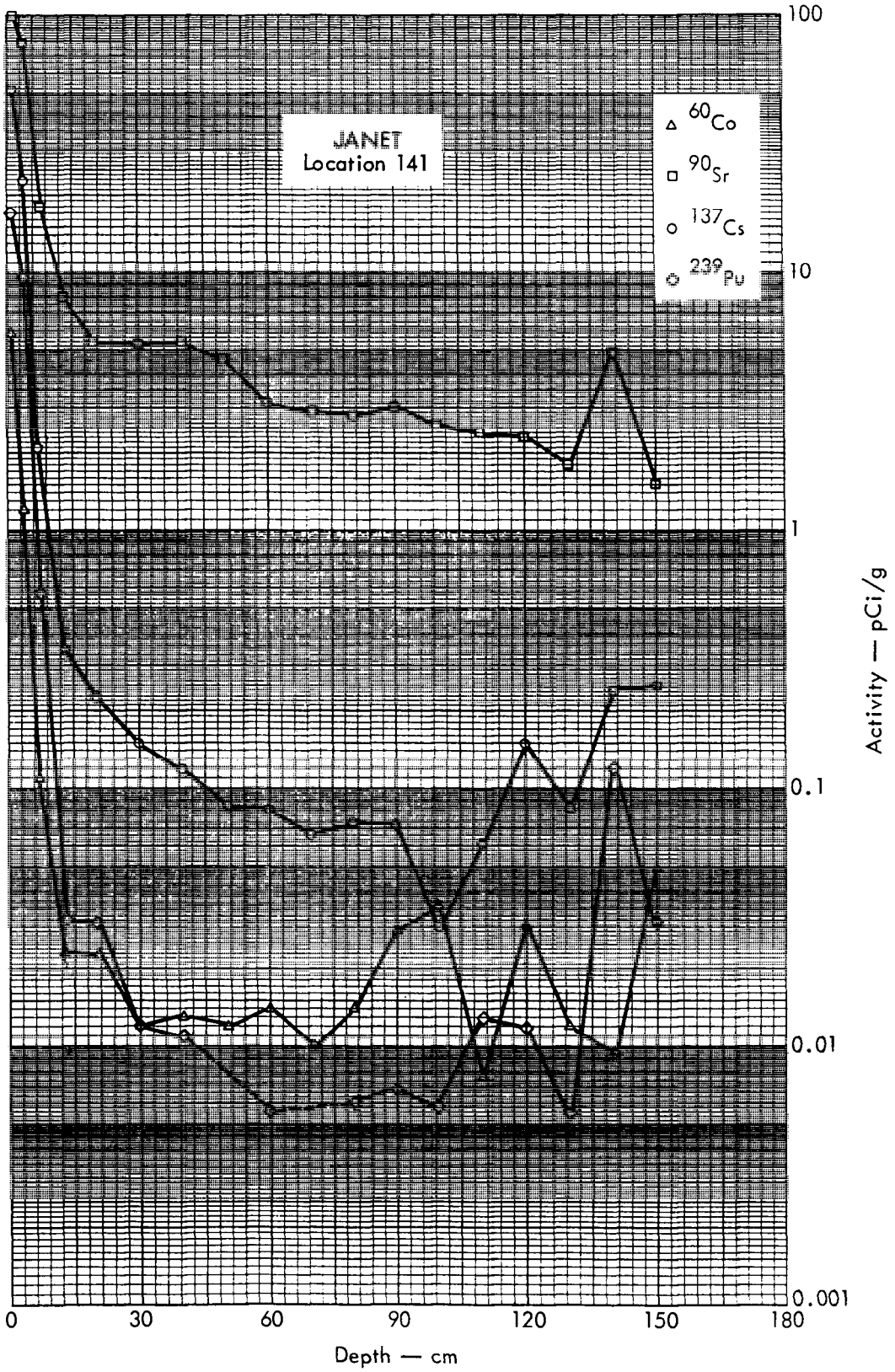

Fig. B.8.2h. Activities of selected radionuclides as a function of soil depth.

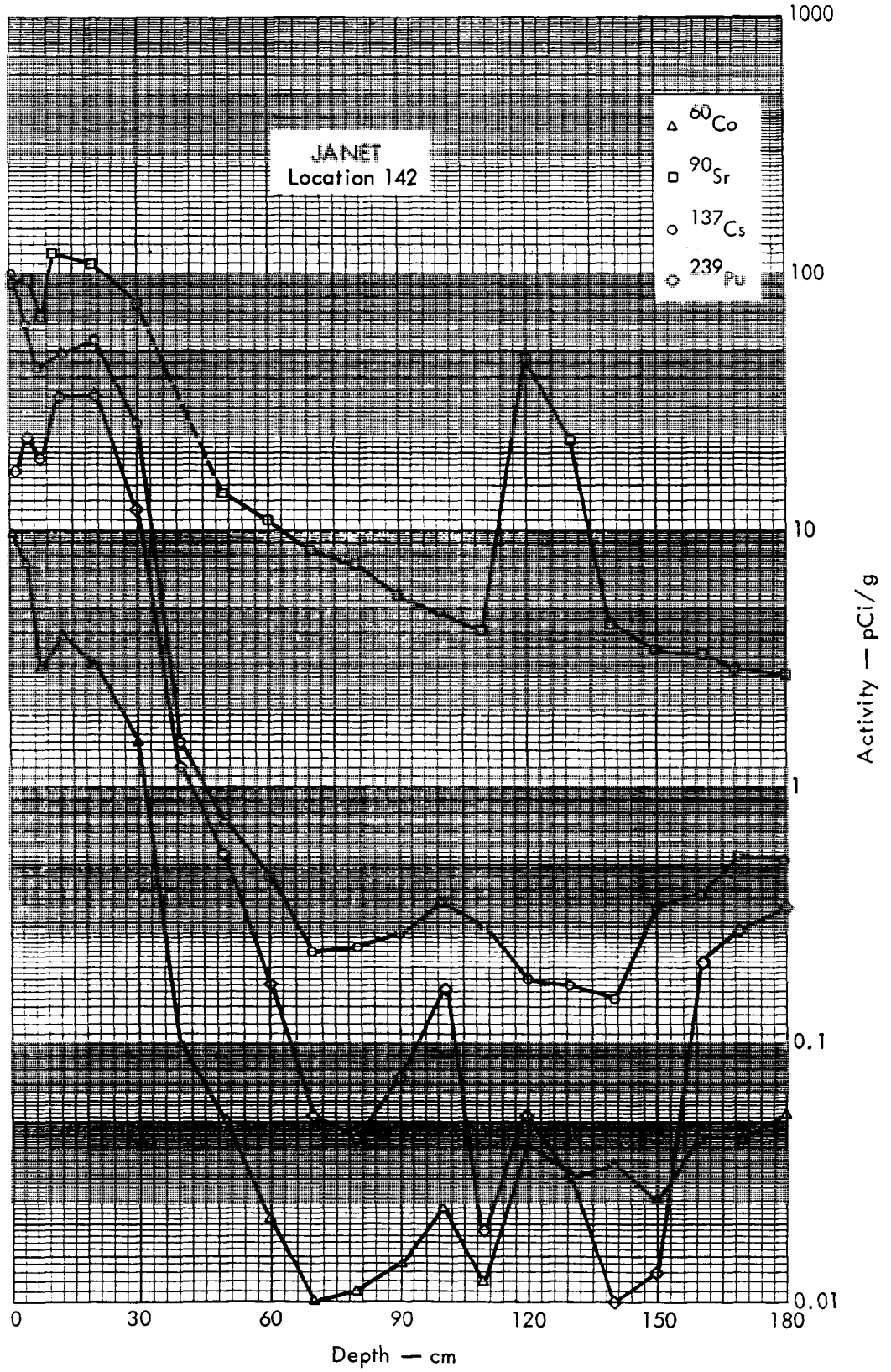

Fig. B.8.2i. Activities of selected radionuclides as a function of soil depth.

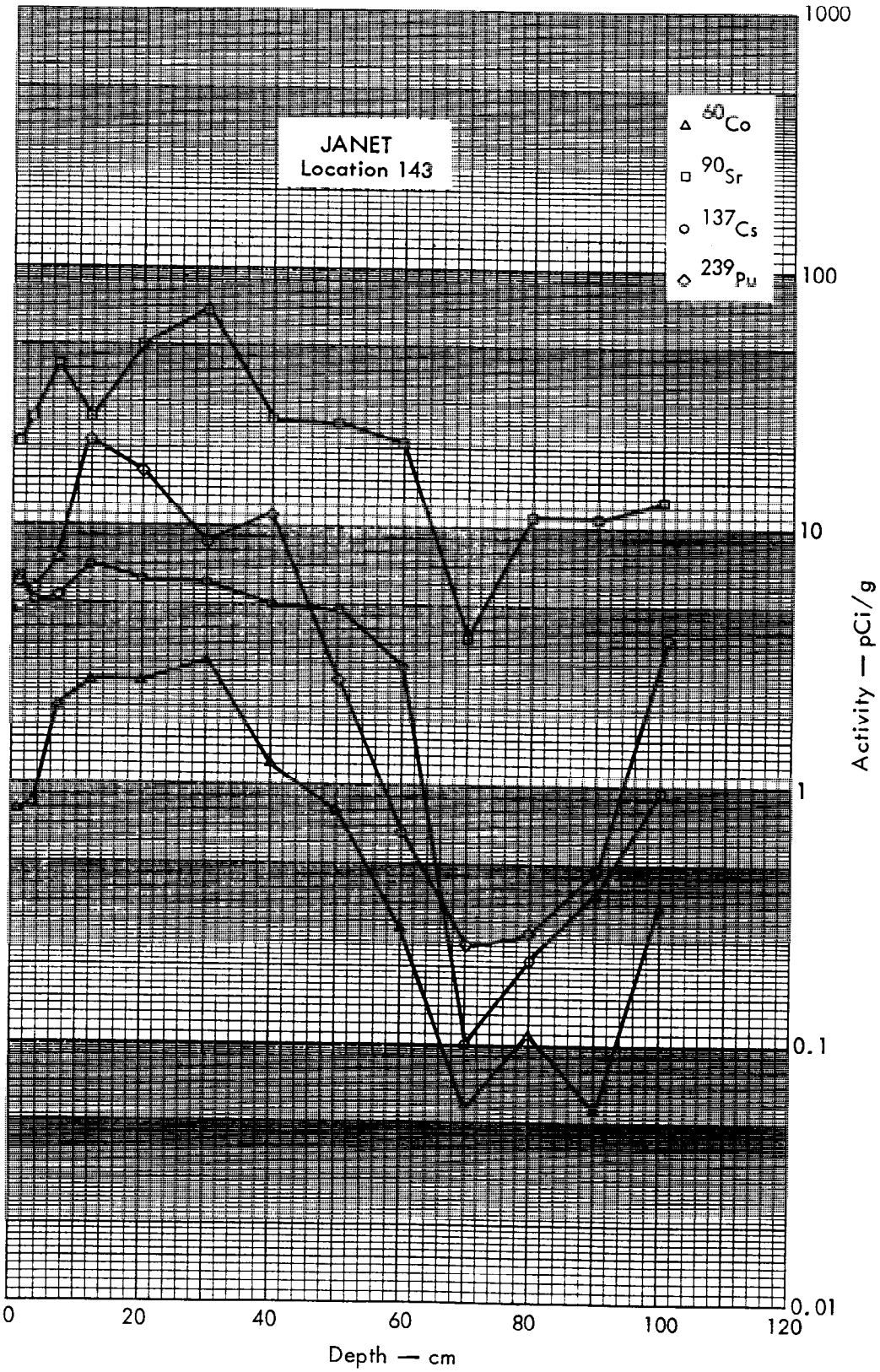

Fig. B. 8.2j. Activities of selected radionuclides as a function of soil depth.

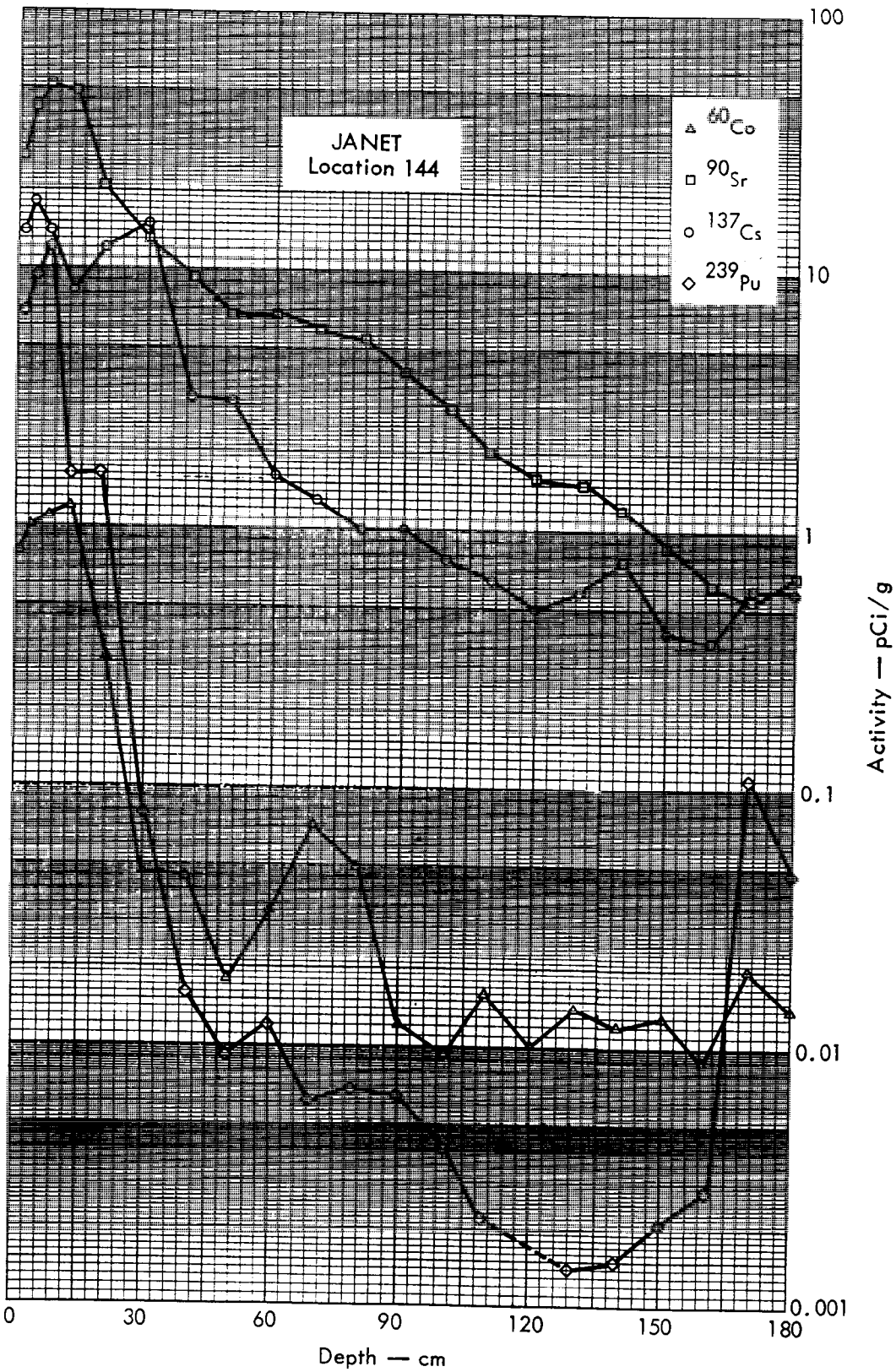

Fig. B.8.2k. Activities of selected radionuclides as a function of soil depth.

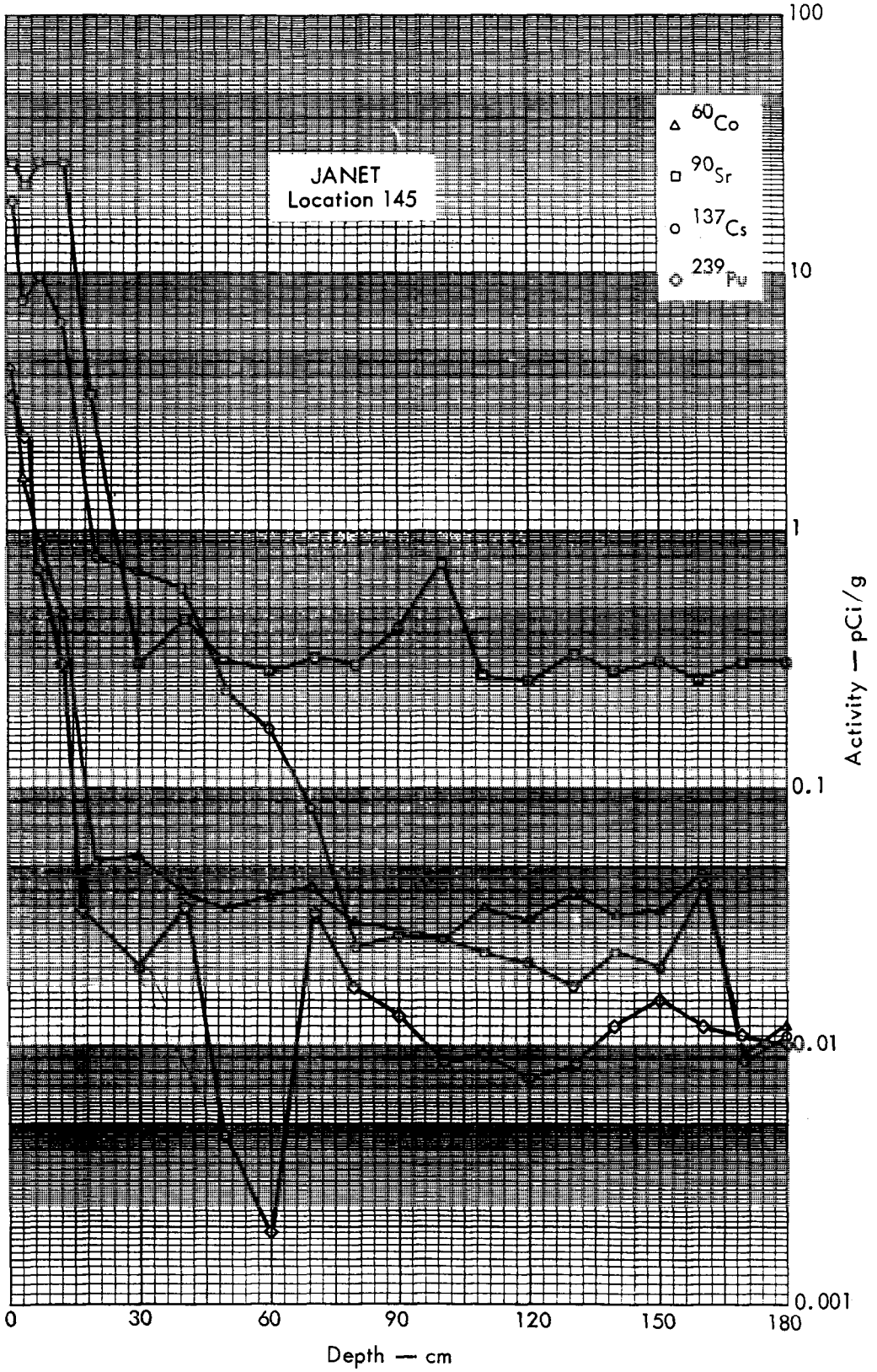

Fig. B. 8.21. Activities of selected radionuclides as a function of soil depth.

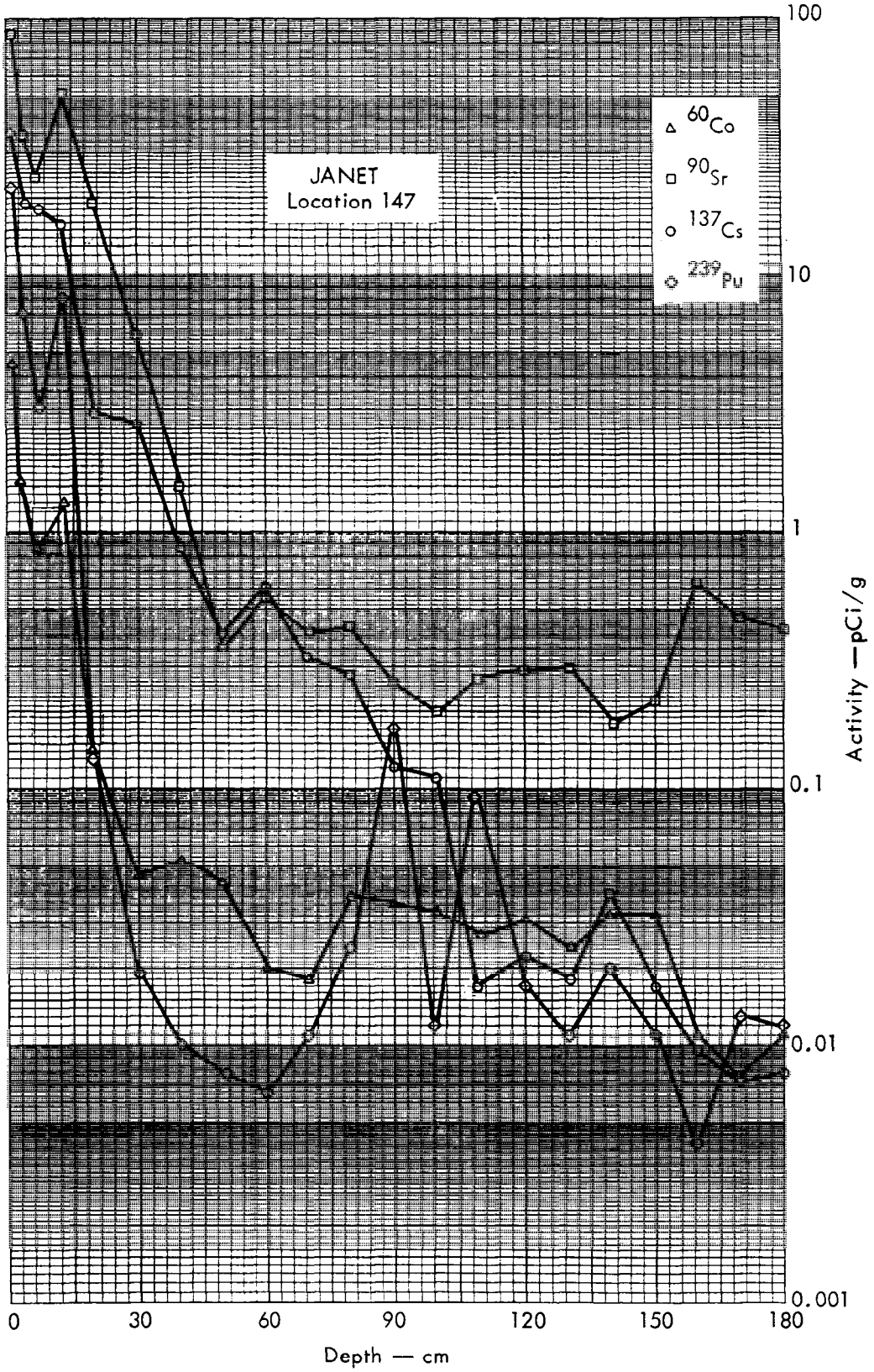

Fig. B.8.2m. Activities of selected radionuclides as a function of soil depth.

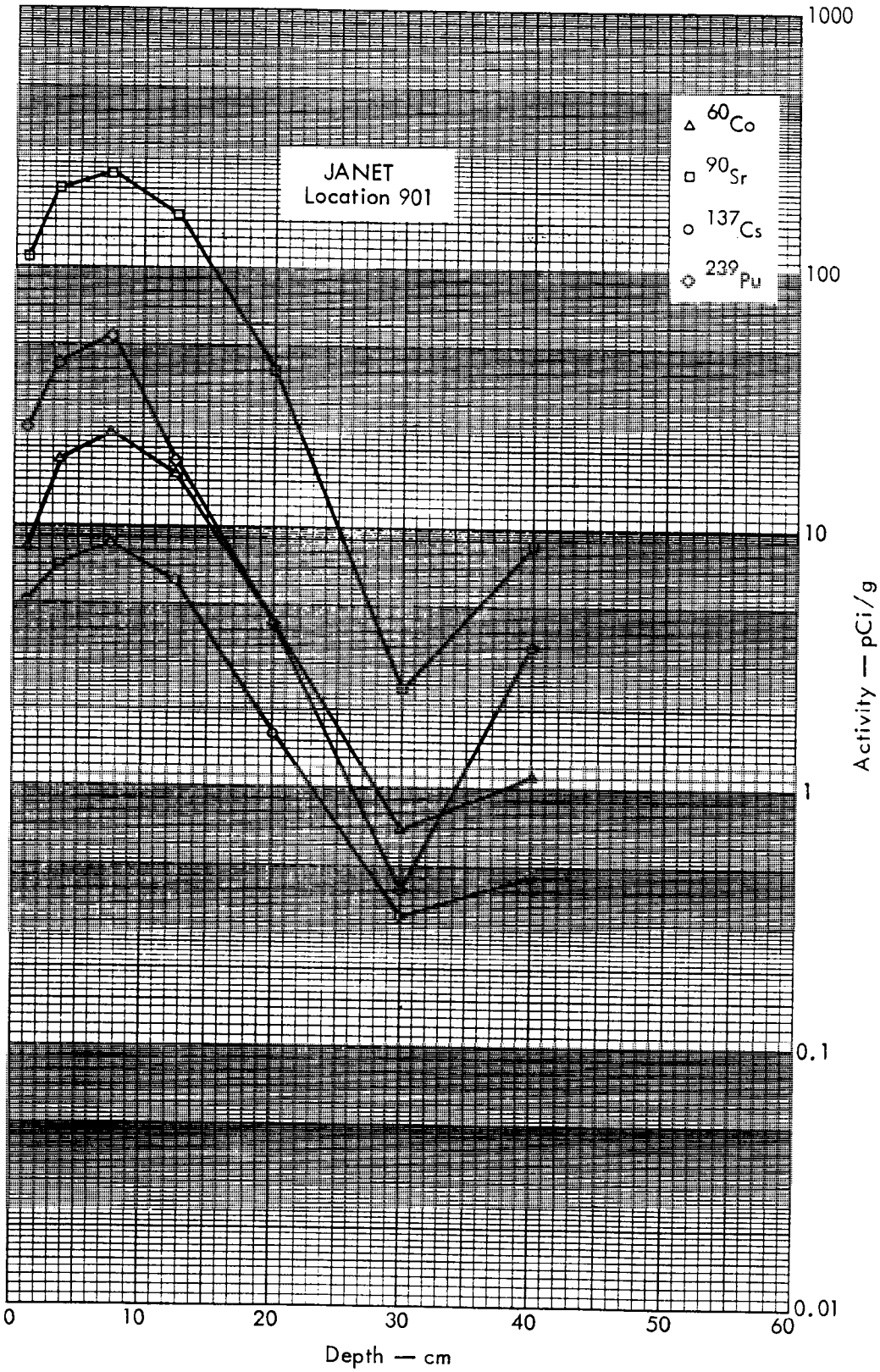

Fig. B.8.2n. Activities of selected radionuclides as a function of soil depth.

Fig. B.9.1.a.

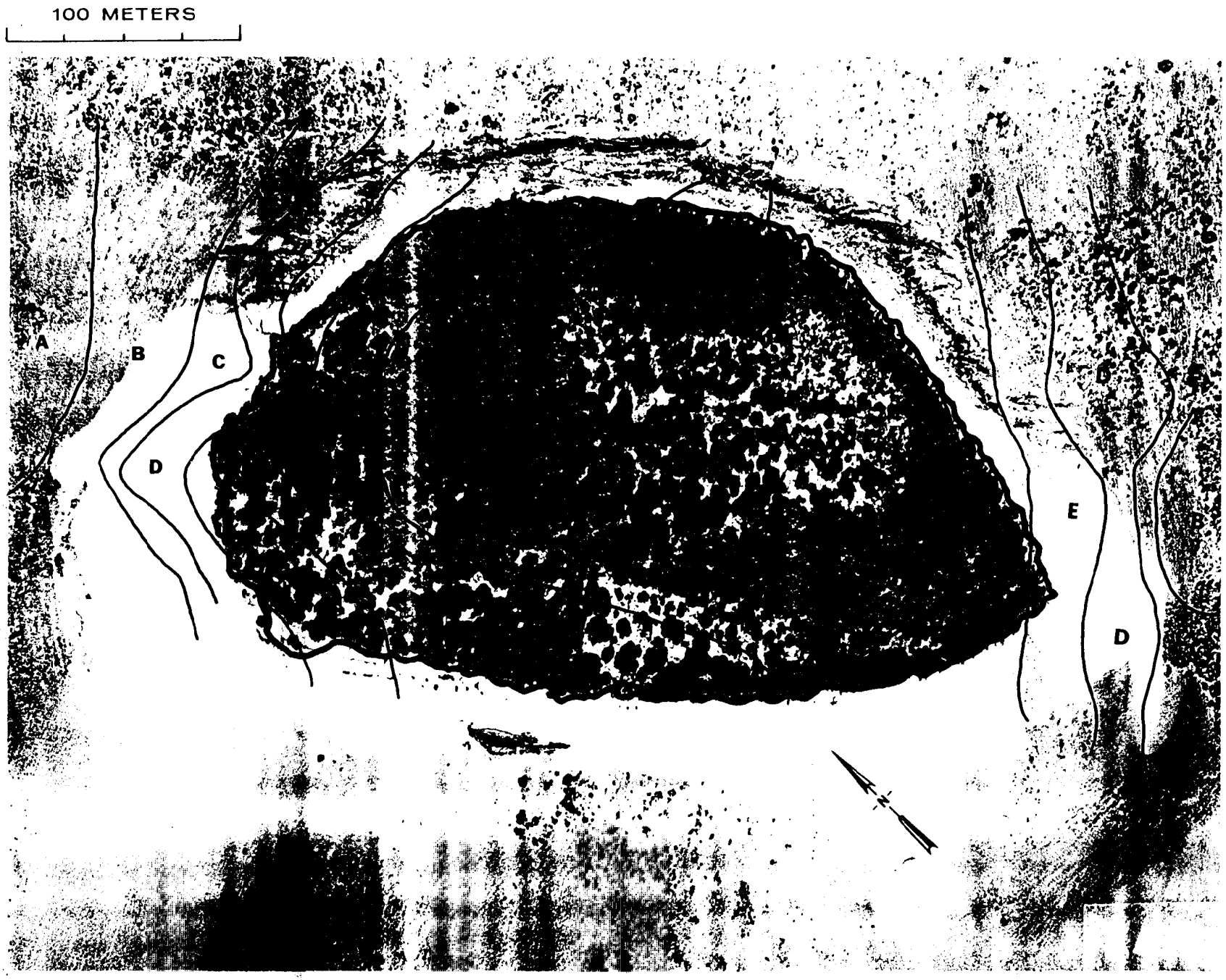

Fig. B.9.1.b. Gross count isoexposure contours. (Refer to alphabetic symbol key in this appendix.)

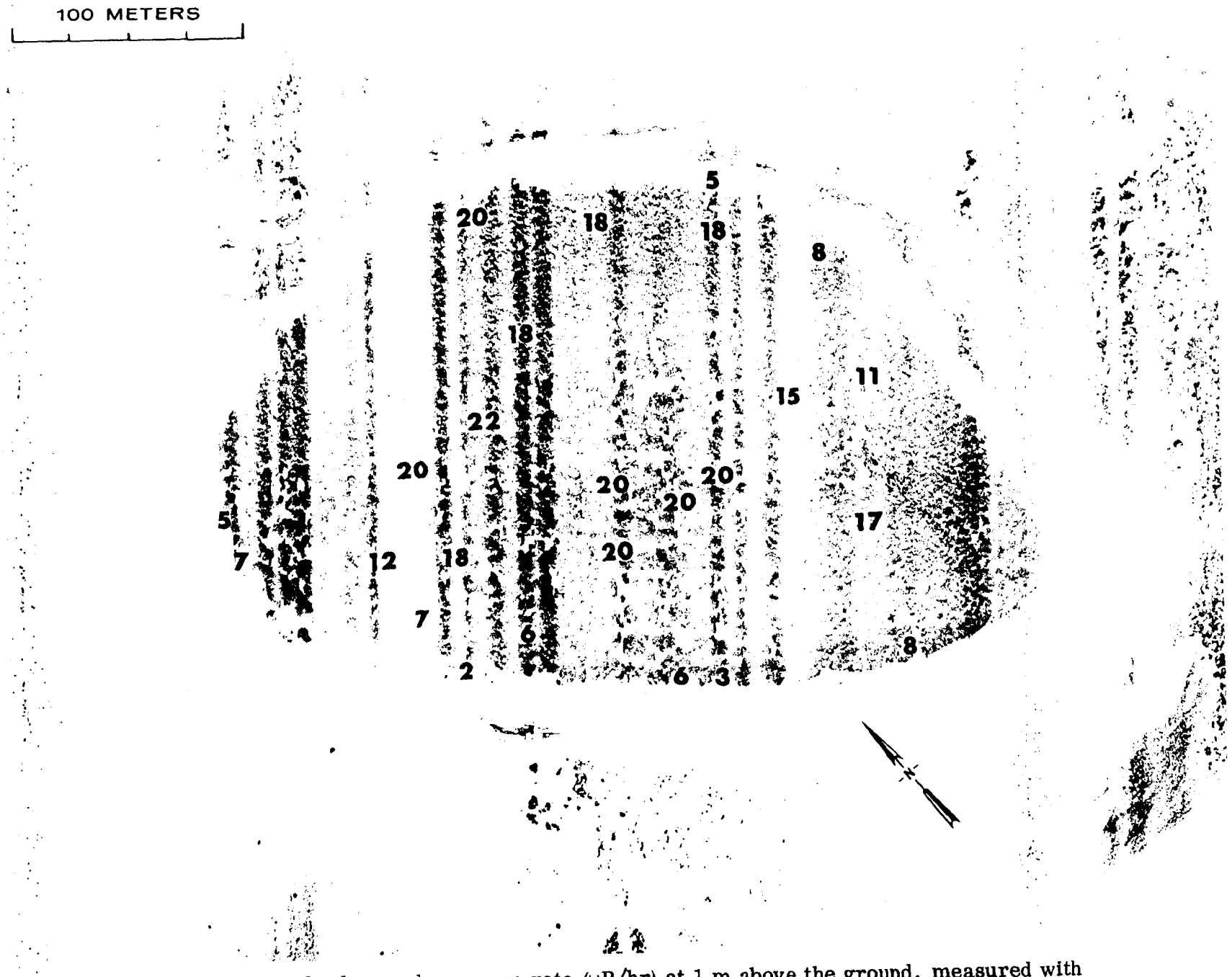

Fig. B.9.1.d. The gamma background exposure rate (μR/hr) at 1 m above the ground, measured with a portable NaI scintillation counter.

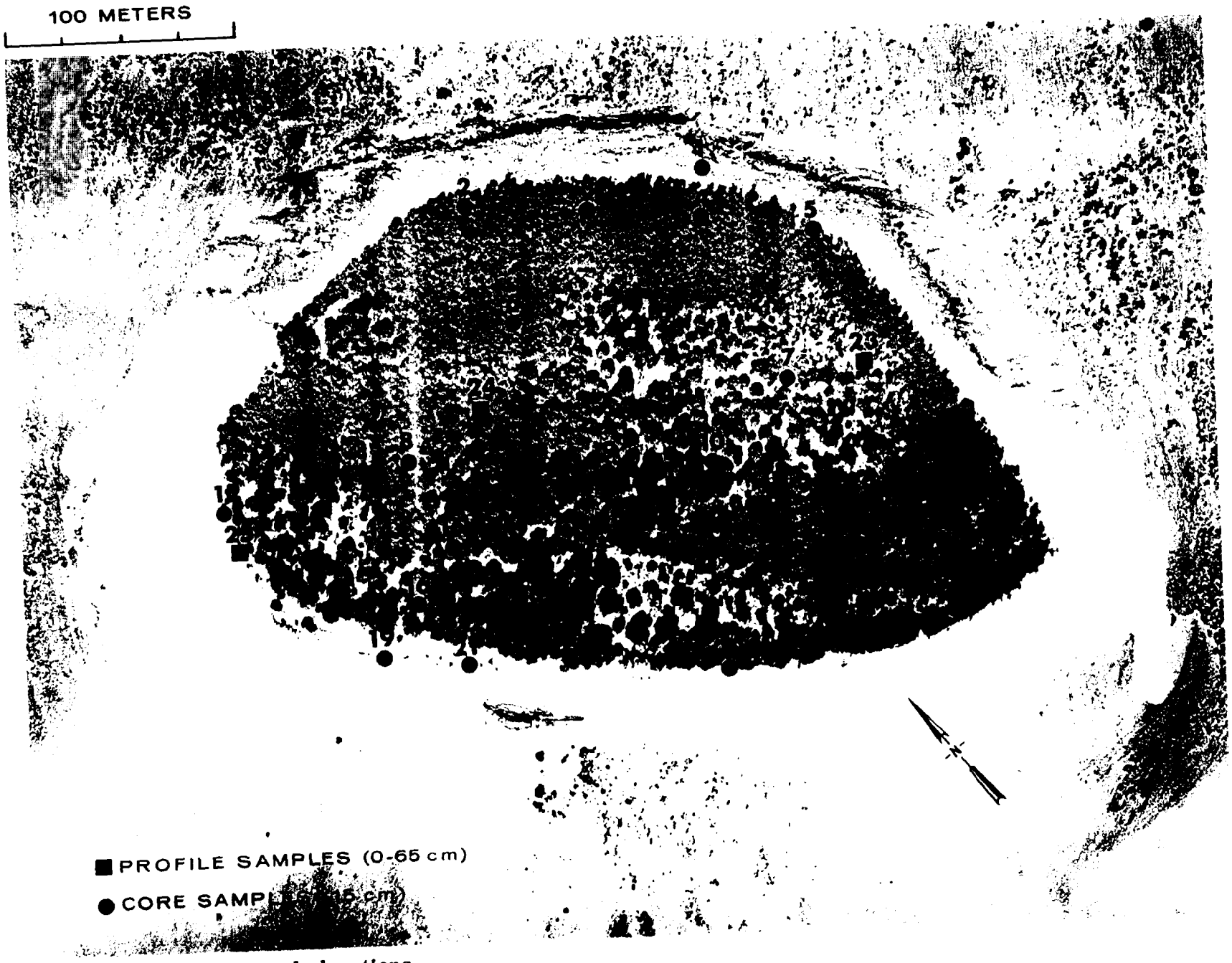

Fig. B.9.1.f. Soil-sample locations.

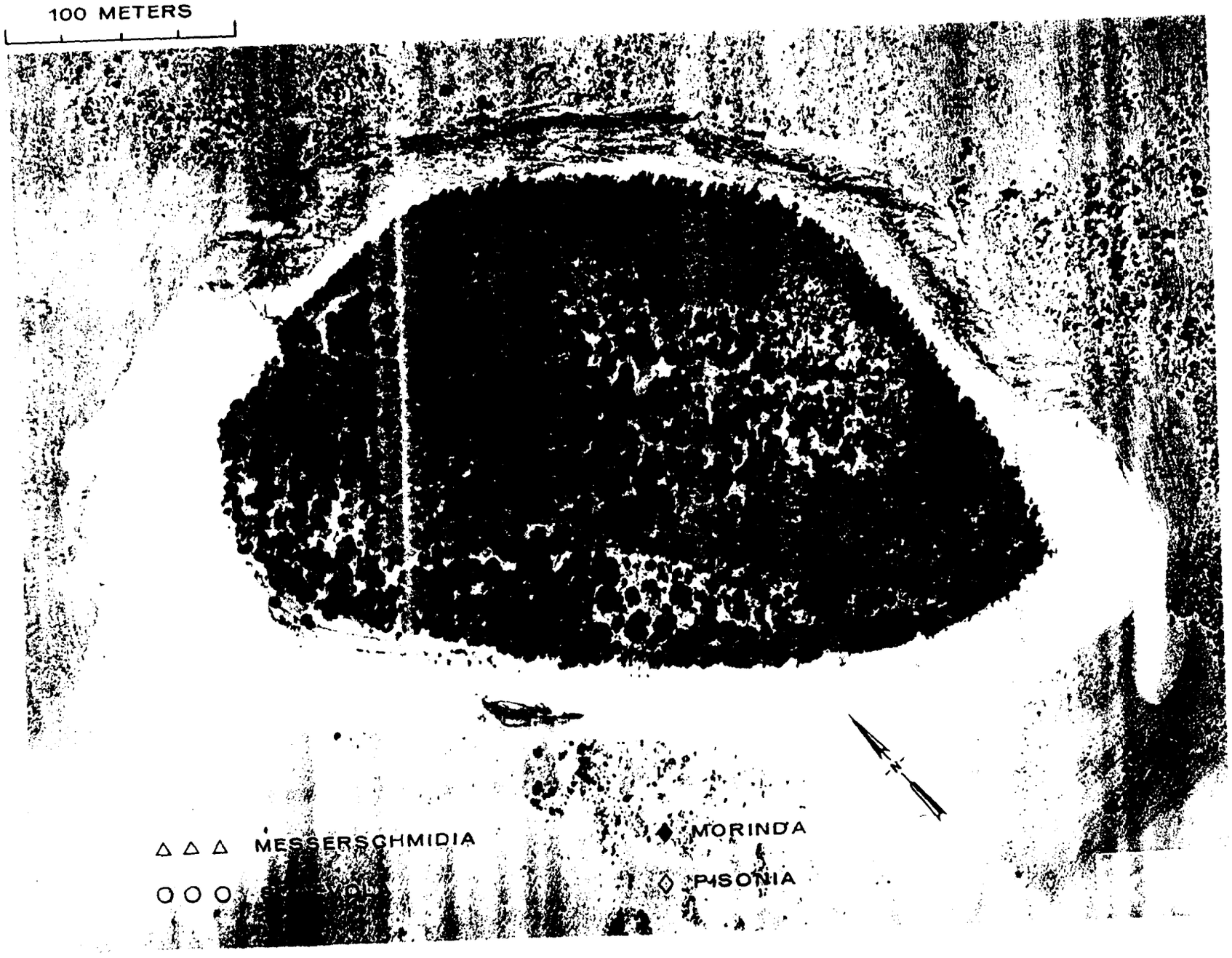

Fig. B.9.1.g. Vegetation sample locations.

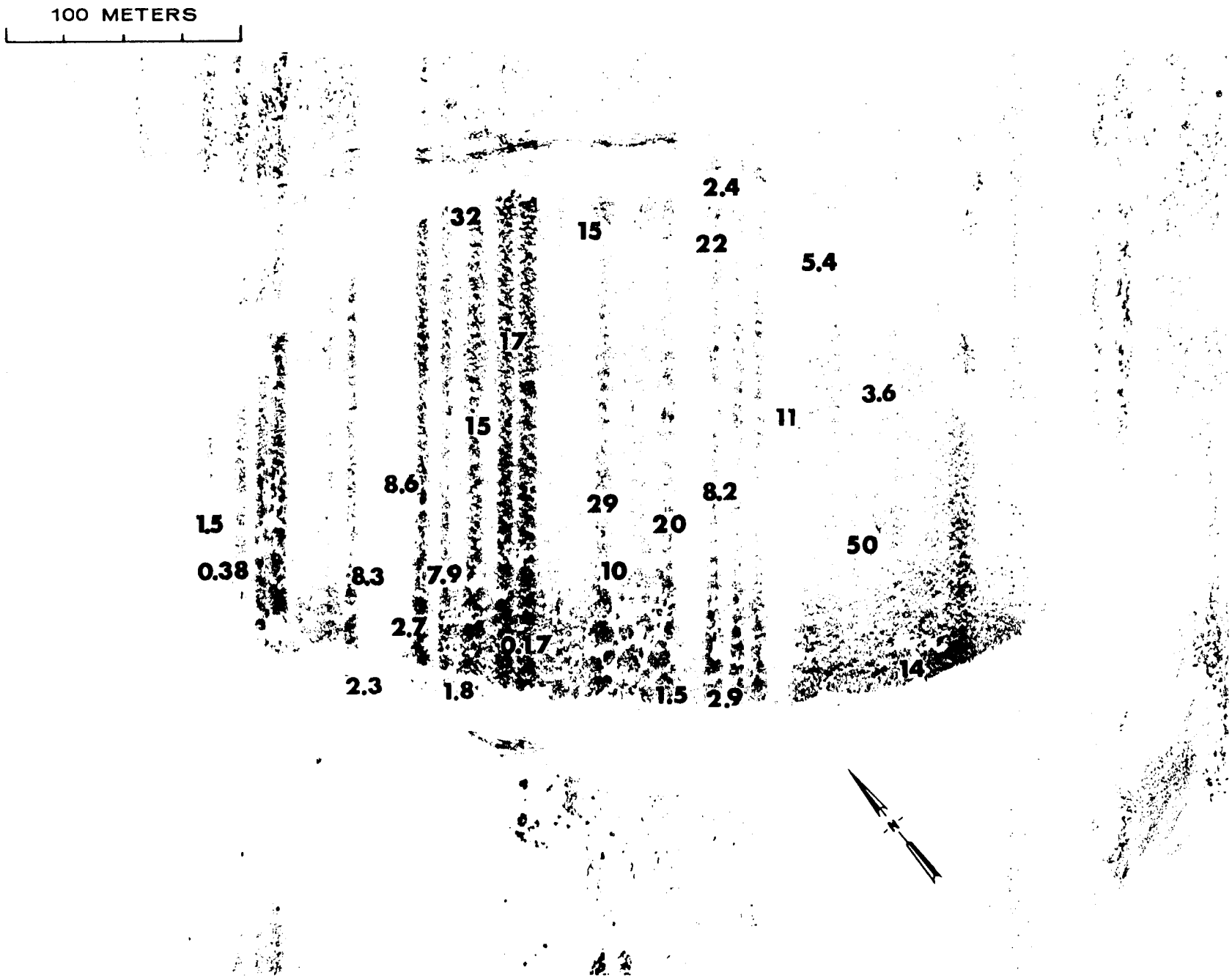

Fig. B.9.1.i. The average ^{239}Pu activities (pCi/g) in soil samples collected to a depth of 15 cm.

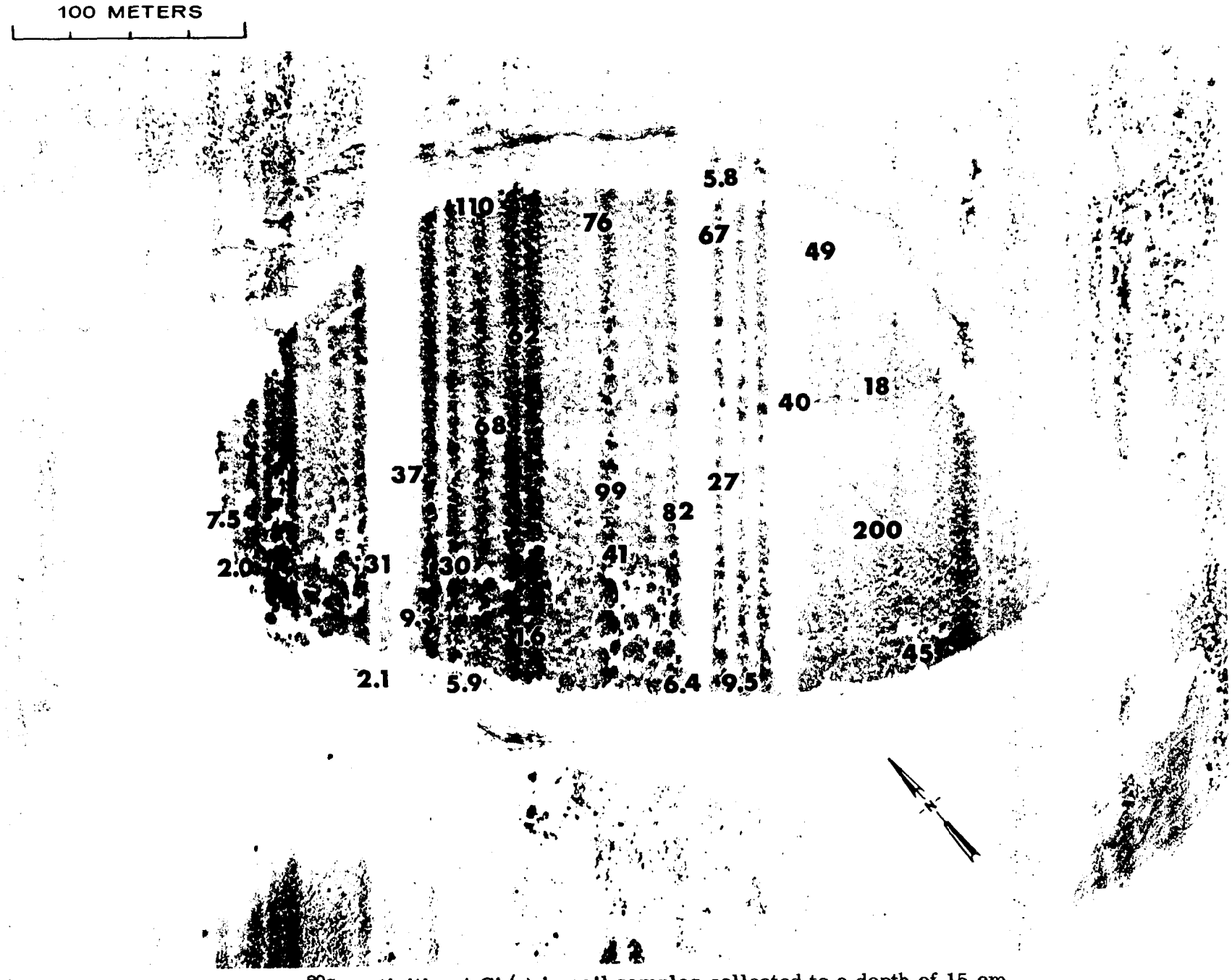

Fig. B.9.1.j. The average ^{90}Sr activities (pCi/g) in soil samples collected to a depth of 15 cm.

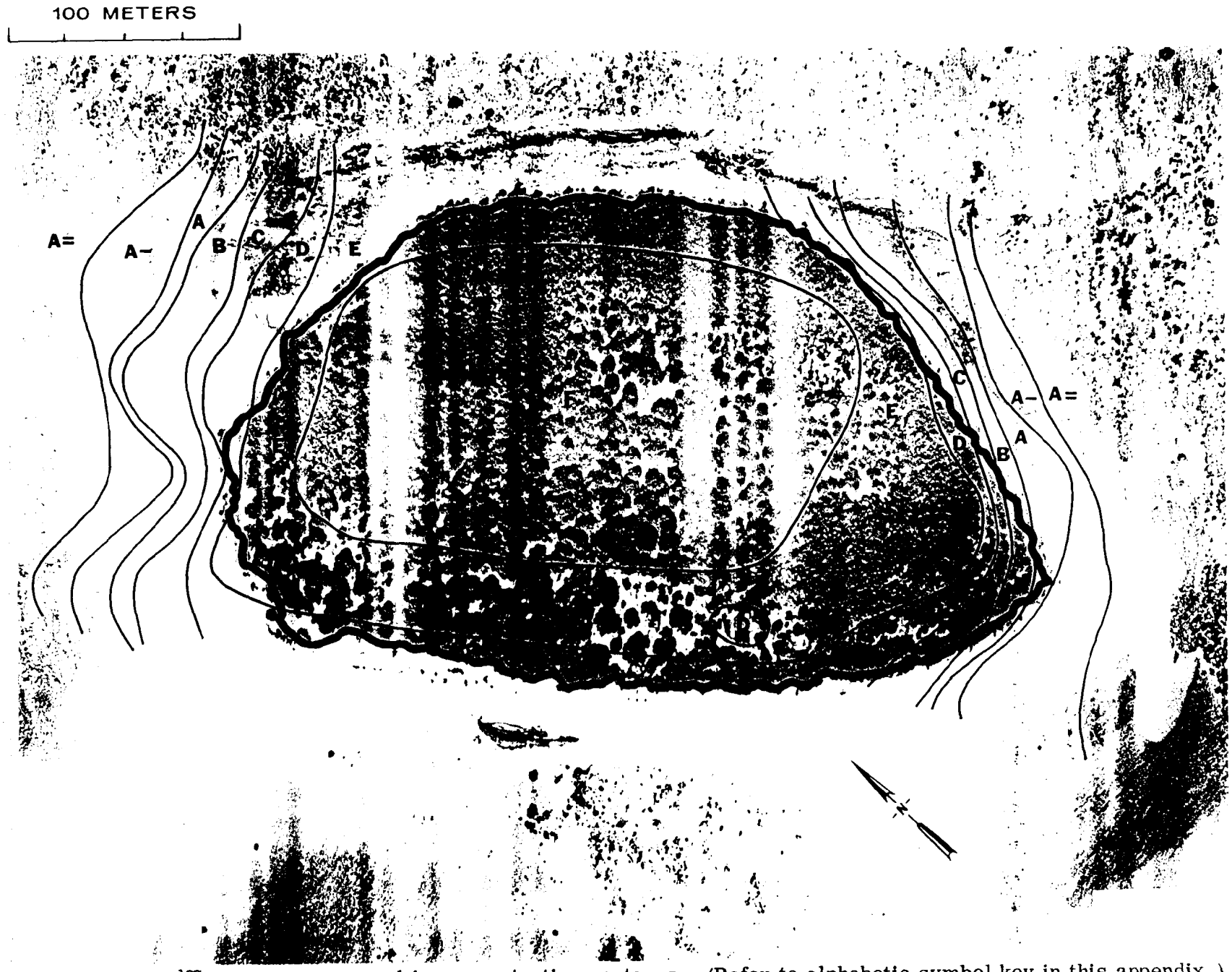

Fig. B.9.1.k. ^{137}Cs isoexposure and isoconcentration contours. (Refer to alphabetic symbol key in this appendix.)

Fig. B.9.1.1. The average ^{137}Cs activities (pCi/g) in soil samples collected to a depth of 15 cm.

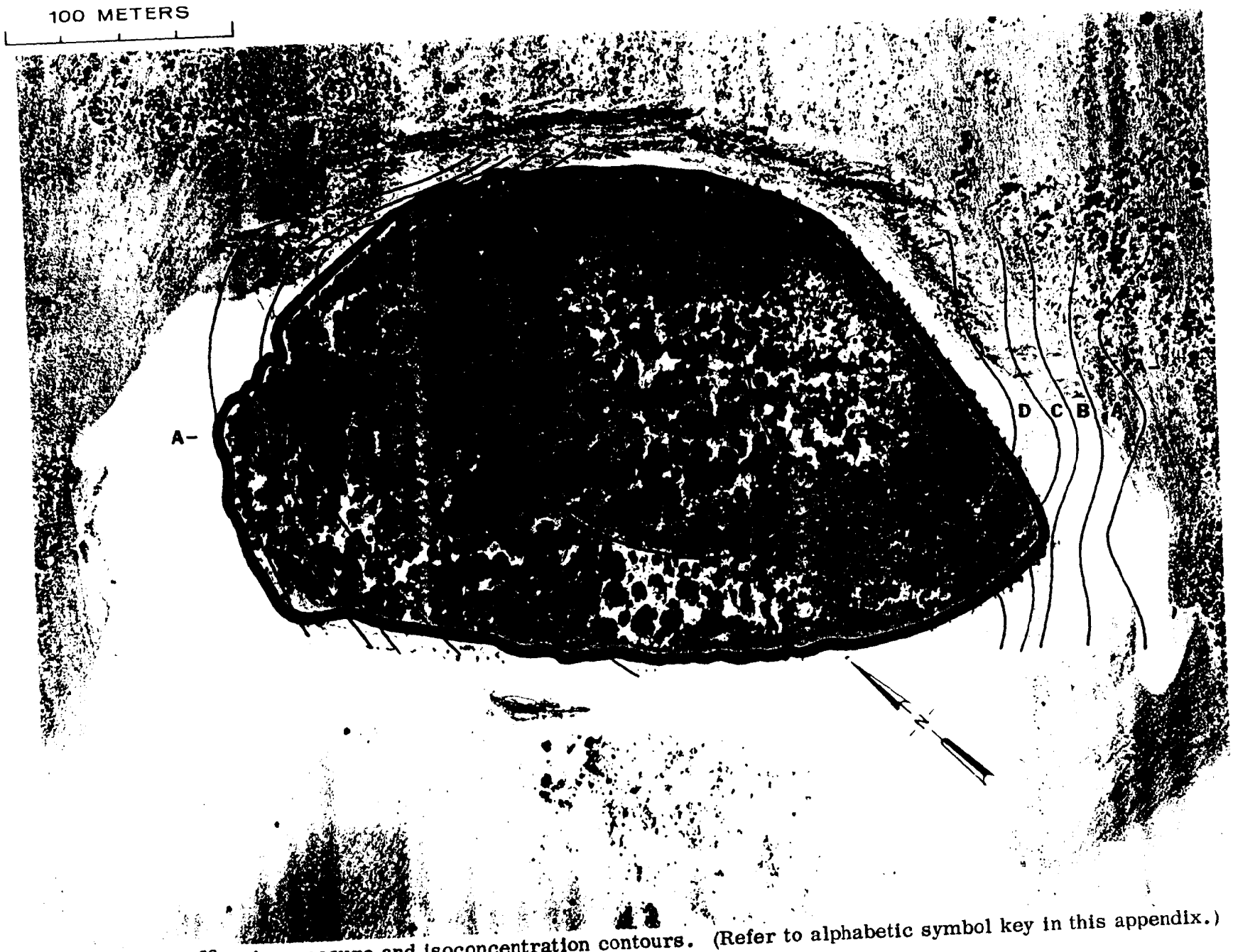

Fig. B.9.1.m. ^{60}Co isoexposure and isoconcentration contours. (Refer to alphabetic symbol key in this appendix.)

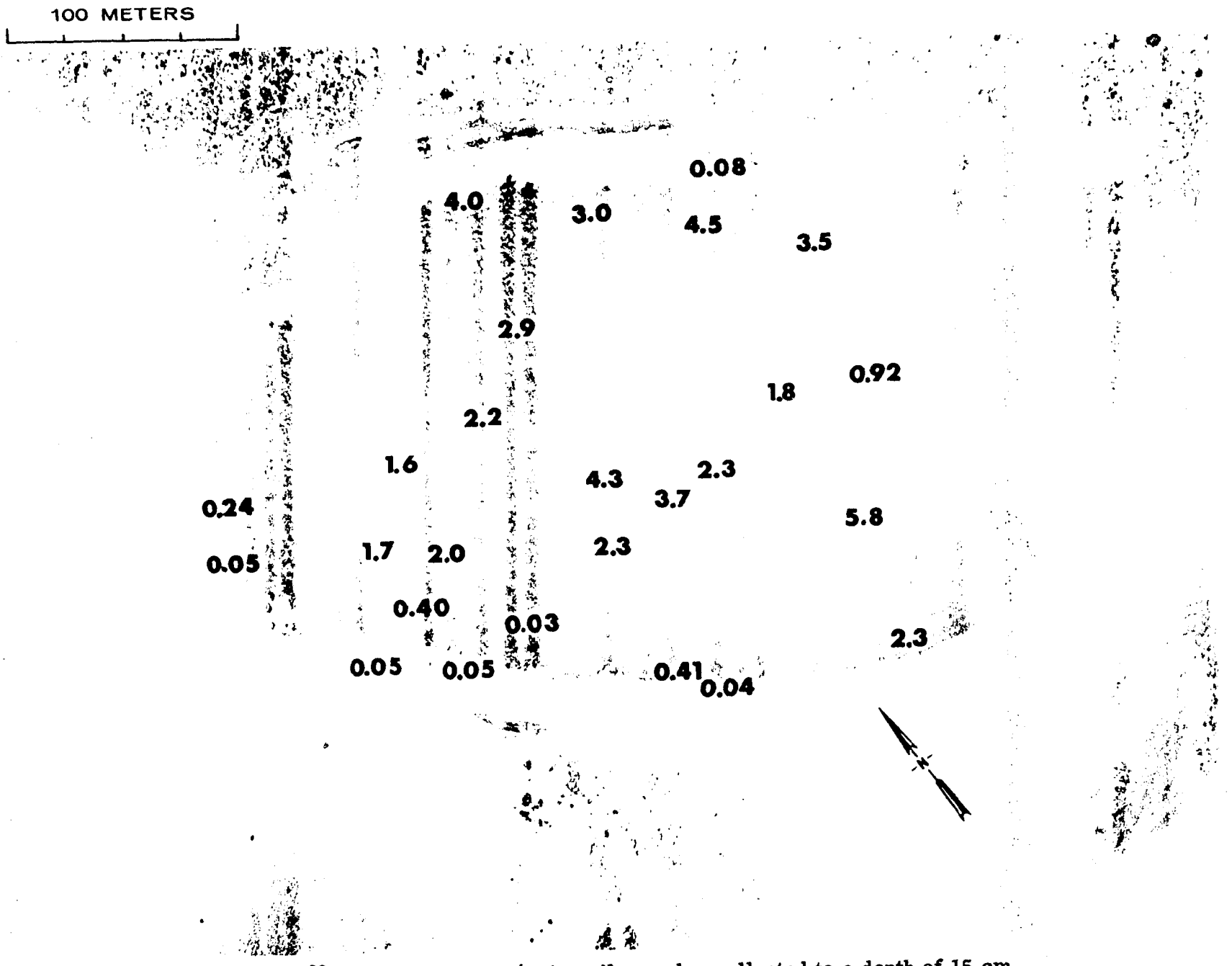

Fig. B.9.1.n. The average ^{60}Co activities (pCi/g) in soil samples collected to a depth of 15 cm.

Fig. B.9.1.o. Terrestrial animal sample locations.

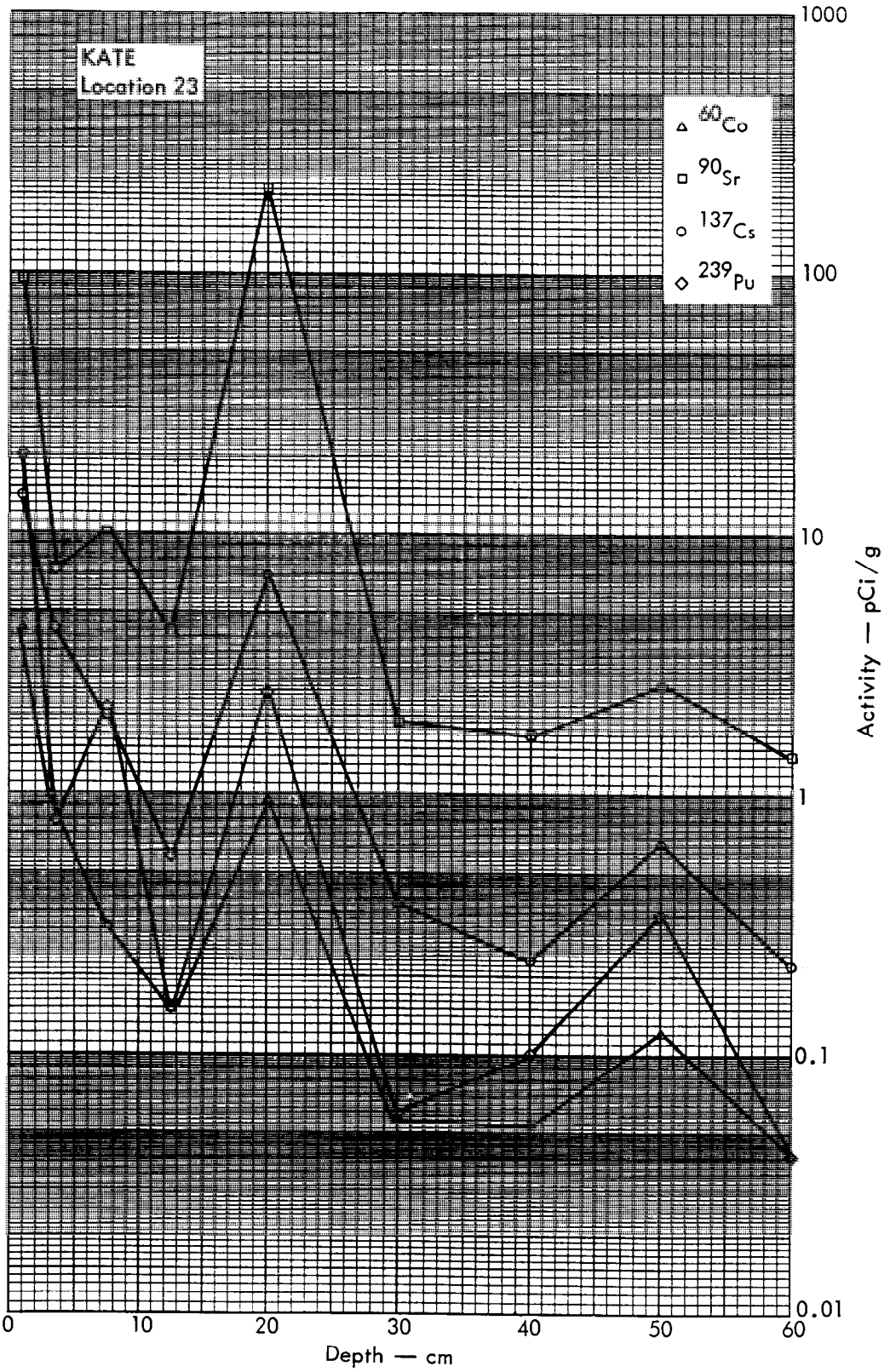

Fig. B.9.2a. Activities of selected radionuclides as a function of soil depth.

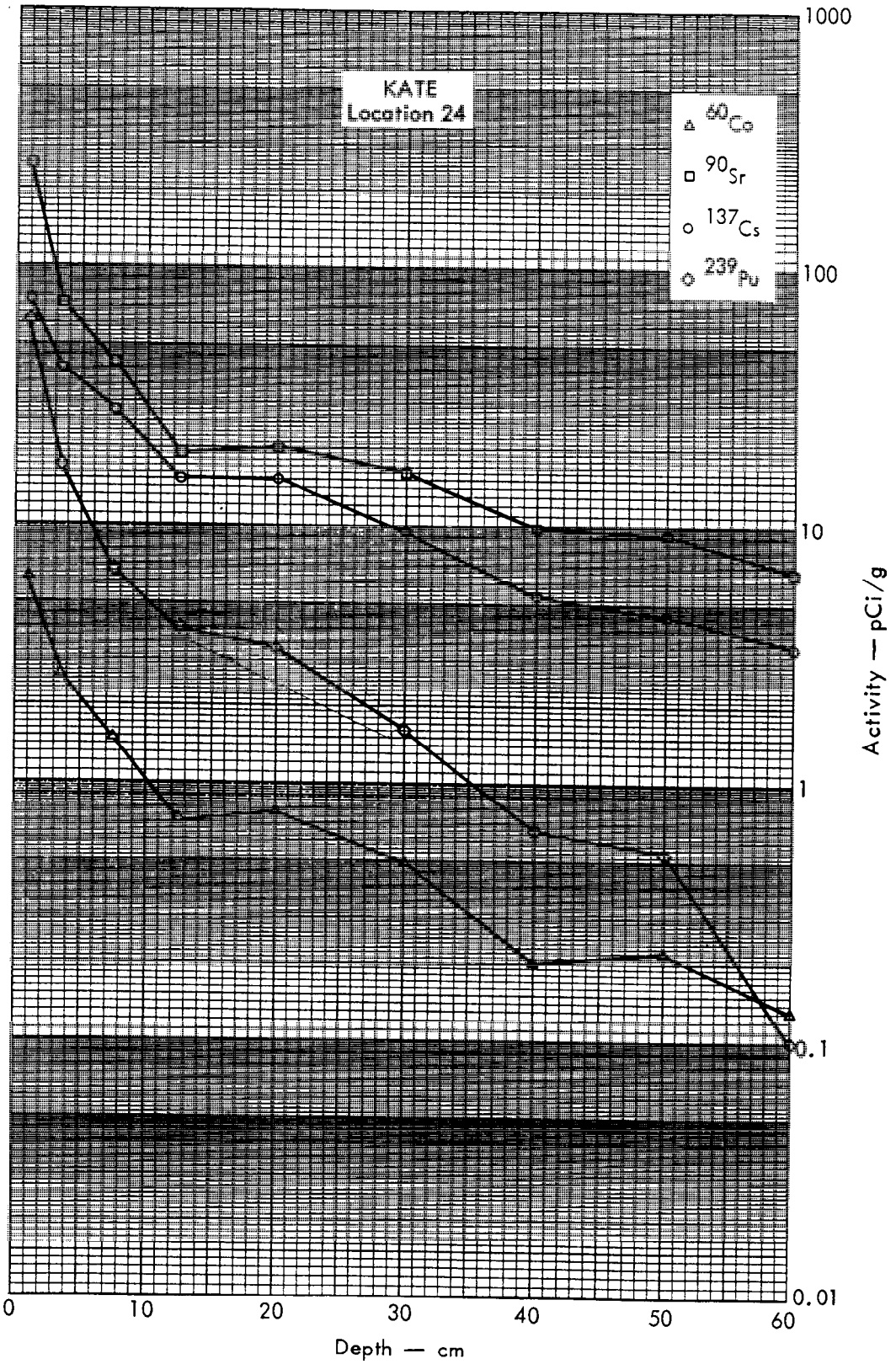

Fig. B. 9. 2b. Activities of selected radionuclides as a function of soil depth.

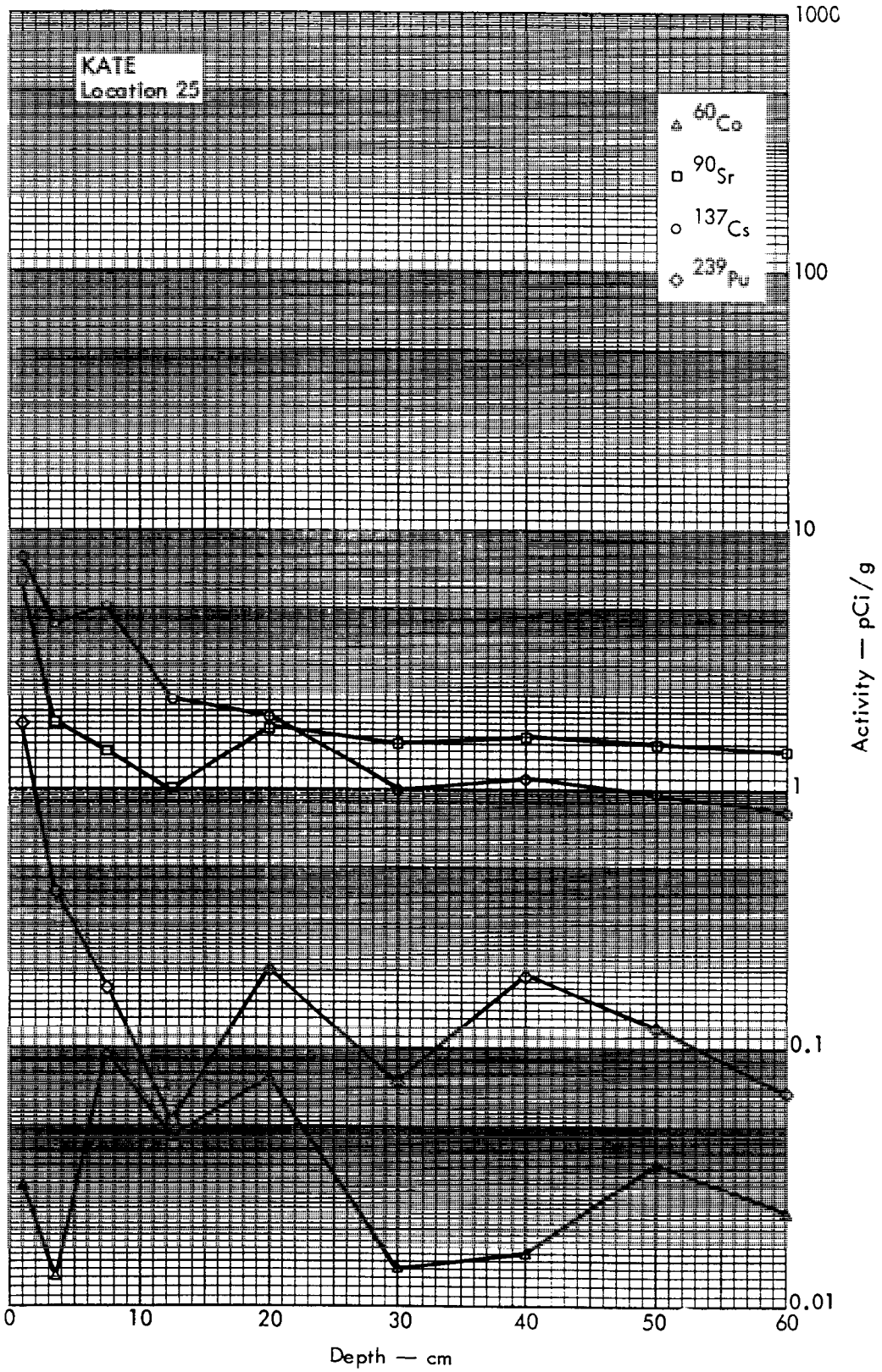

Fig. B.9.2c. Activities of selected radionuclides as a function of soil depth.

Fig. B.10.1.a.

Fig. B.10.1.b. **Gross count isoexposure contours.** (Refer to alphabetic symbol key in this appendix.)

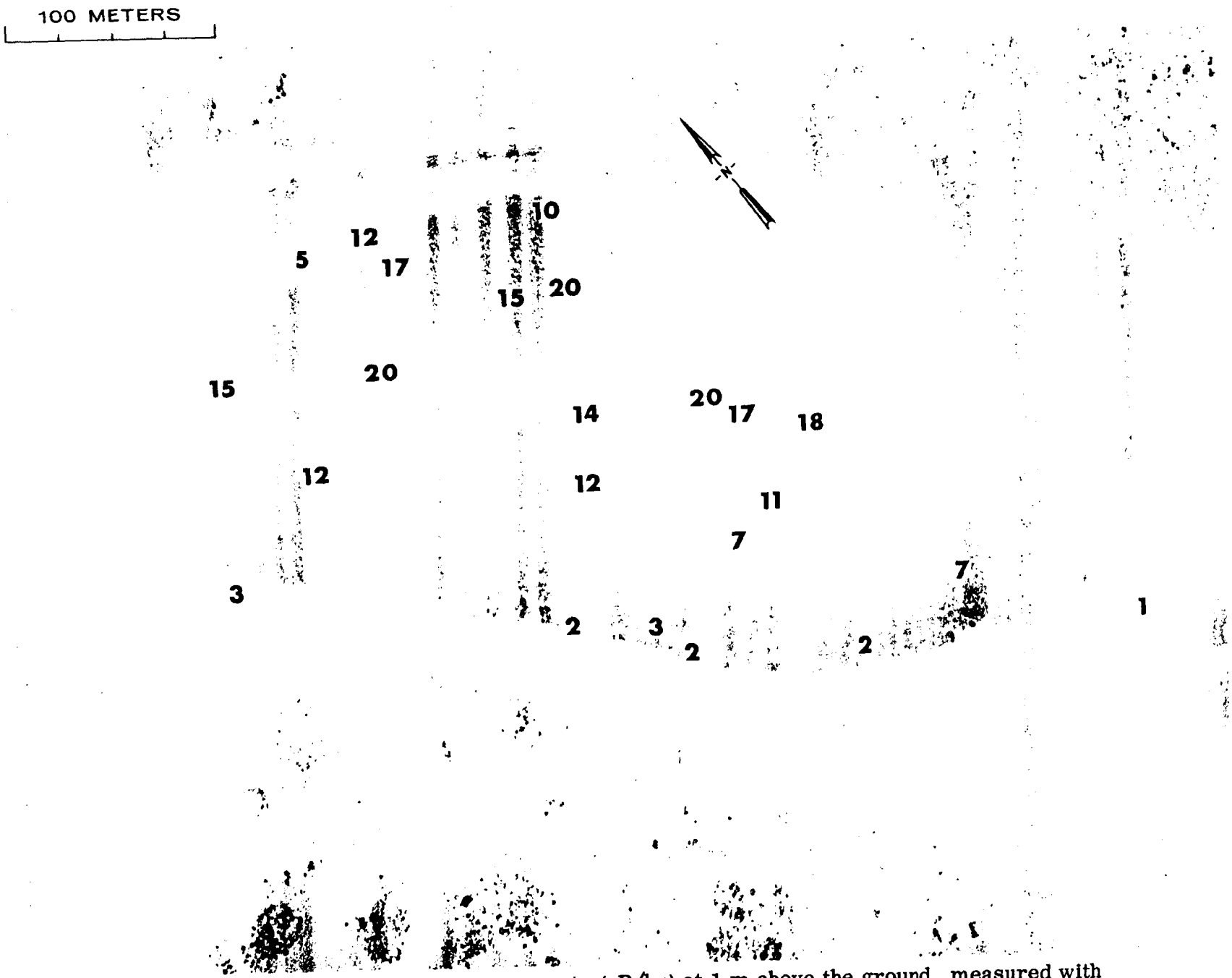

Fig. B.10.1.d. The gamma background exposure rate (μR/hr) at 1 m above the ground, measured with a portable NaI scintillation counter.

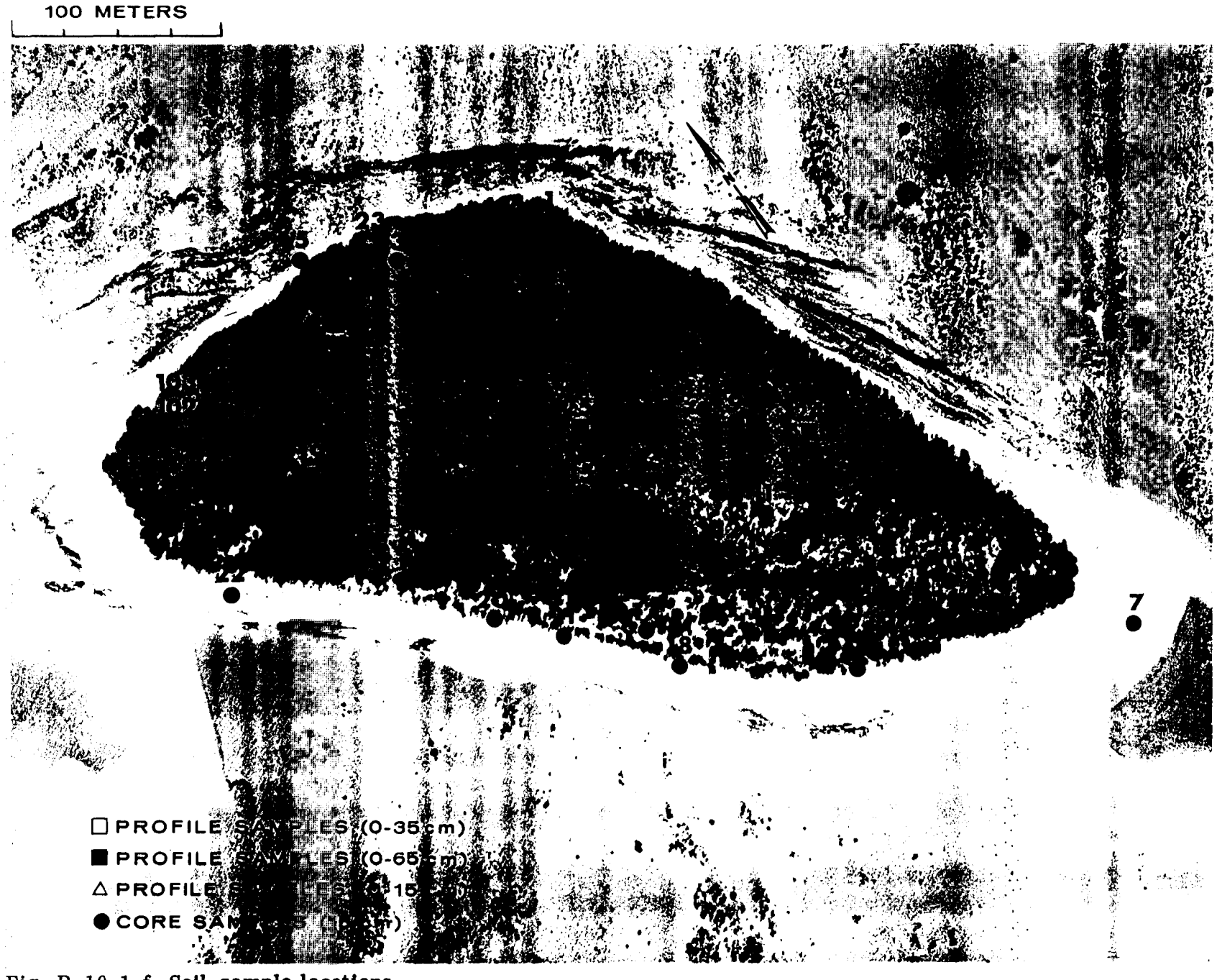

Fig. B.10.1.f. Soil-sample locations.

Fig. B.10.1.g. Vegetation sample locations.

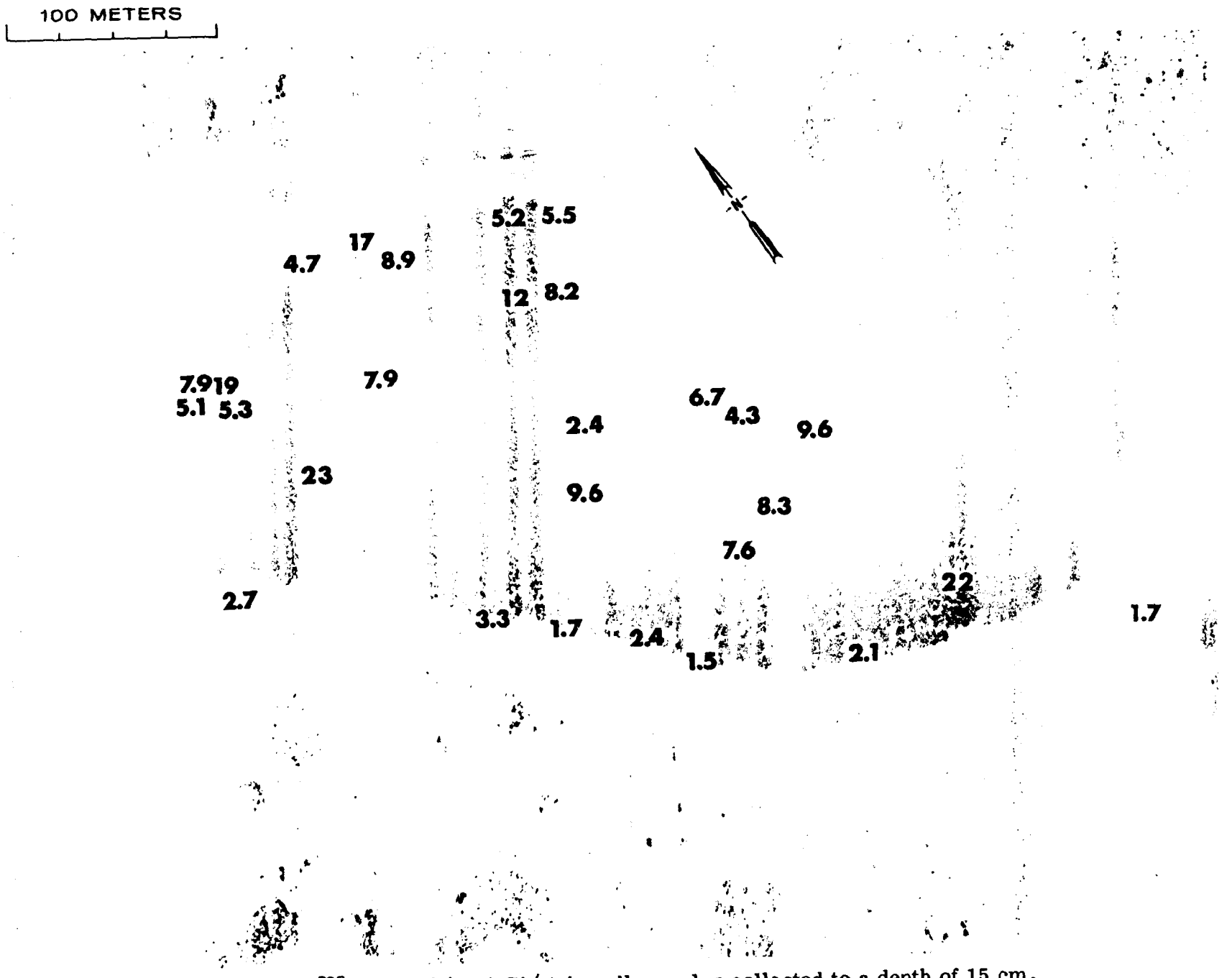

Fig. B.10.1.1. The average ^{239}Pu activities (pCi/g) in soil samples collected to a depth of 15 cm.

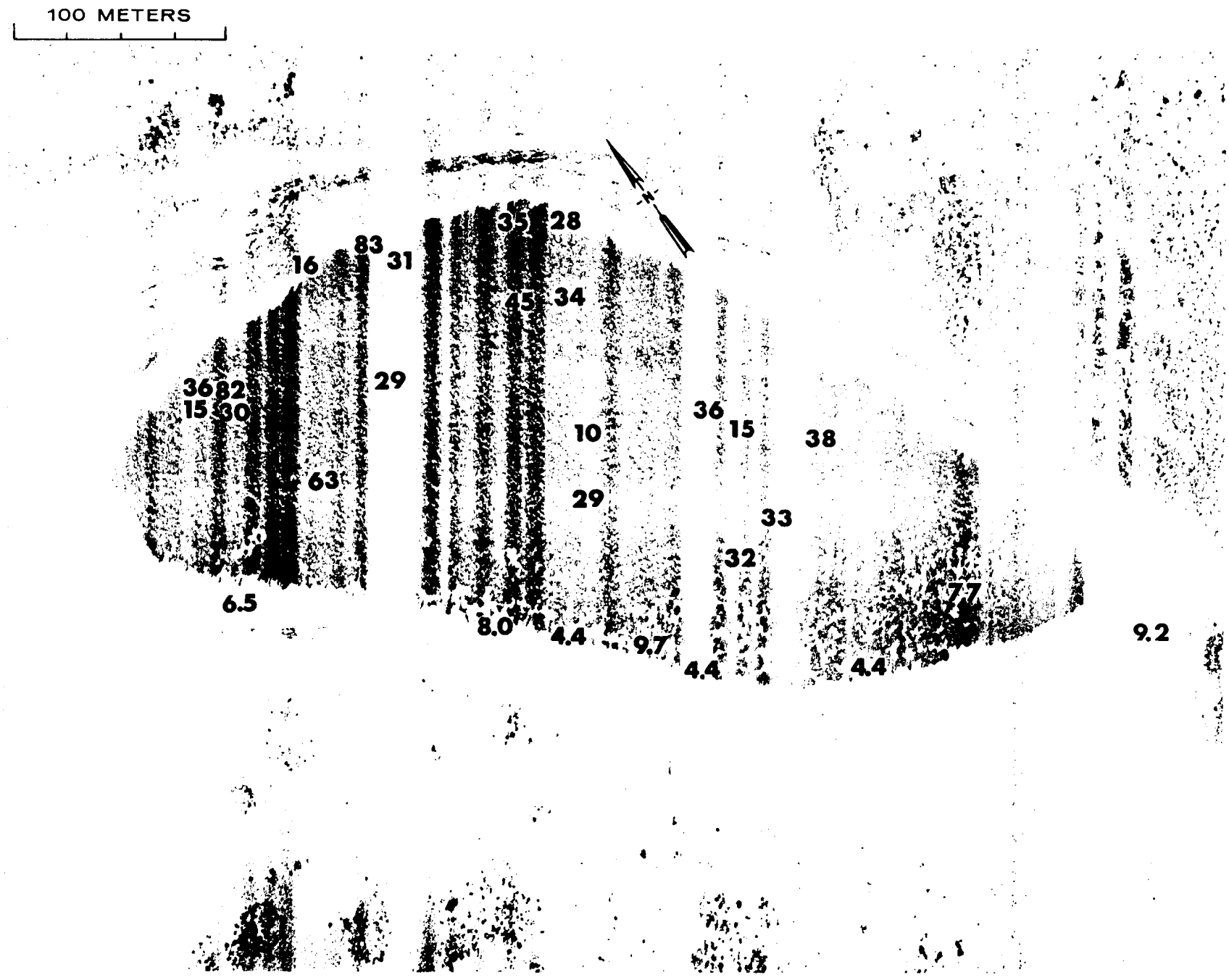

Fig. B.10.1.j. The average ^{90}Sr activities (pCi/g) in soil samples collected to a depth of 15 cm.

Fig. B.10.1.k. ^{137}Cs isoexposure and isoconcentration contours. (Refer to alphabetic symbol key in this appendix.)

Fig. B.10.1.1. The average ^{137}Cs activities (pCi/g) in soil samples collected to a depth of 15 cm.

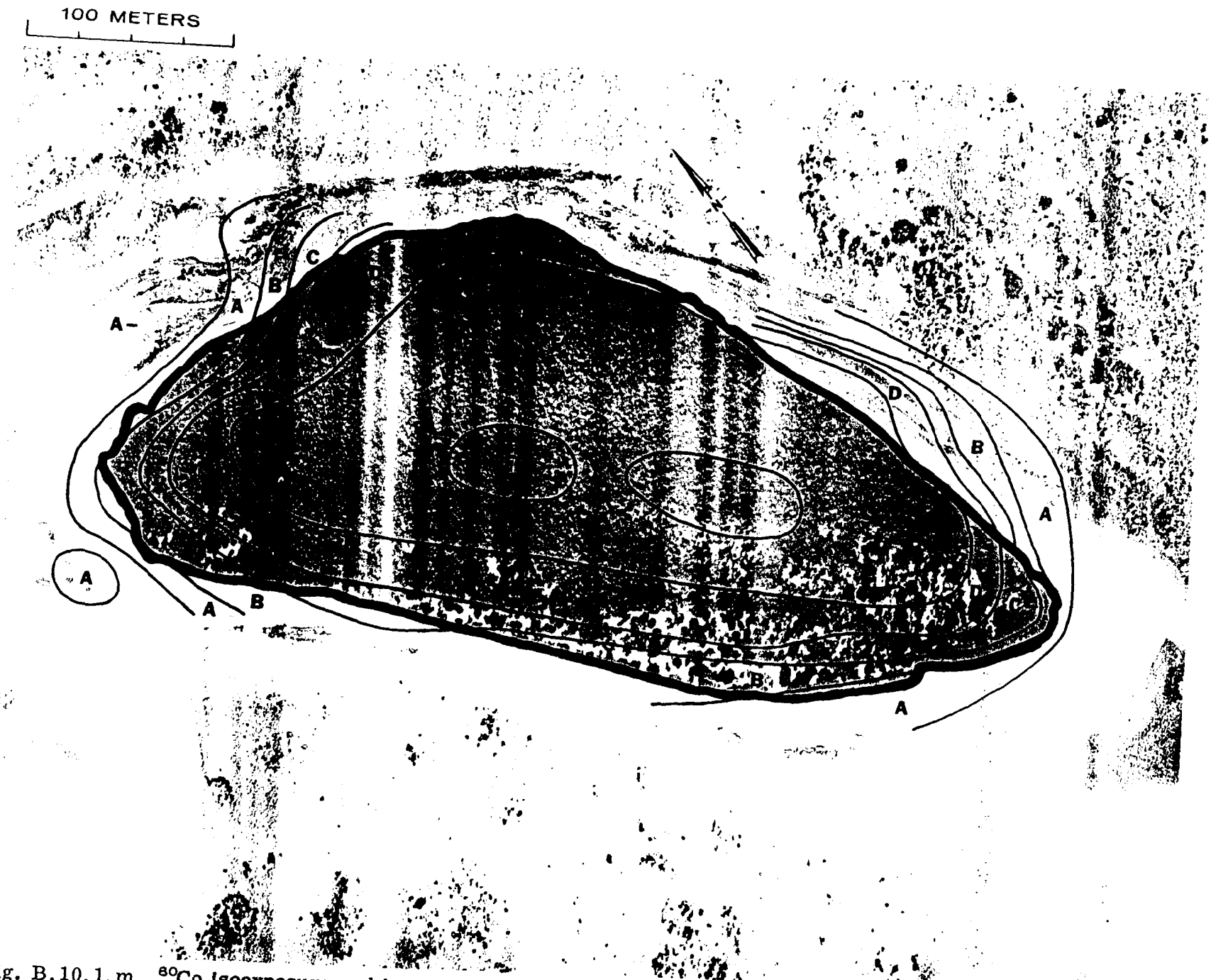

Fig. B.10.1.m. ^{60}Co isoexposure and isoconcentration contours. (Refer to alphabetic symbol key in this appendix.)

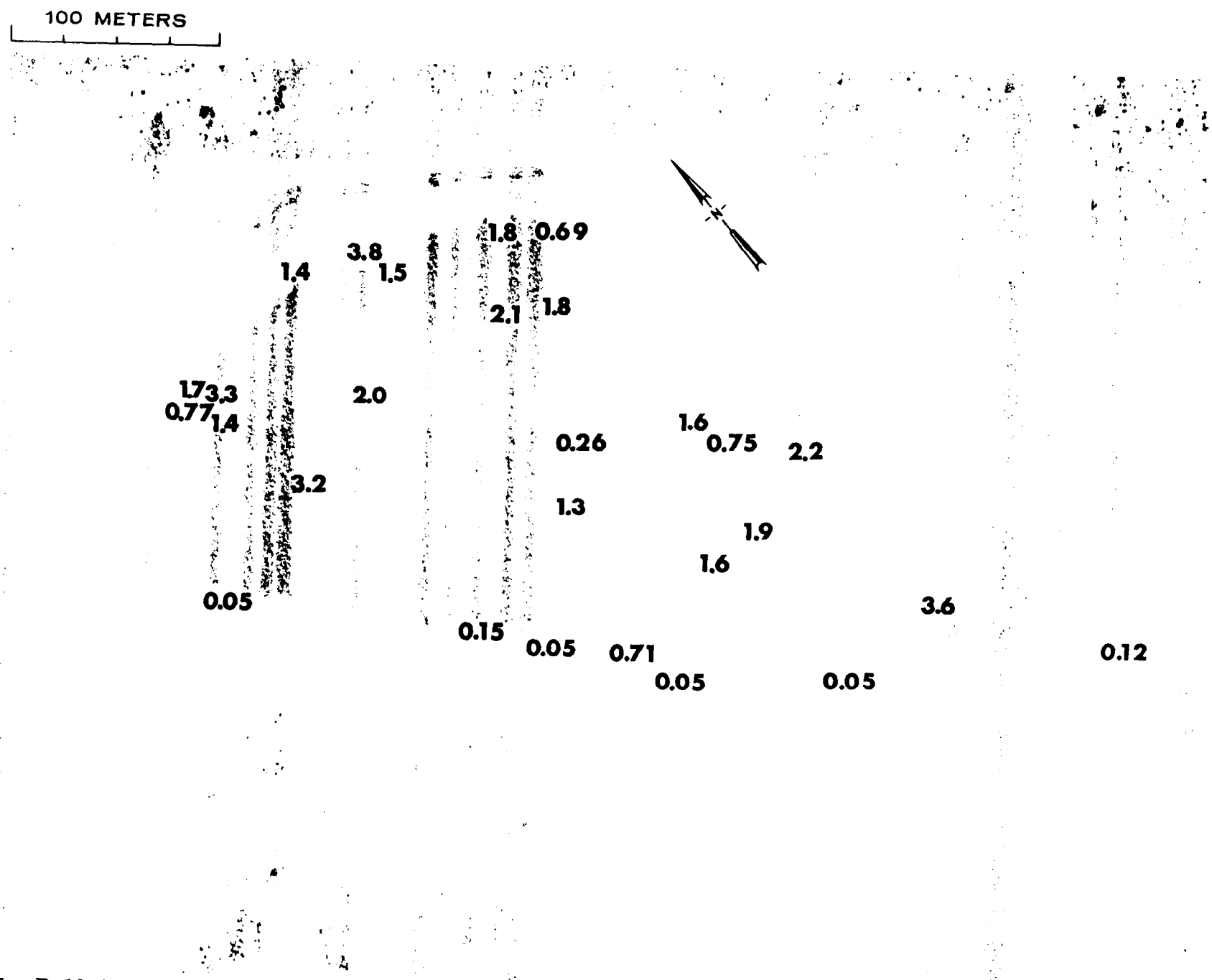

Fig. B.10.1.n. The average ^{60}Co activities (pCi/g) in soil samples collected to a depth of 15 cm.

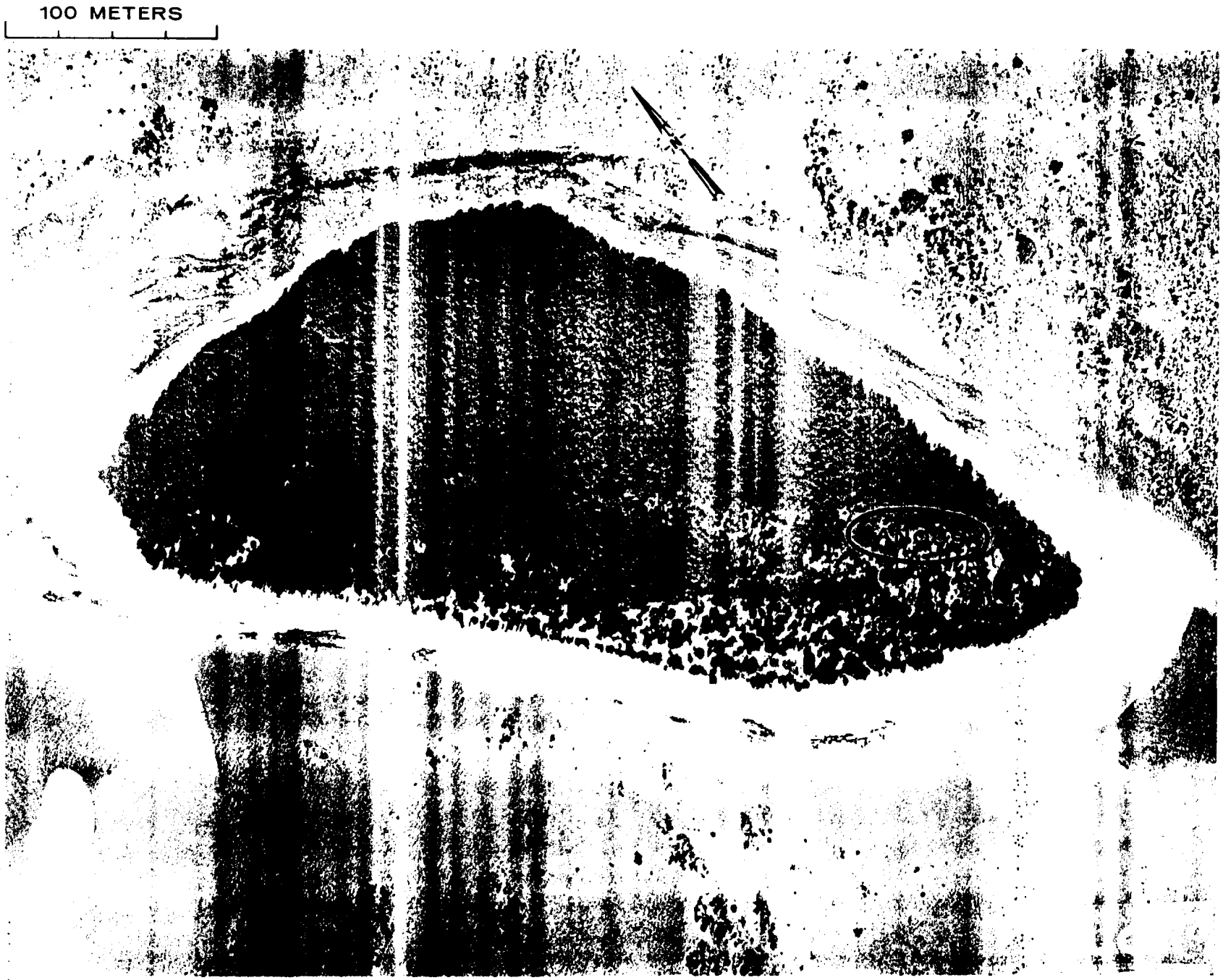

Fig. B.10.1.o. Terrestrial animal sample locations.

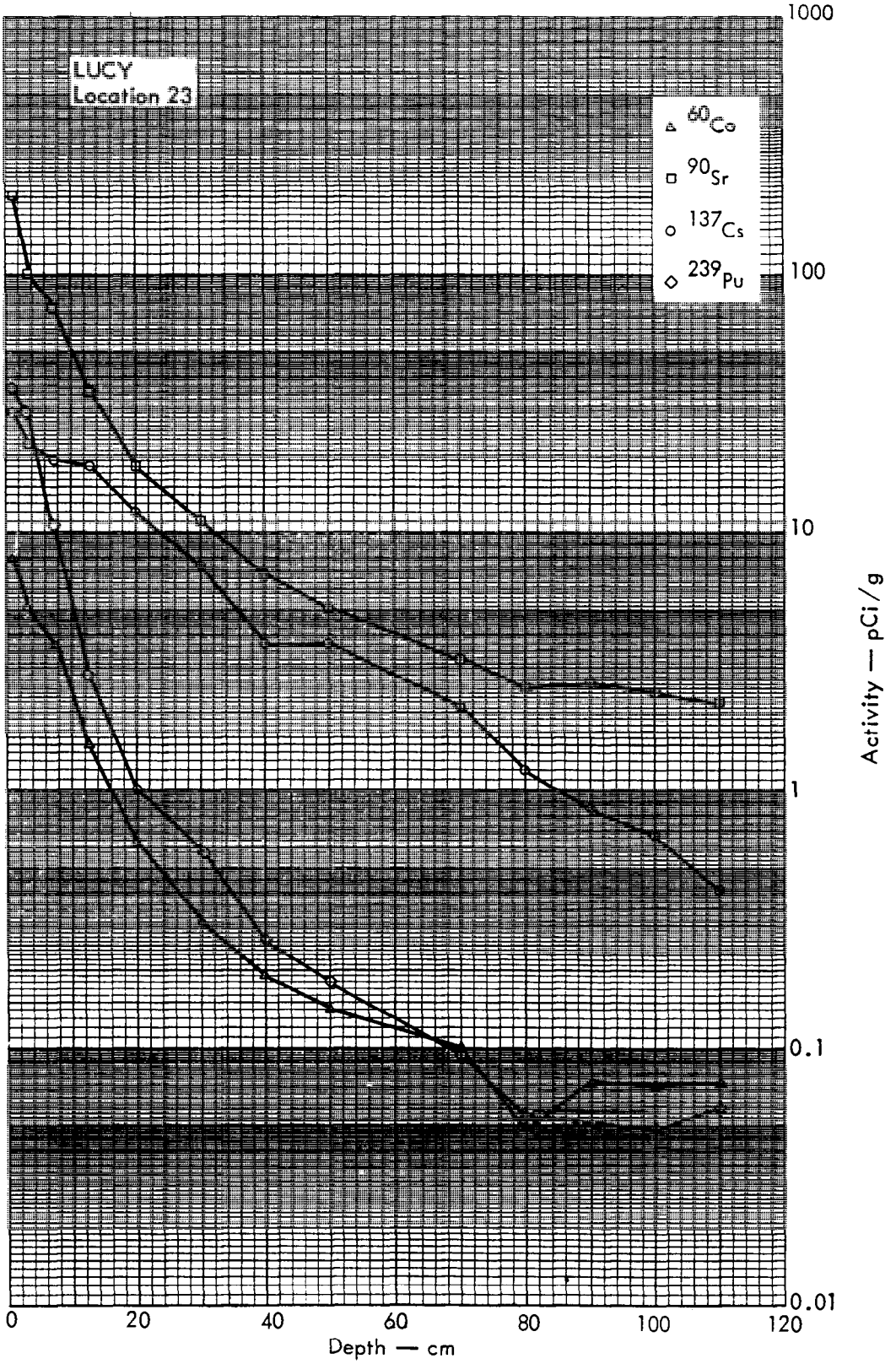

Fig. B.10.2a. Activities of selected radionuclides as a function of soil depth.

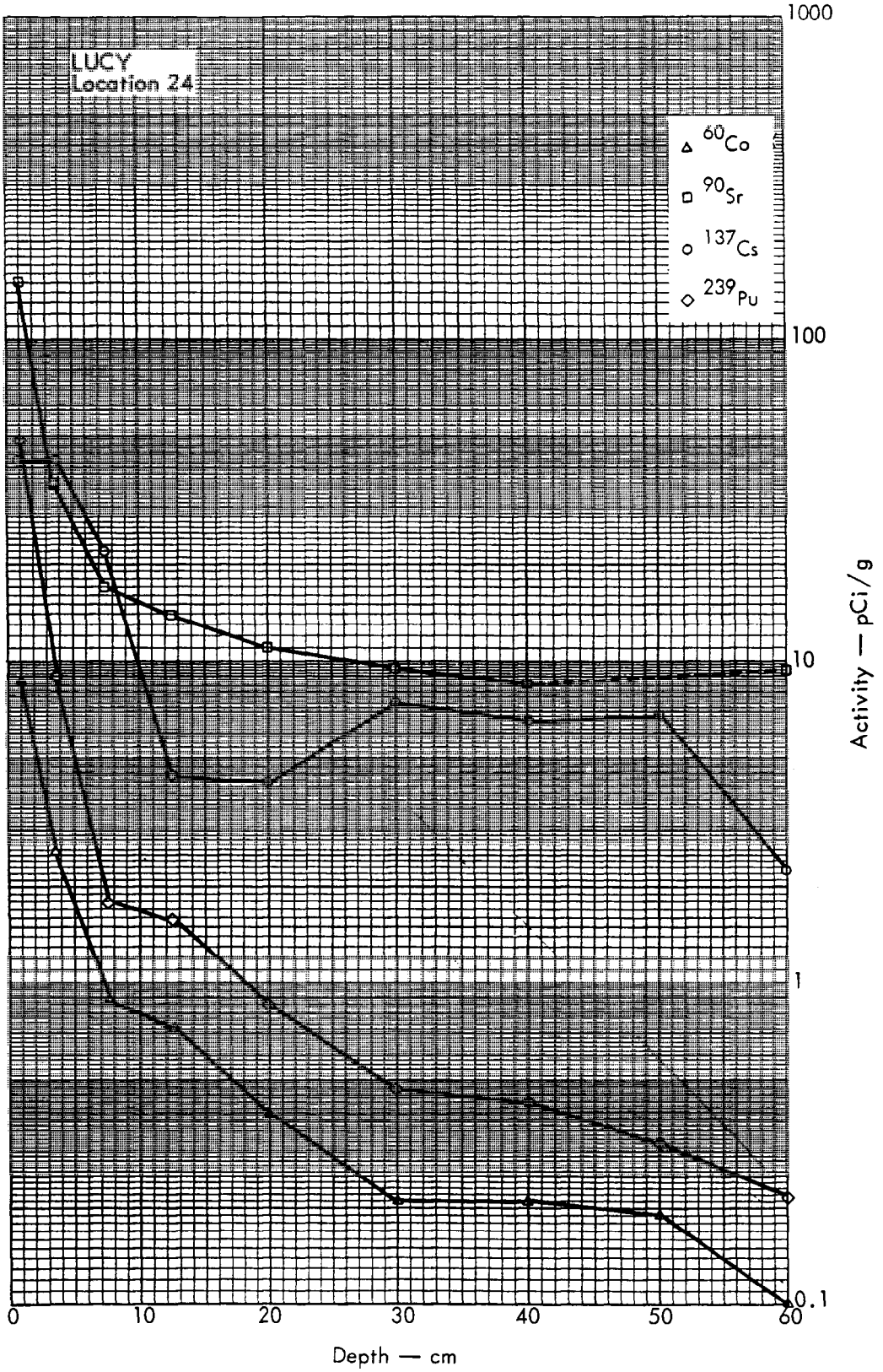

Fig. B.10.2b. Activities of selected radionuclides as a function of soil depth.

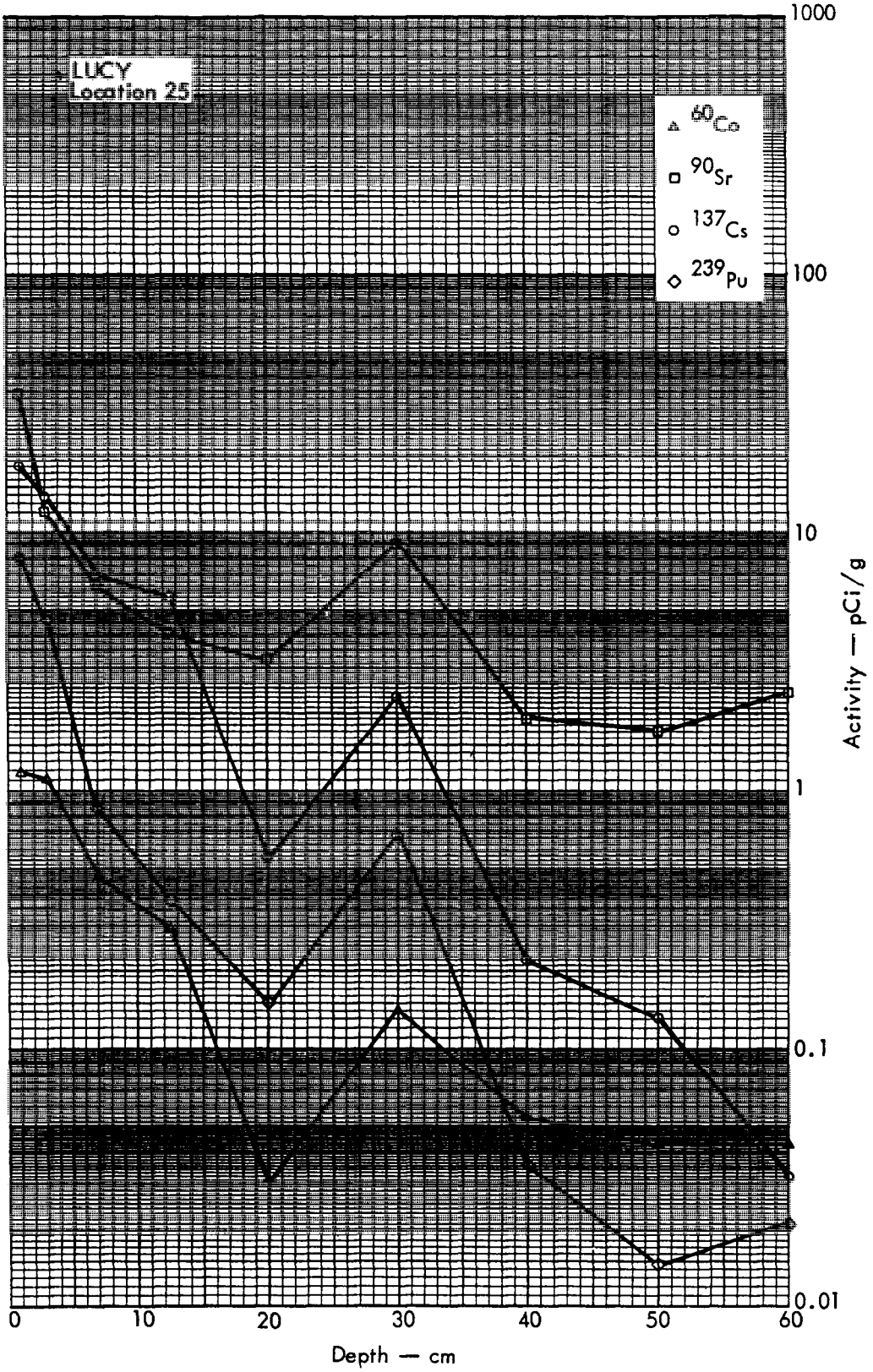

Fig. B.10.2c. Activities of selected radionuclides as a function of soil depth.

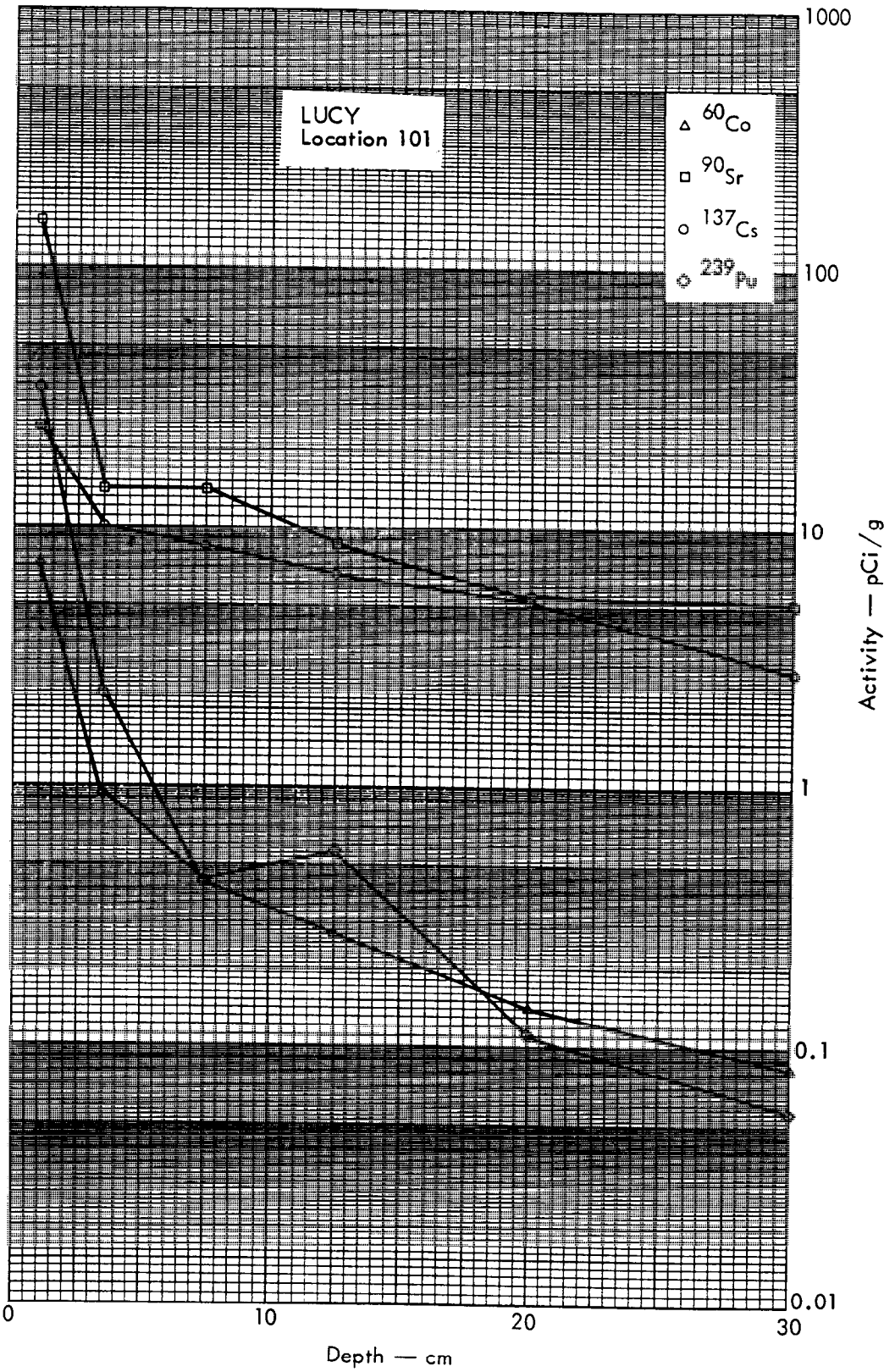

Fig. B.10.2d. Activities of selected radionuclides as a function of soil depth.

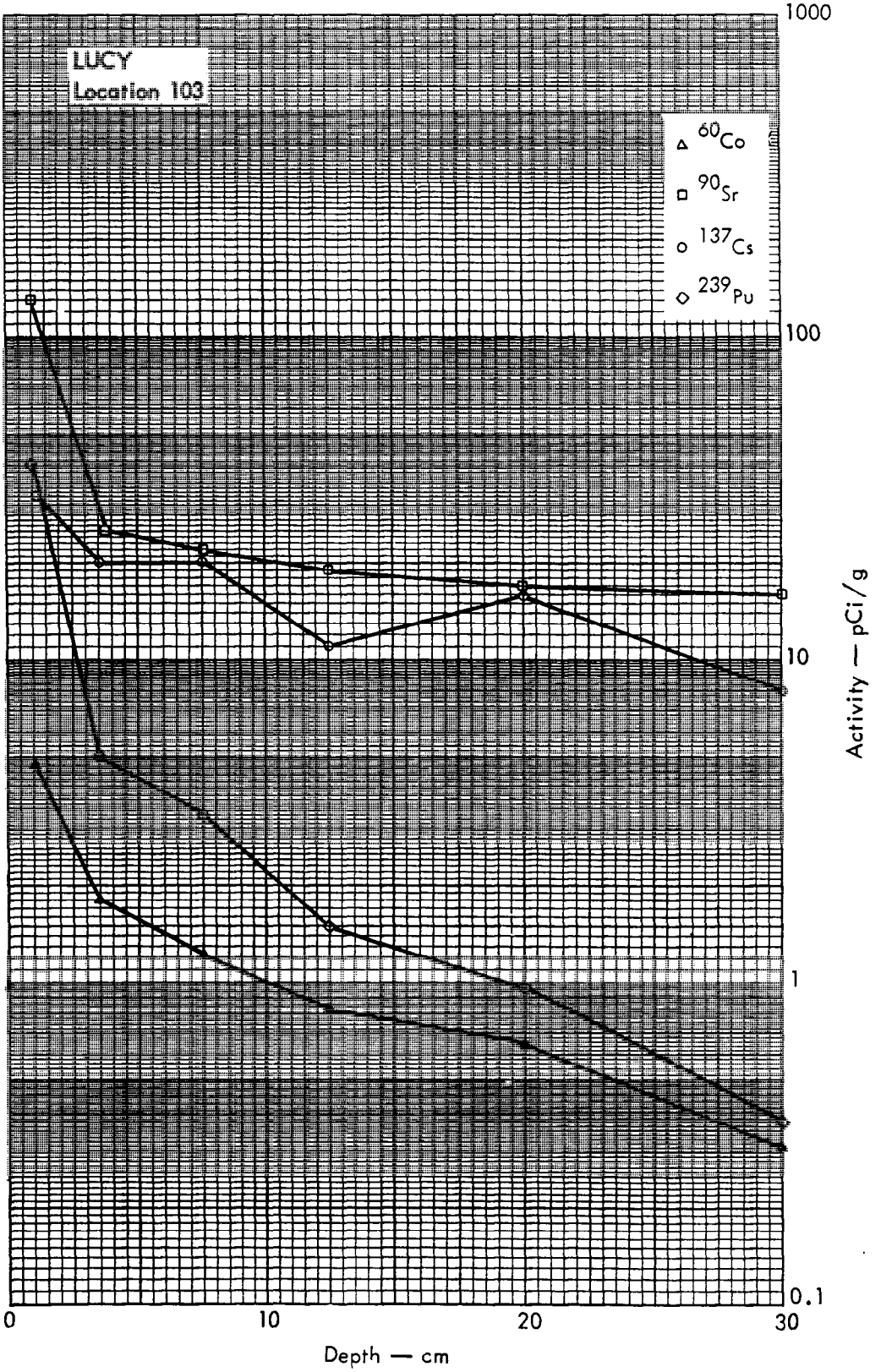

Fig. B.10.2e. Activities of selected radionuclides as a function of soil depth.

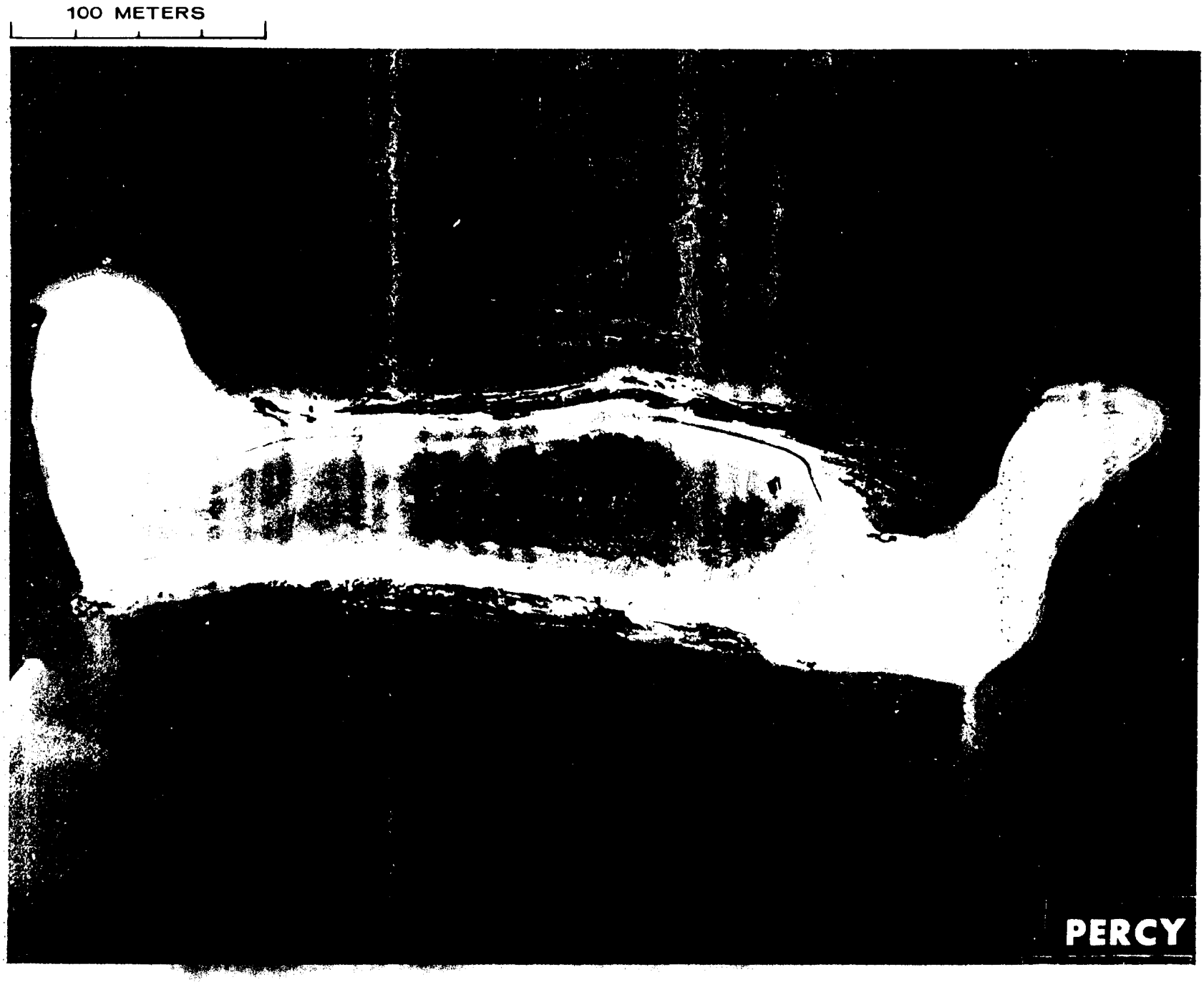

Fig. B.11.1.a.

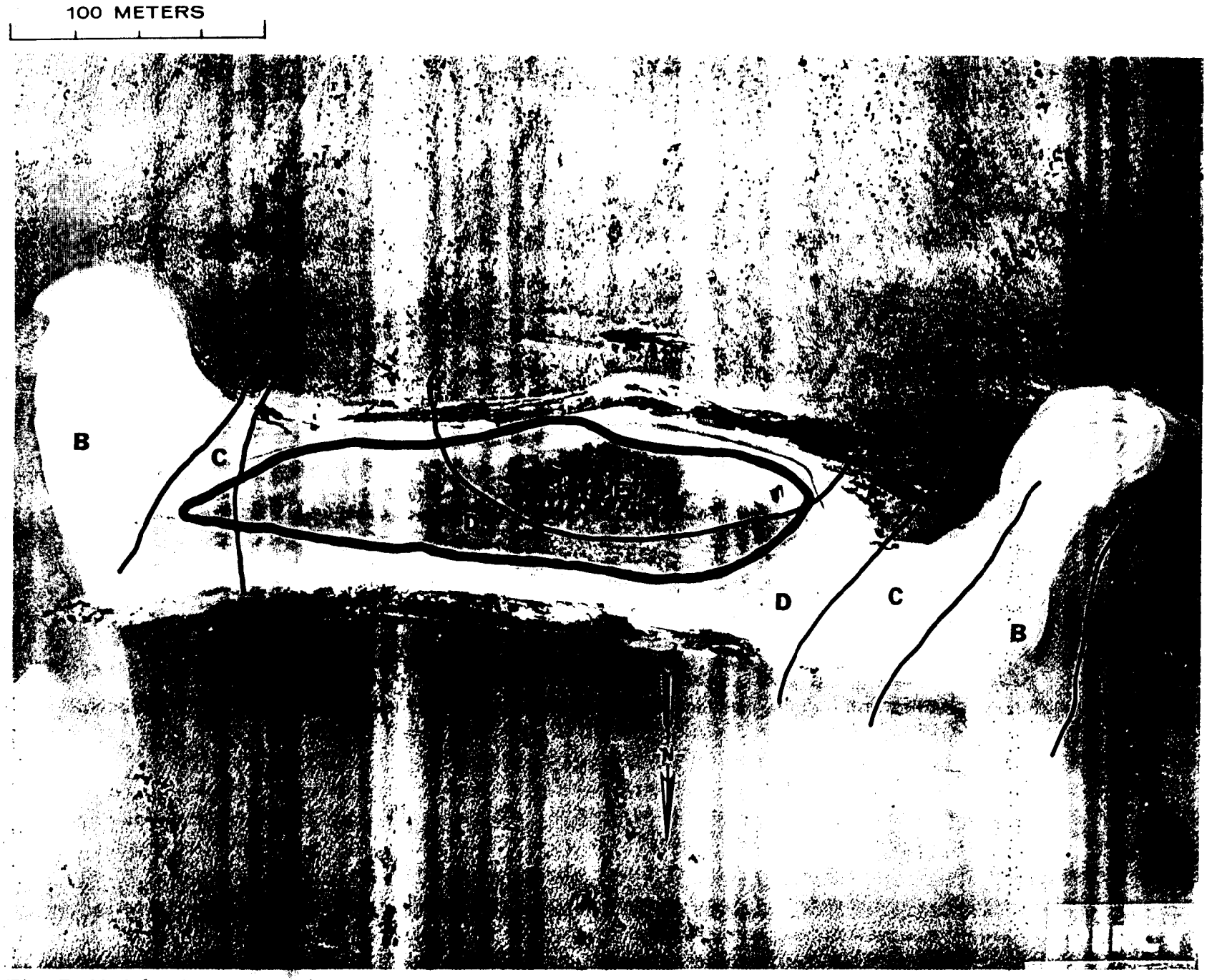

Fig. B.11.1.b. Gross count isoexposure contours. (Refer to alphabetic symbol key in this appendix.)

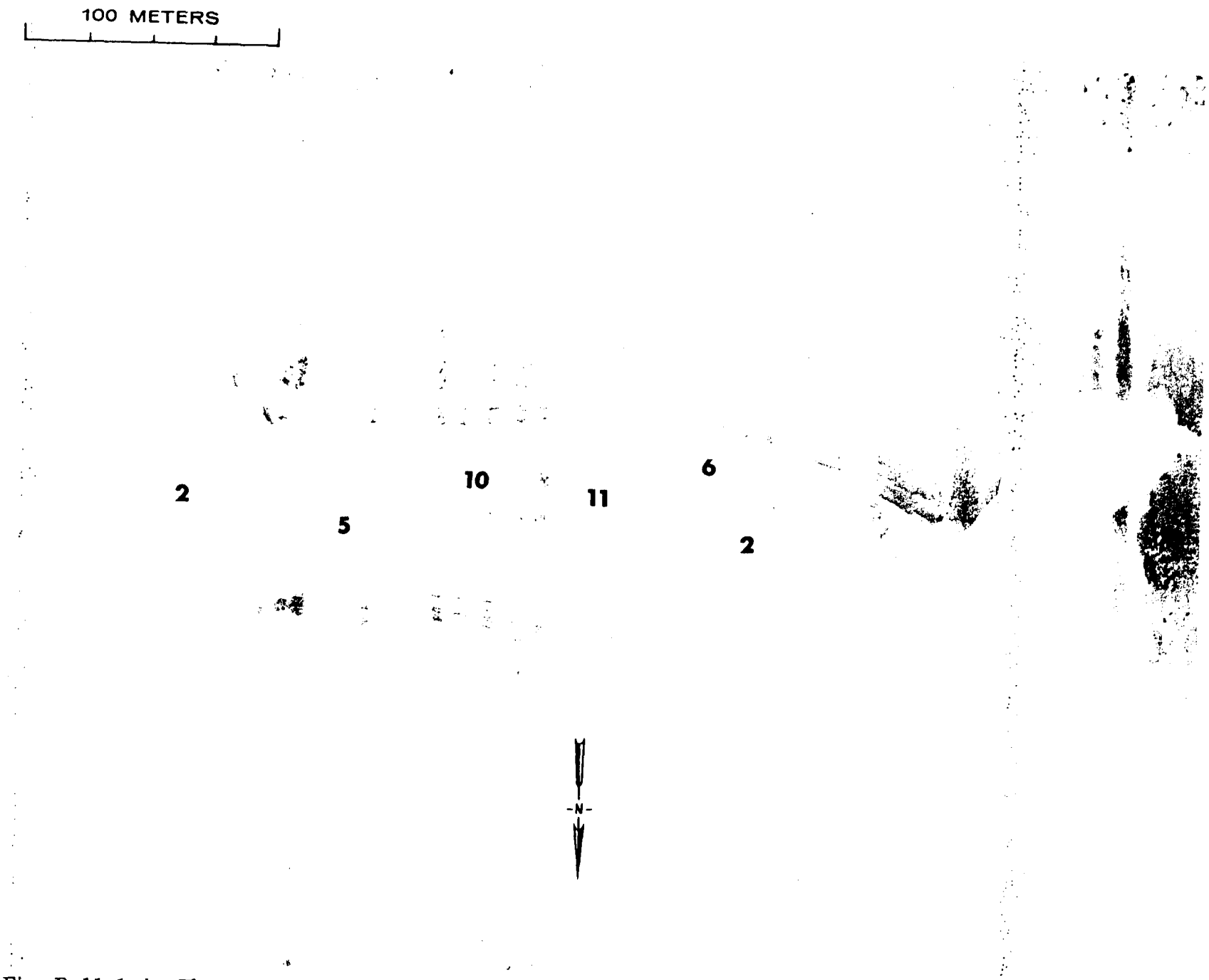

Fig. B.11.1.d. The gamma background exposure rate (μR/hr) at 1 m above the ground, measured with a portable NaI scintillation counter.

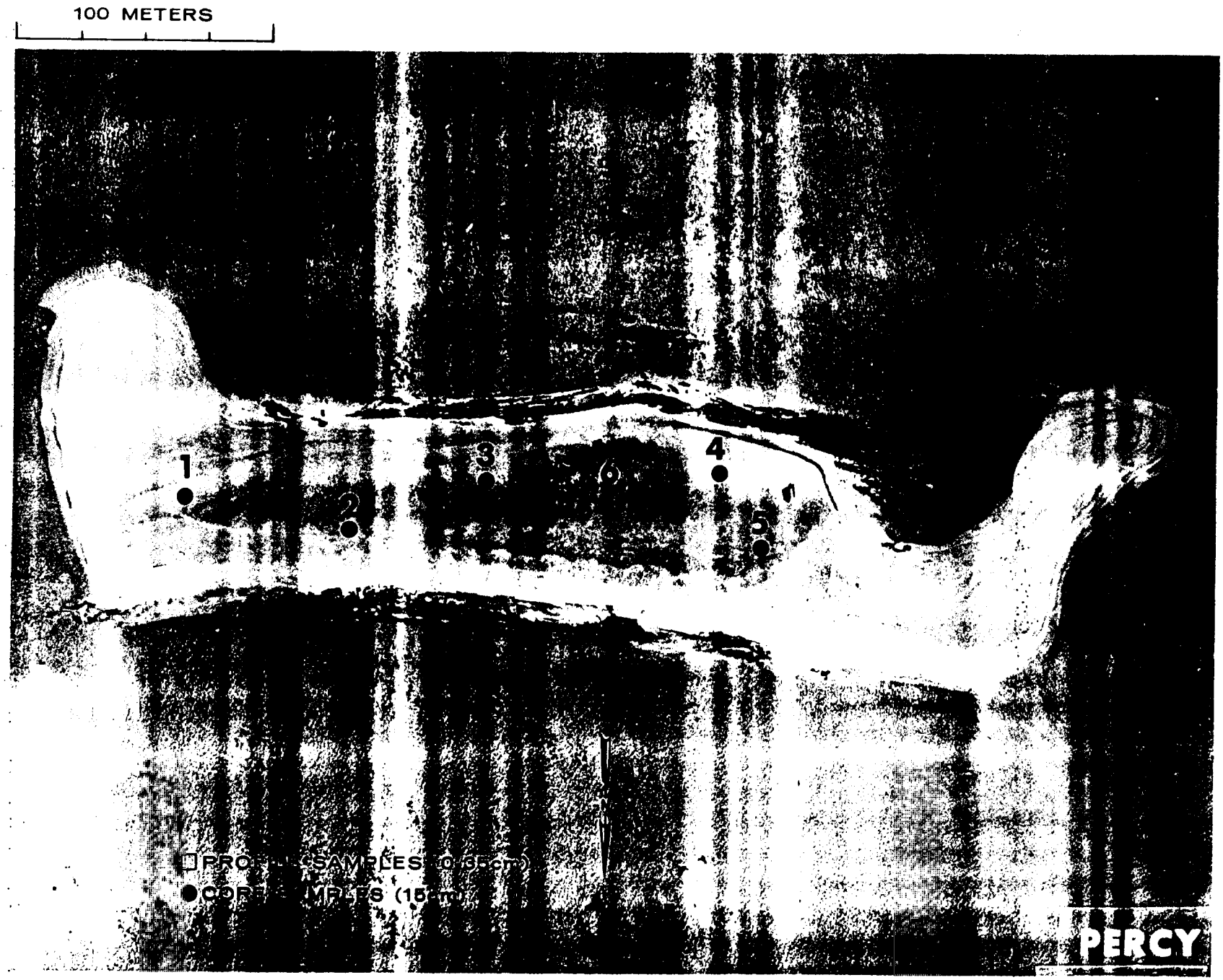

Fig. B.11.1.f. Soil-sample locations.

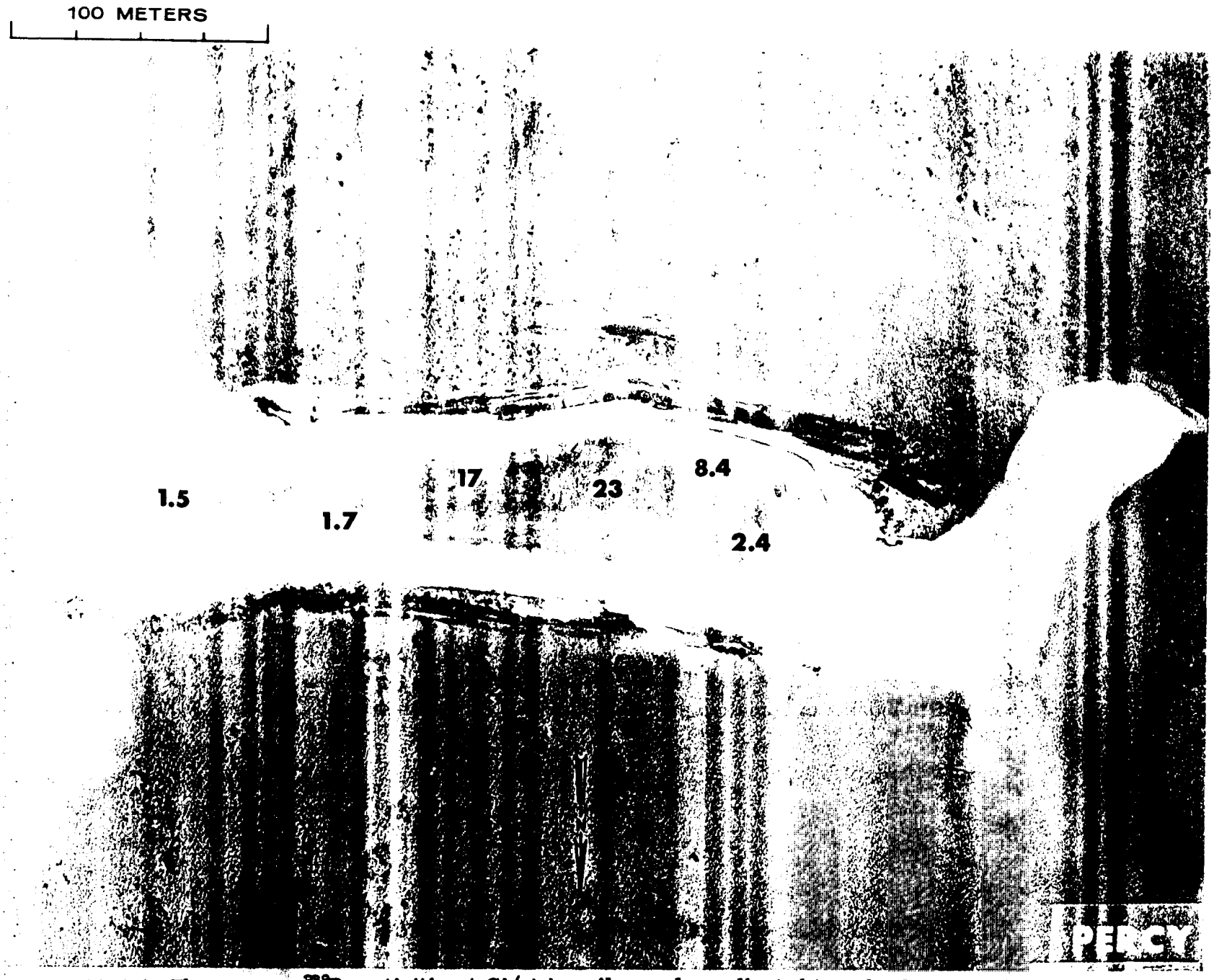

Fig. B.11.1.i. The average ^{239}Pu activities (pCi/g) in soil samples collected to a depth of 15 cm.

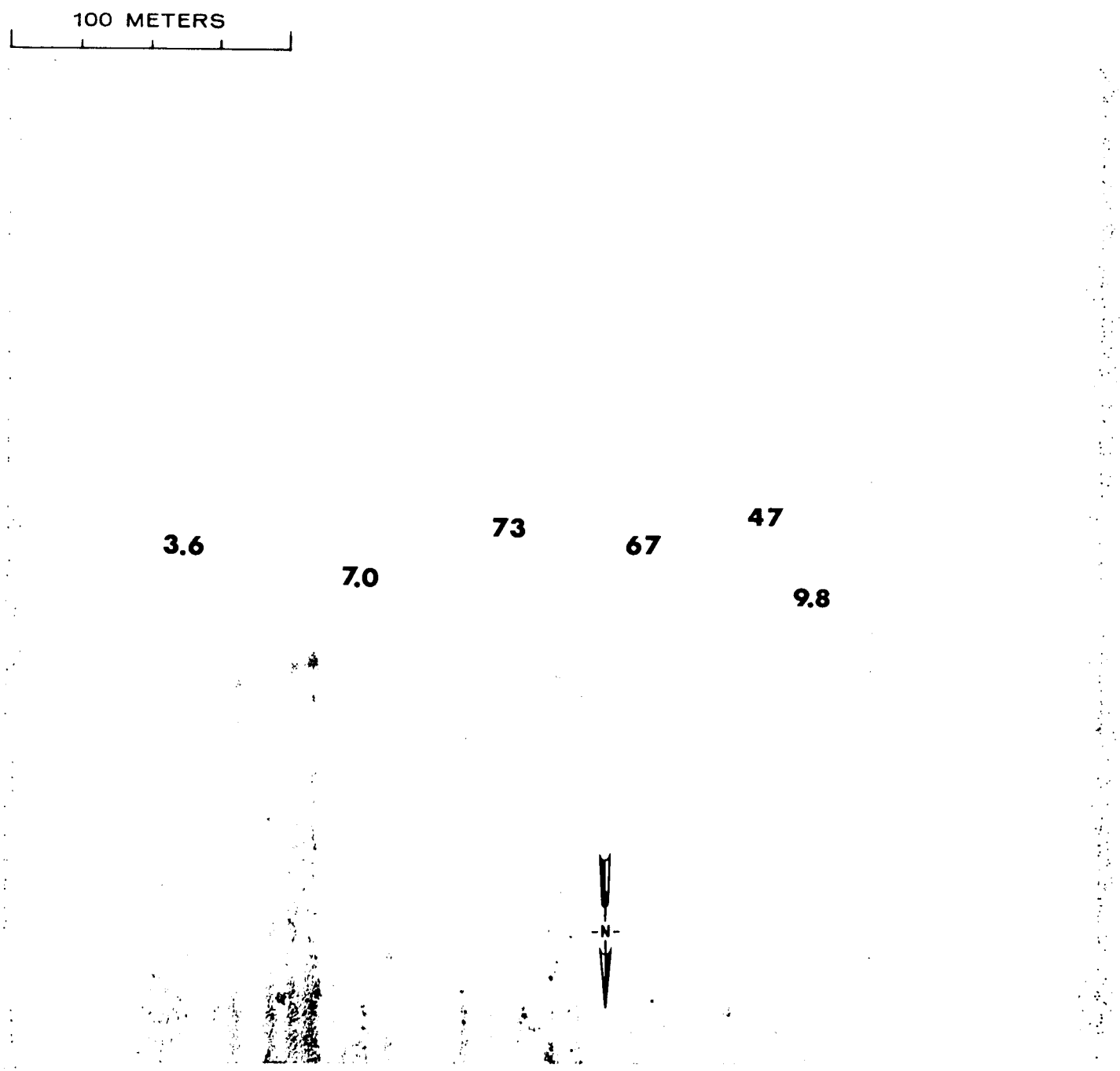

Fig. B.11.1.j. The average ^{90}Sr activities (pCi/g) in soil samples collected to a depth of 15 cm.

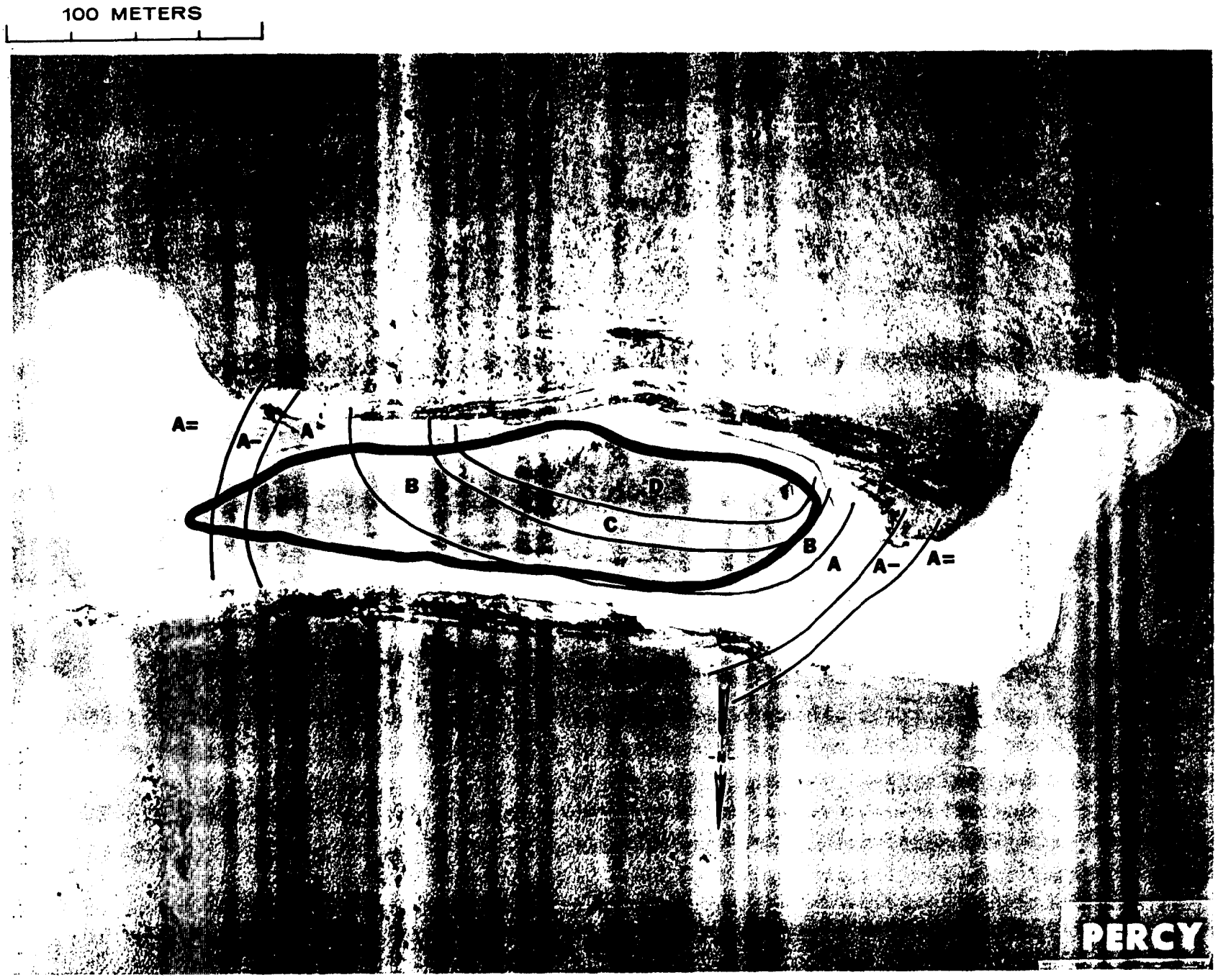

Fig. B.11.1.k. ^{137}Cs isoexposure and isoconcentration contours. (Refer to alphabetic symbol key in this appendix.)

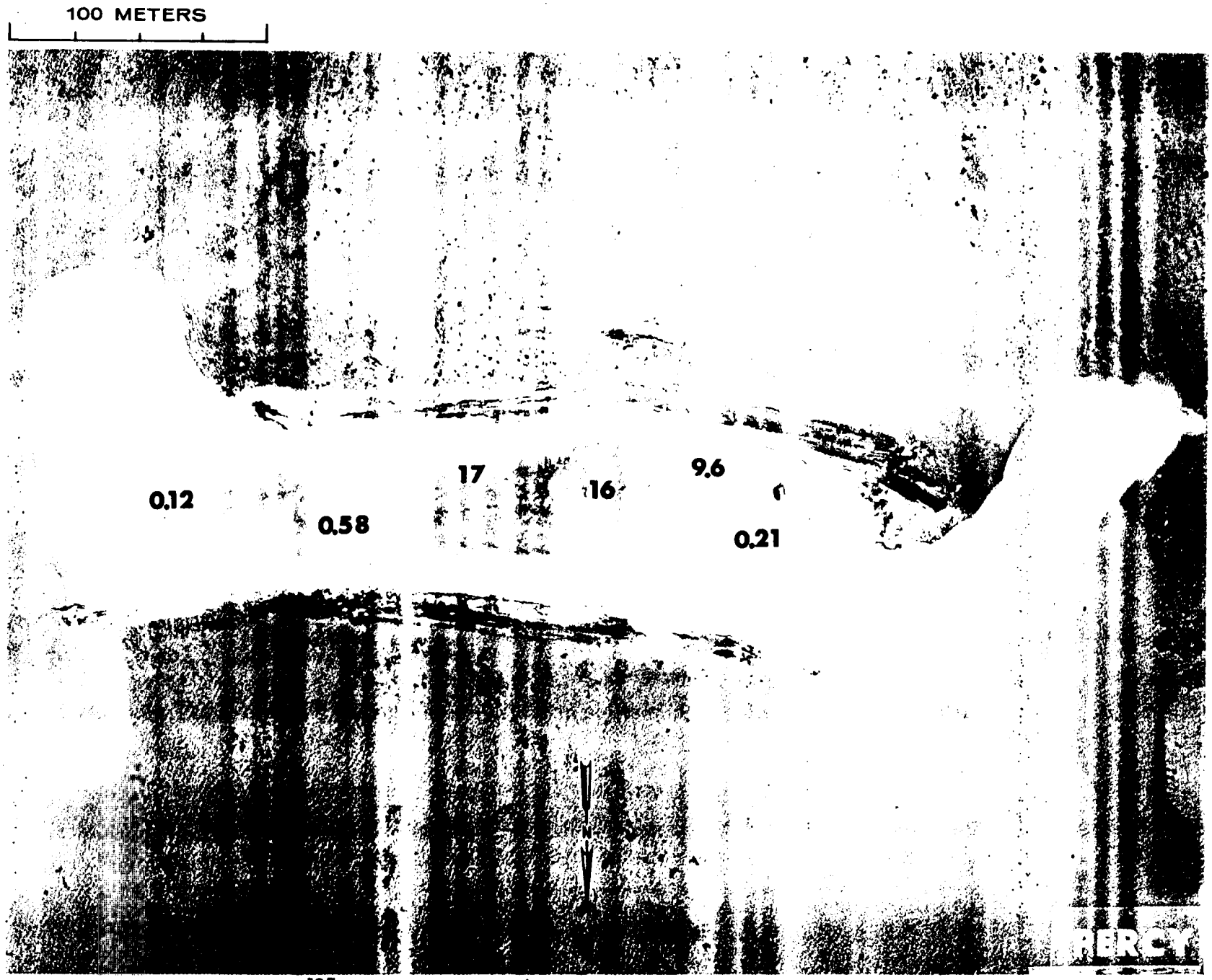

Fig. B.11.1.1. The average ^{137}Cs activities (pCi/g) in soil samples collected to a depth of 15 cm.

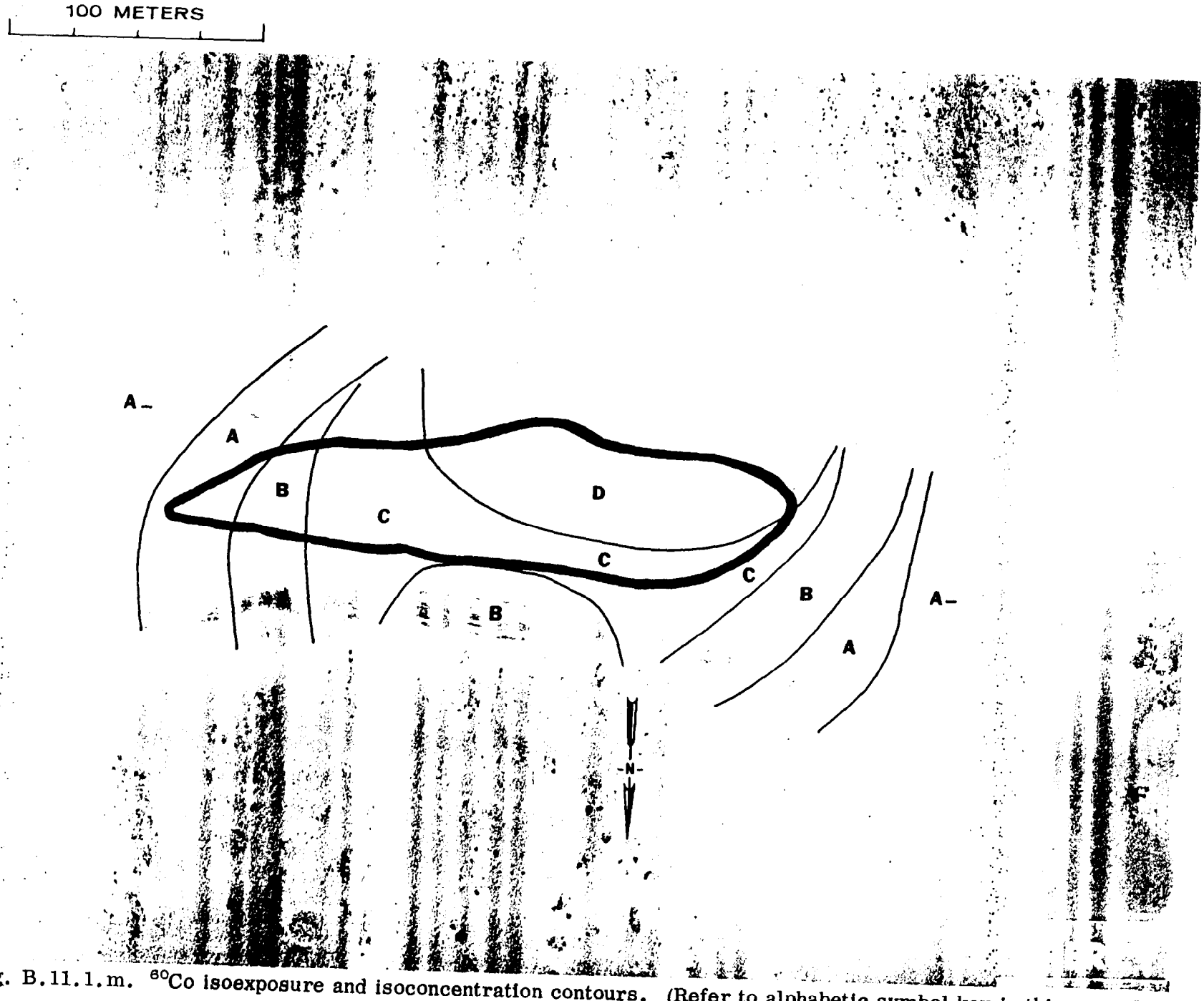

Fig. B.11.1.m. ^{60}Co isoexposure and isoconcentration contours. (Refer to alphabetic symbol key in this appendix.)

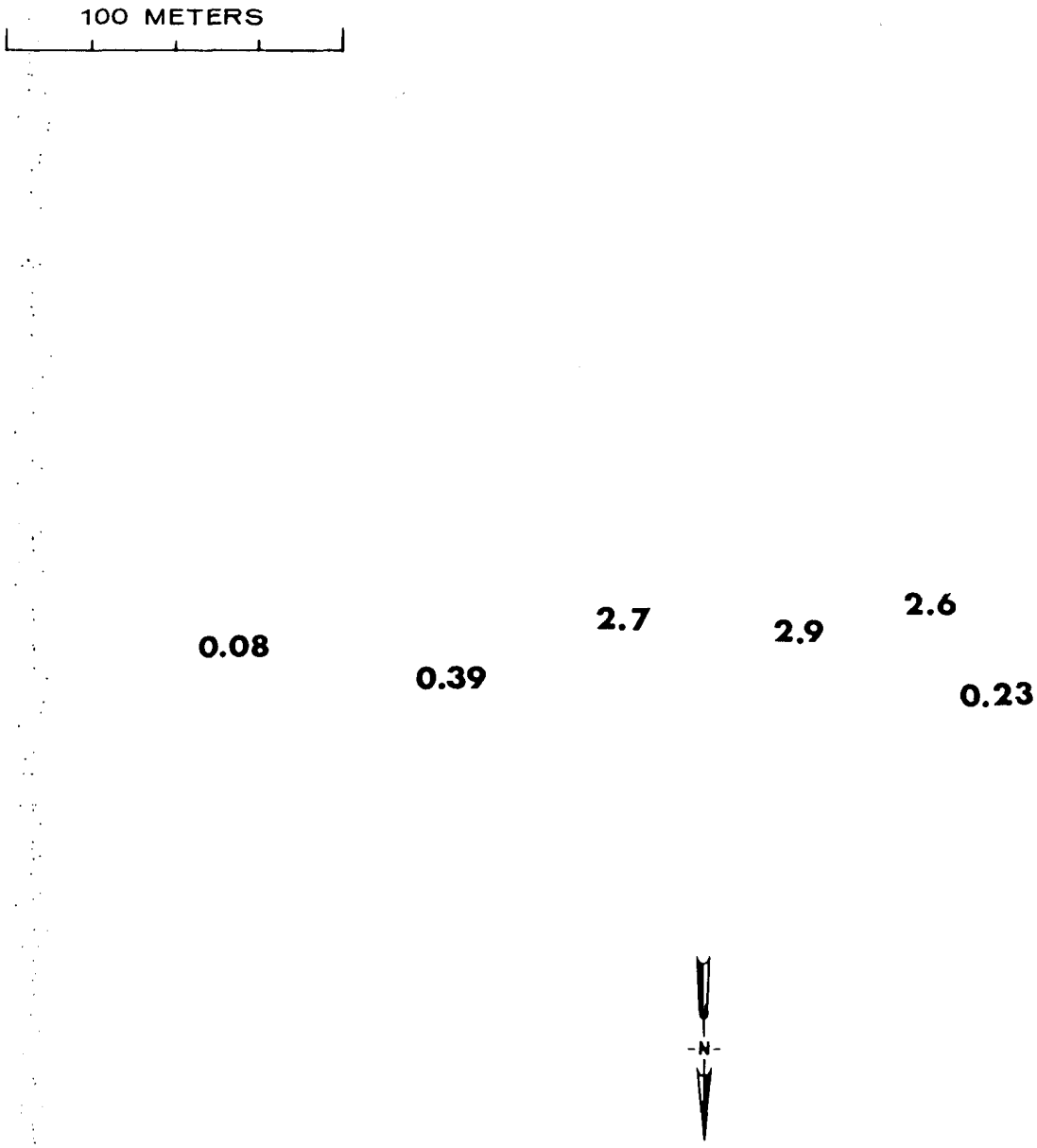

Fig. B.11.1.n. The average ^{60}Co activities (pCi/g) in soil samples collected to a depth of 15 cm.

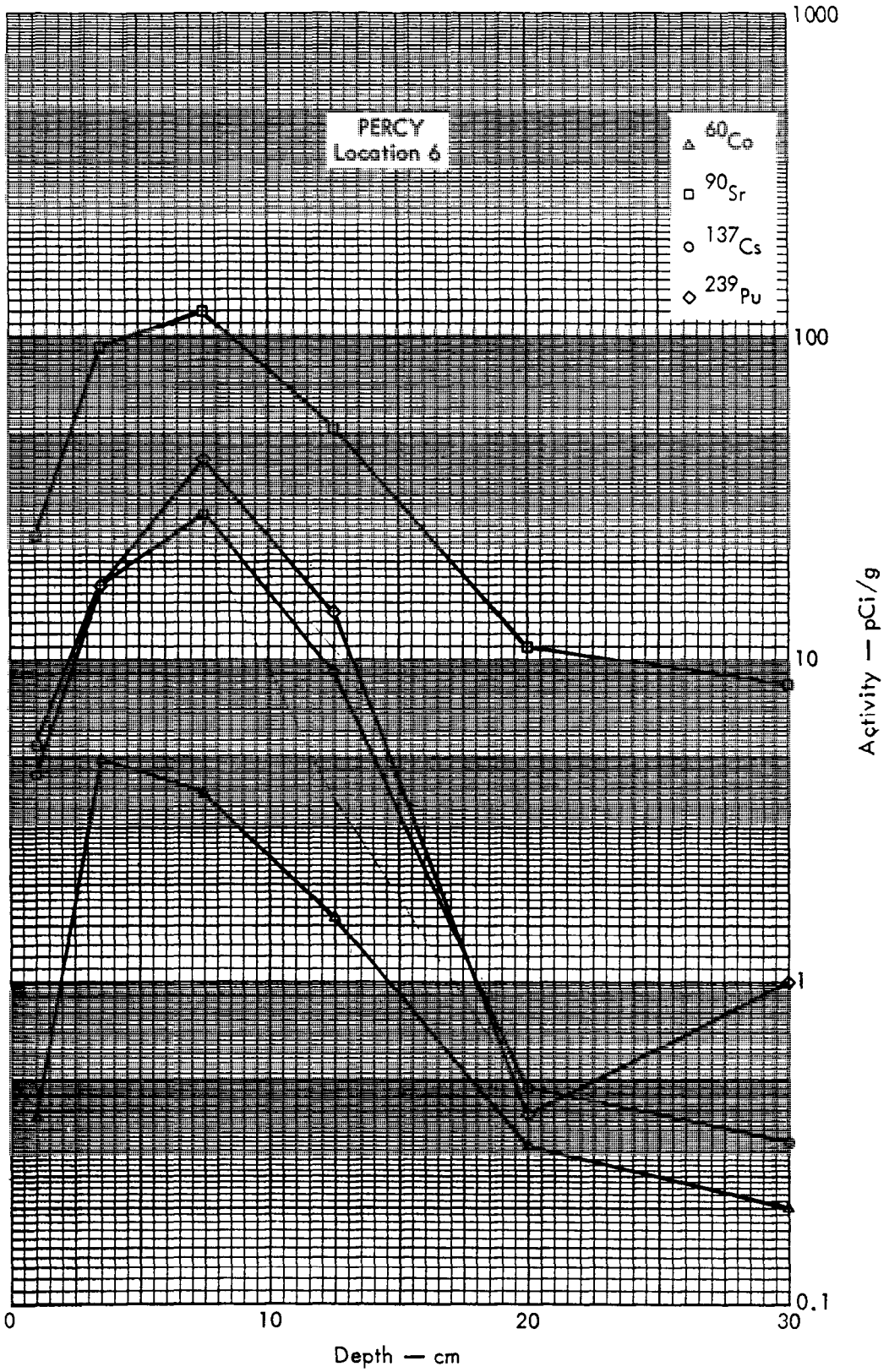

Fig. B.11.2a. Activities of selected radionuclides as a function of soil depth.

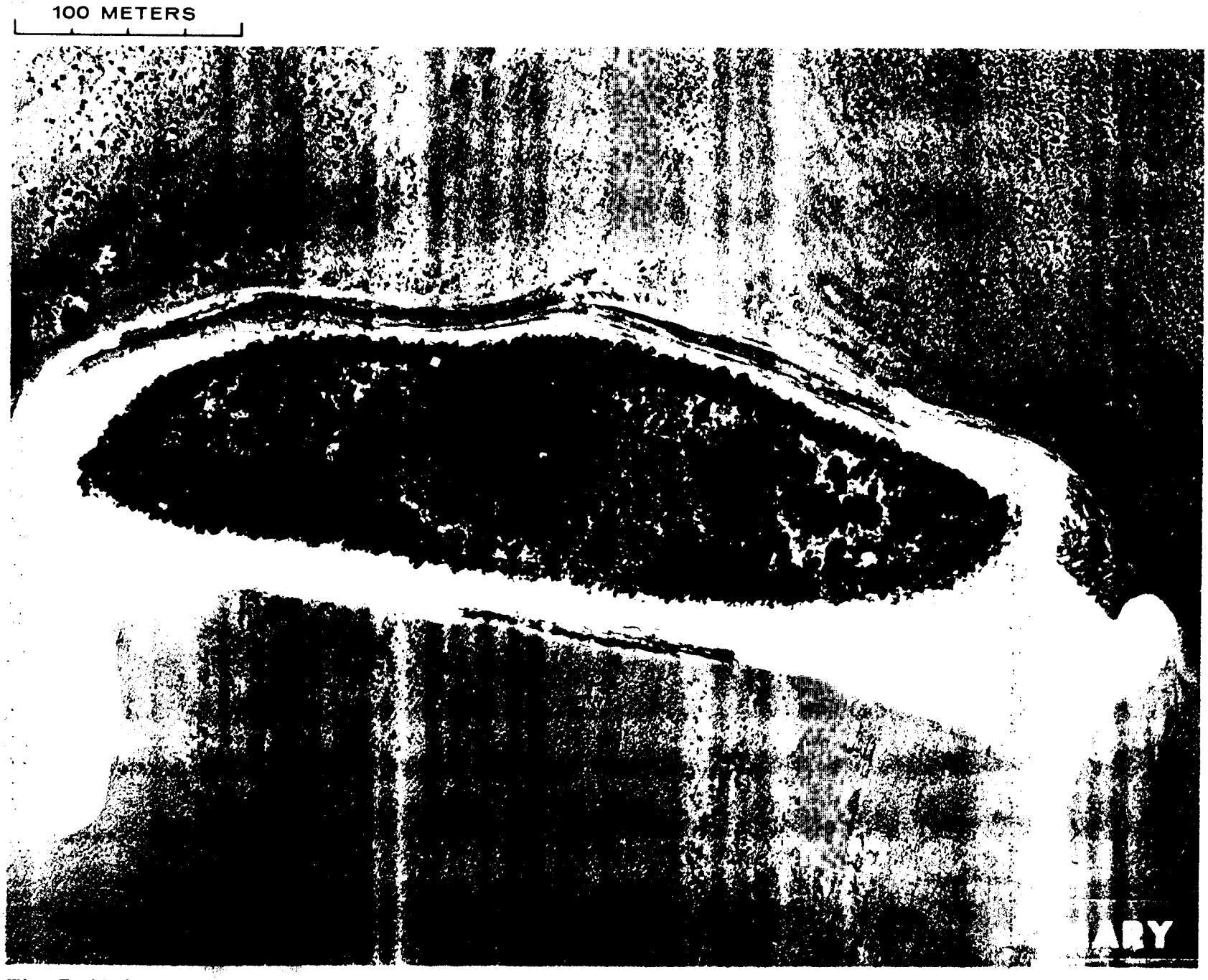

Fig. B.12.1.a.

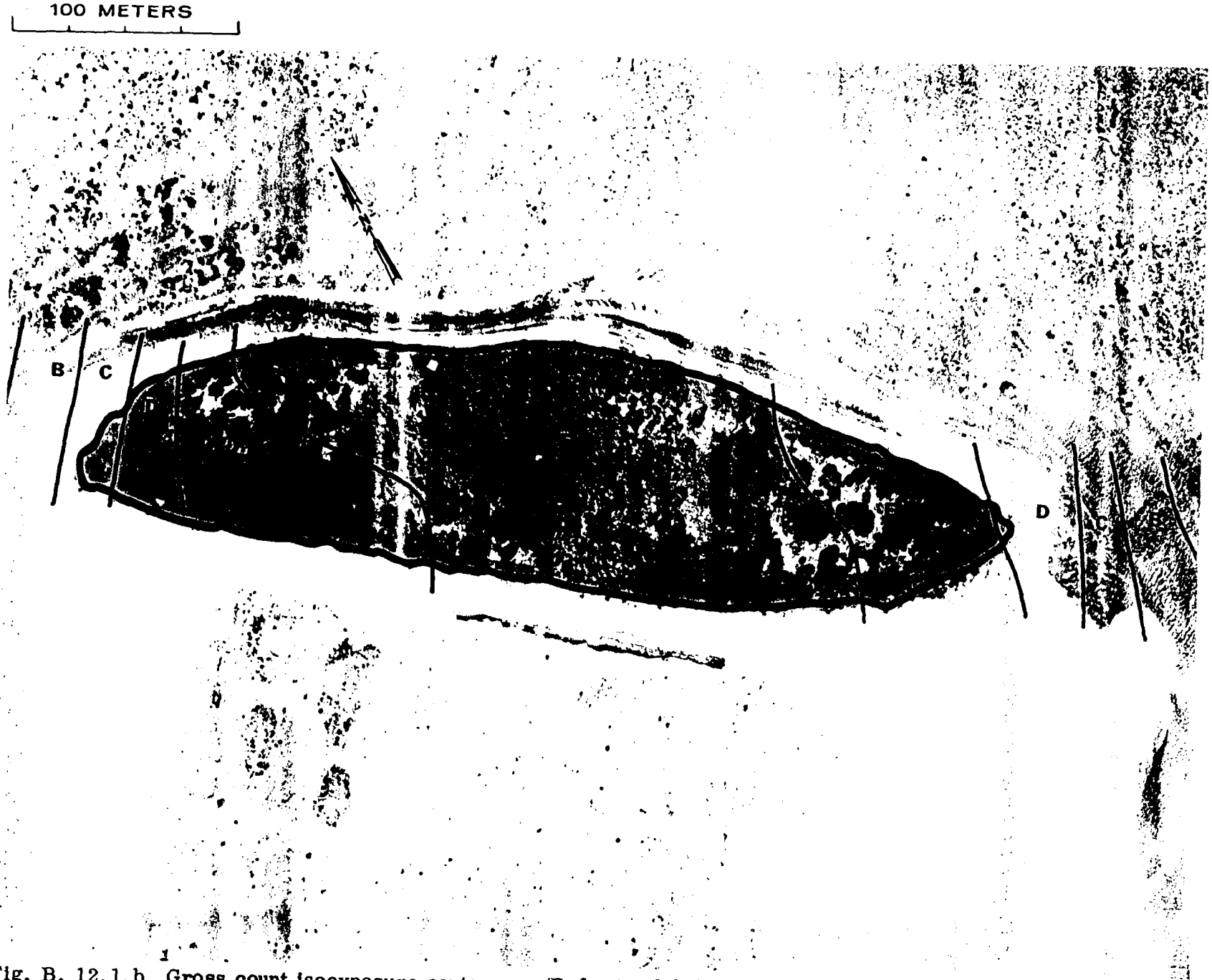

Fig. B. 12.1.b. Gross count isoexposure contours. (Refer to alphabetic symbol key in this appendix.)

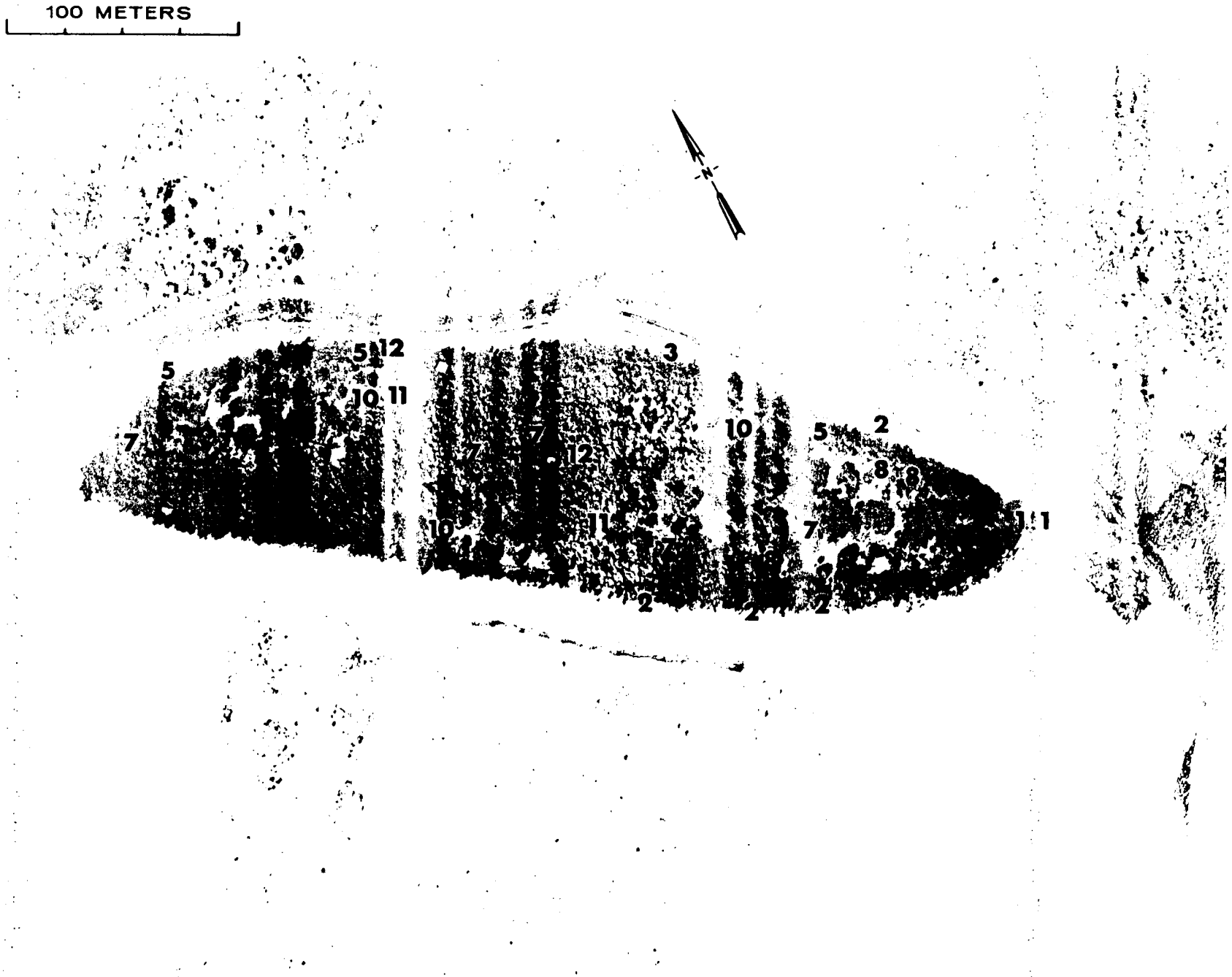

Fig. B.12.1.d. The gamma background exposure rate (μR/hr) at 1 m above the ground, measured with a portable NaI scintillation counter.

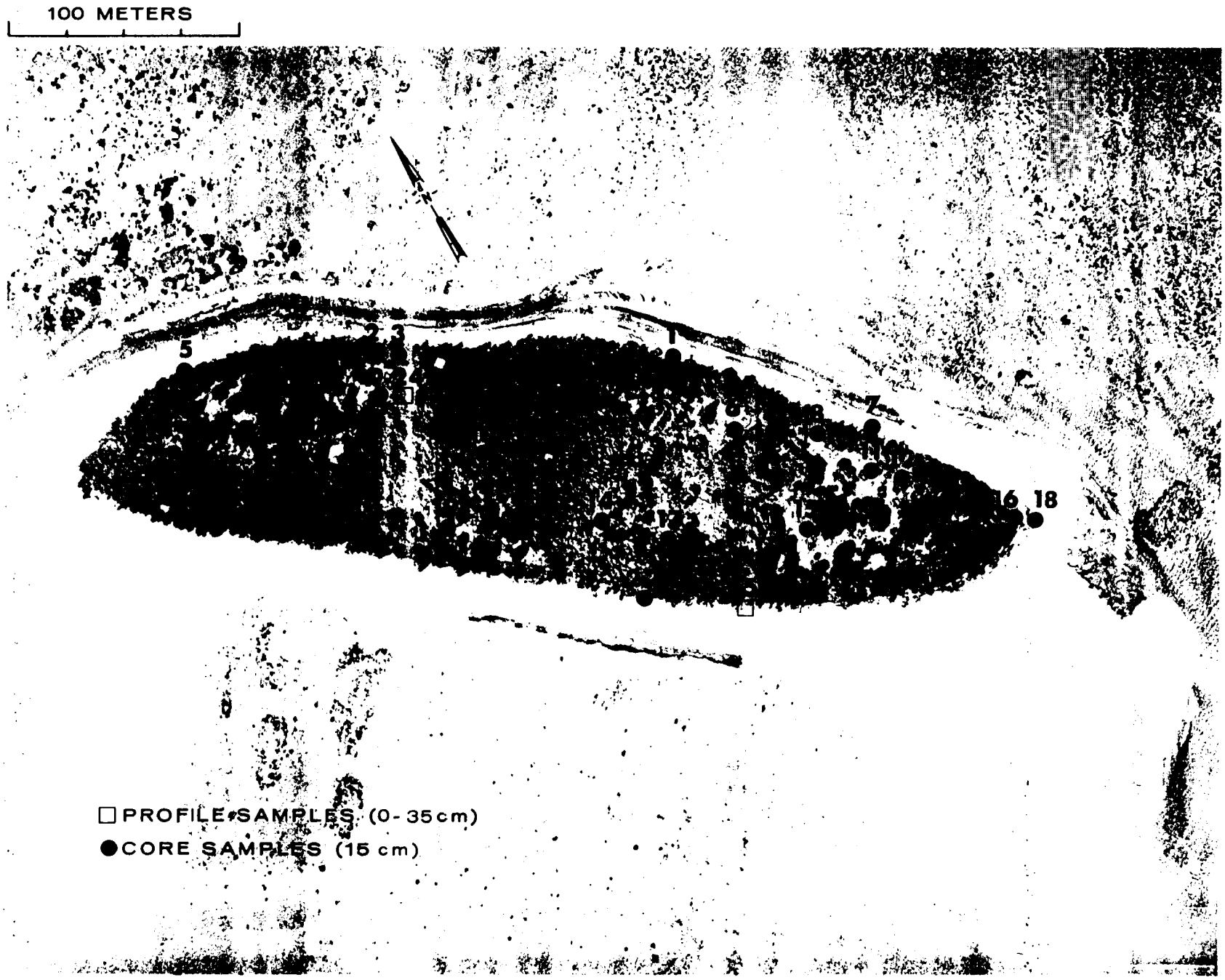

Fig. B.12.1.f. Soil-sample locations.

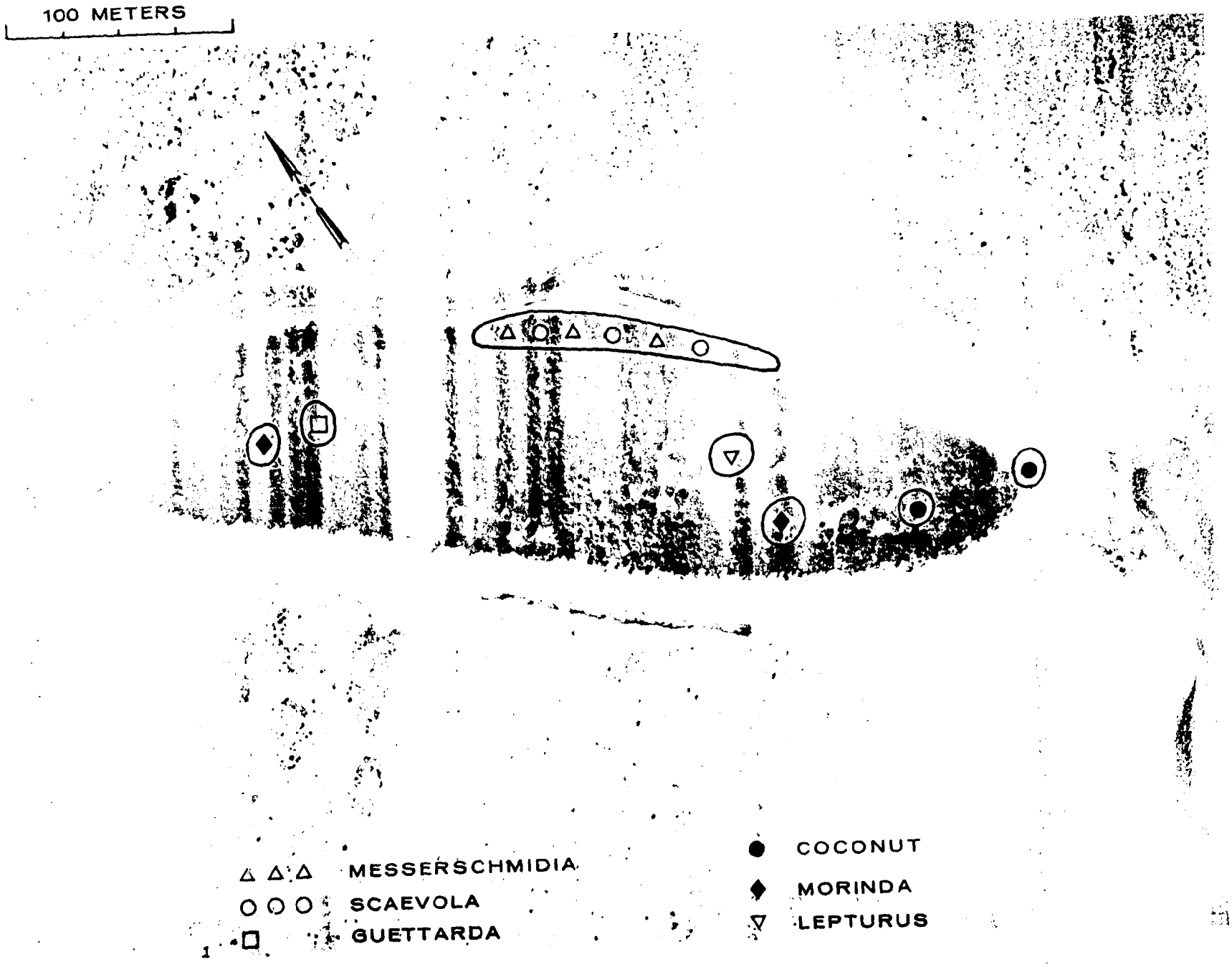

Fig. B.12.1.g. Vegetation sample locations.

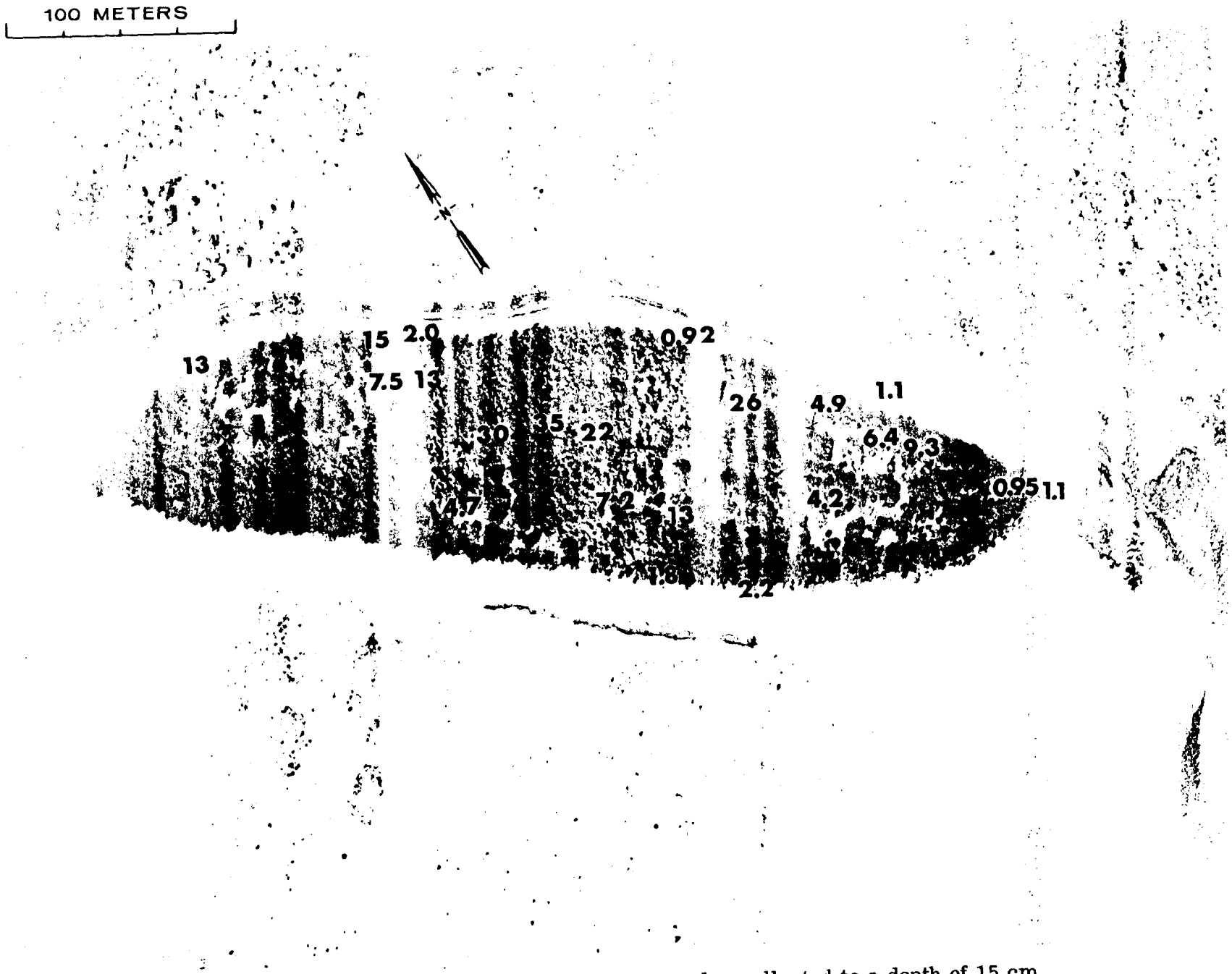

Fig. B.12.1.i. The average ^{239}Pu activities (pCi/g) in soil samples collected to a depth of 15 cm.

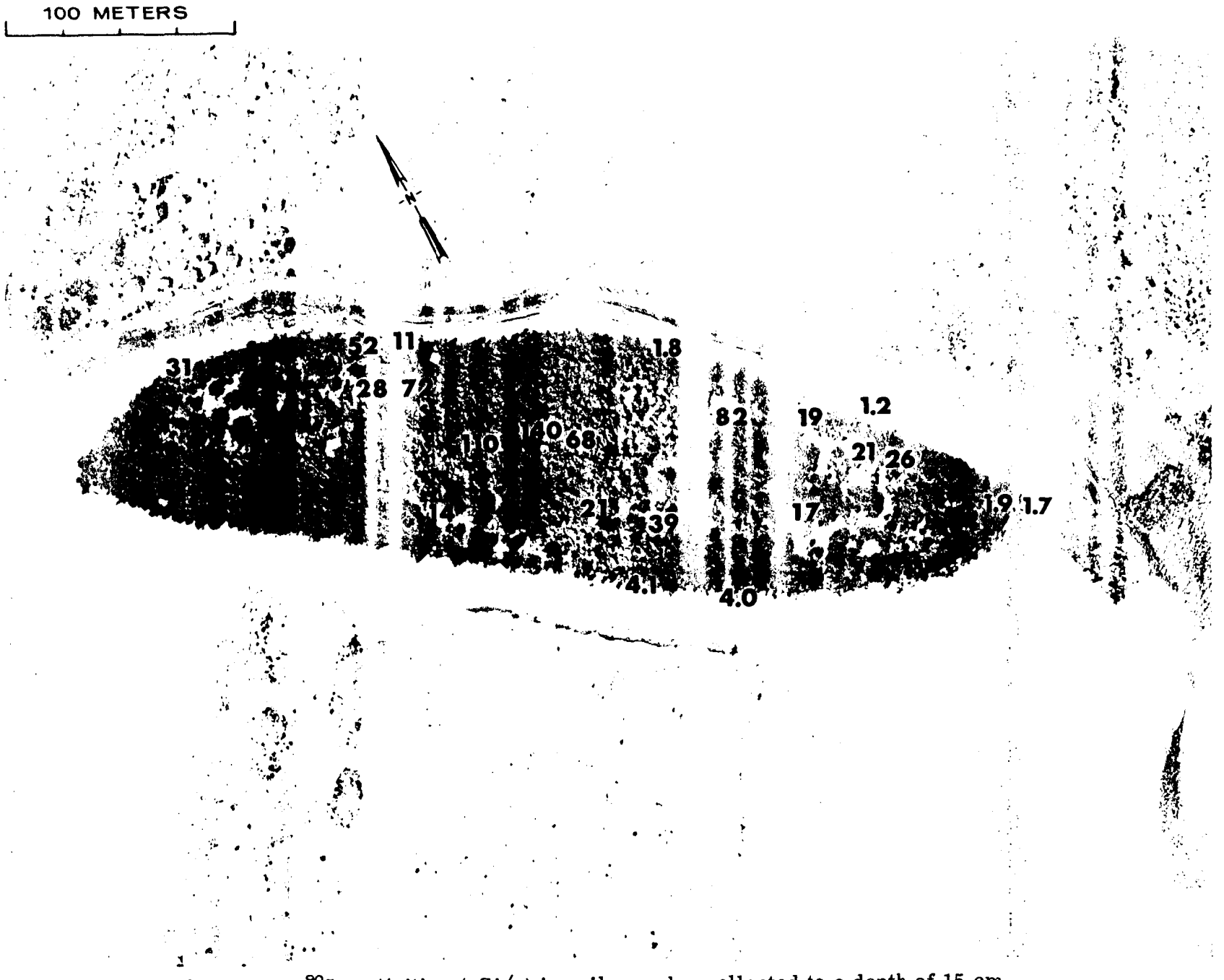

Fig. B.12.1.j. The average ^{90}Sr activities (pCi/g) in soil samples collected to a depth of 15 cm.

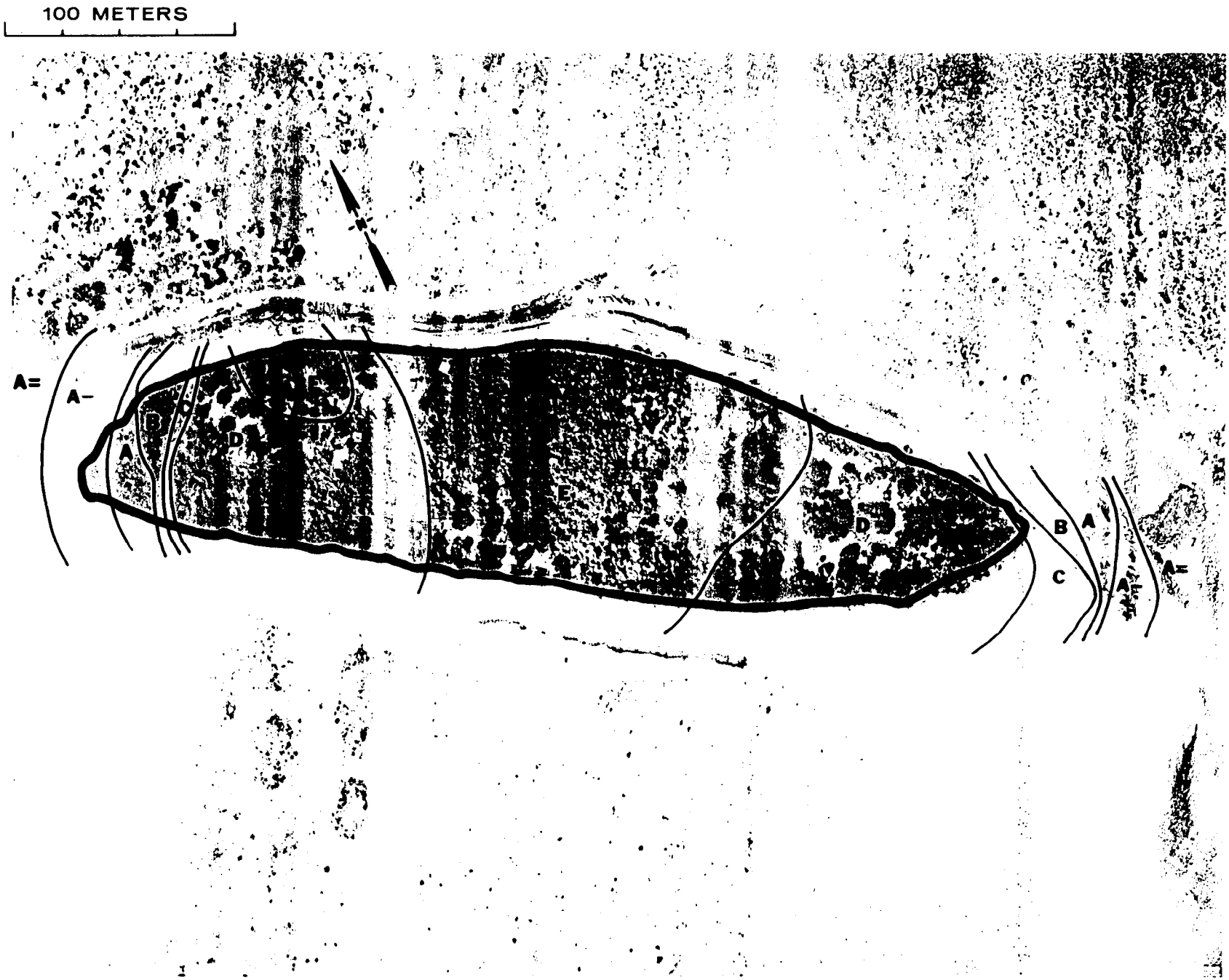

Fig. B.12.1.k. ^{137}Cs isoexposure and isoconcentration contours. (Refer to alphabetic symbol key in this appendix.)

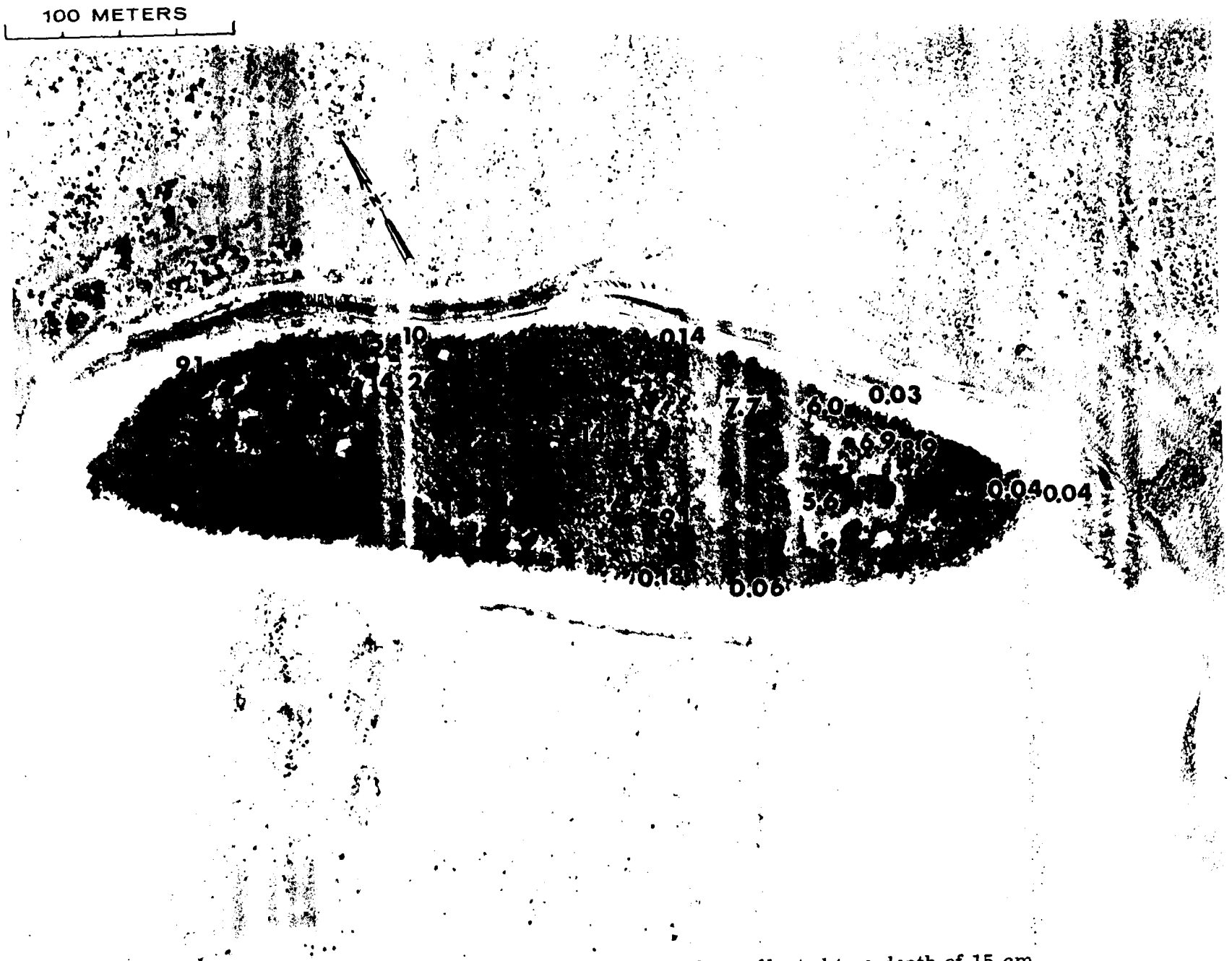

Fig. B.12.1.1. The average ^{137}Cs activities (pCi/g) in soil samples collected to a depth of 15 cm.

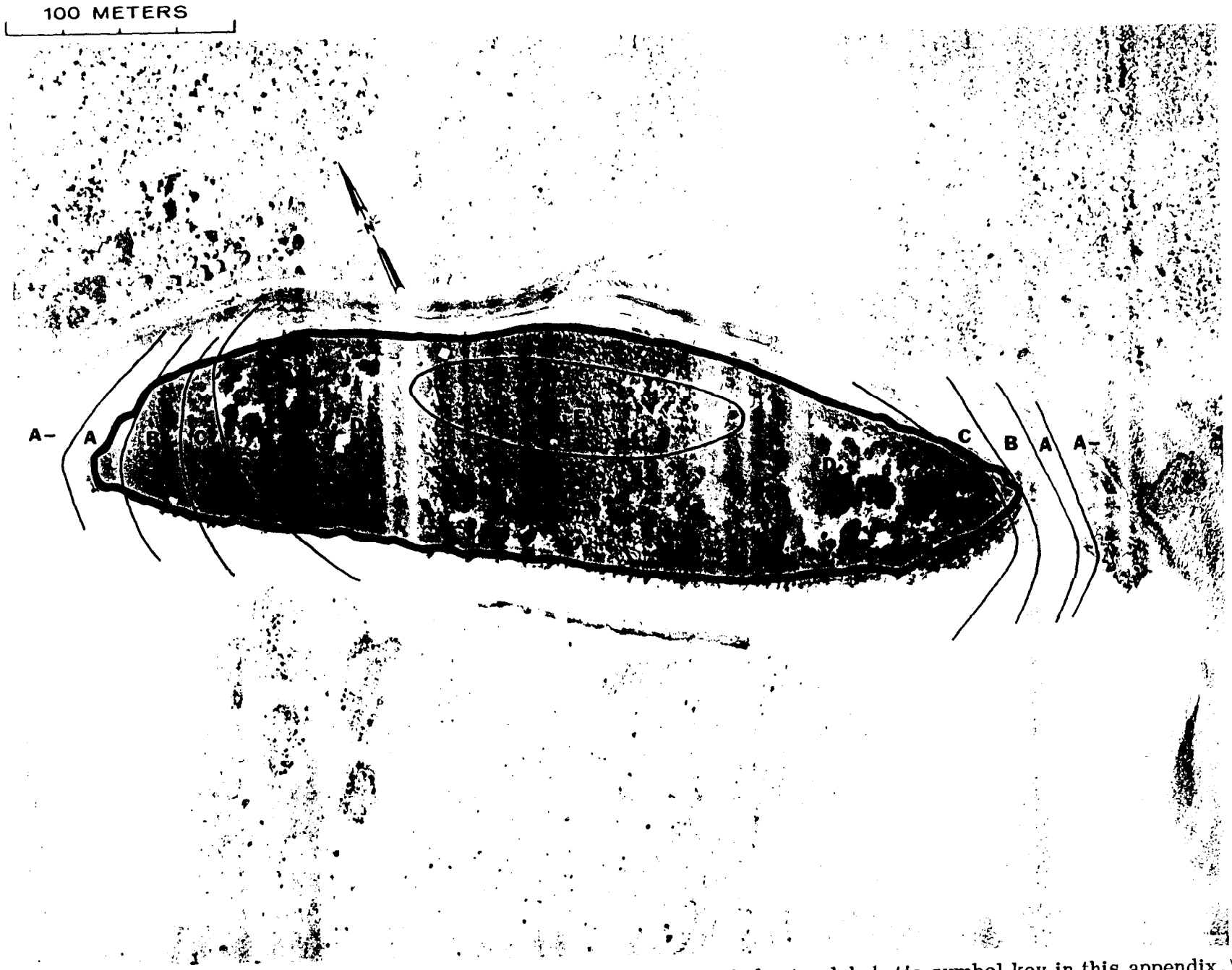

Fig. B.12.1.m. ^{60}Co isoexposure and isoconcentration contours. (Refer to alphabetic symbol key in this appendix.)

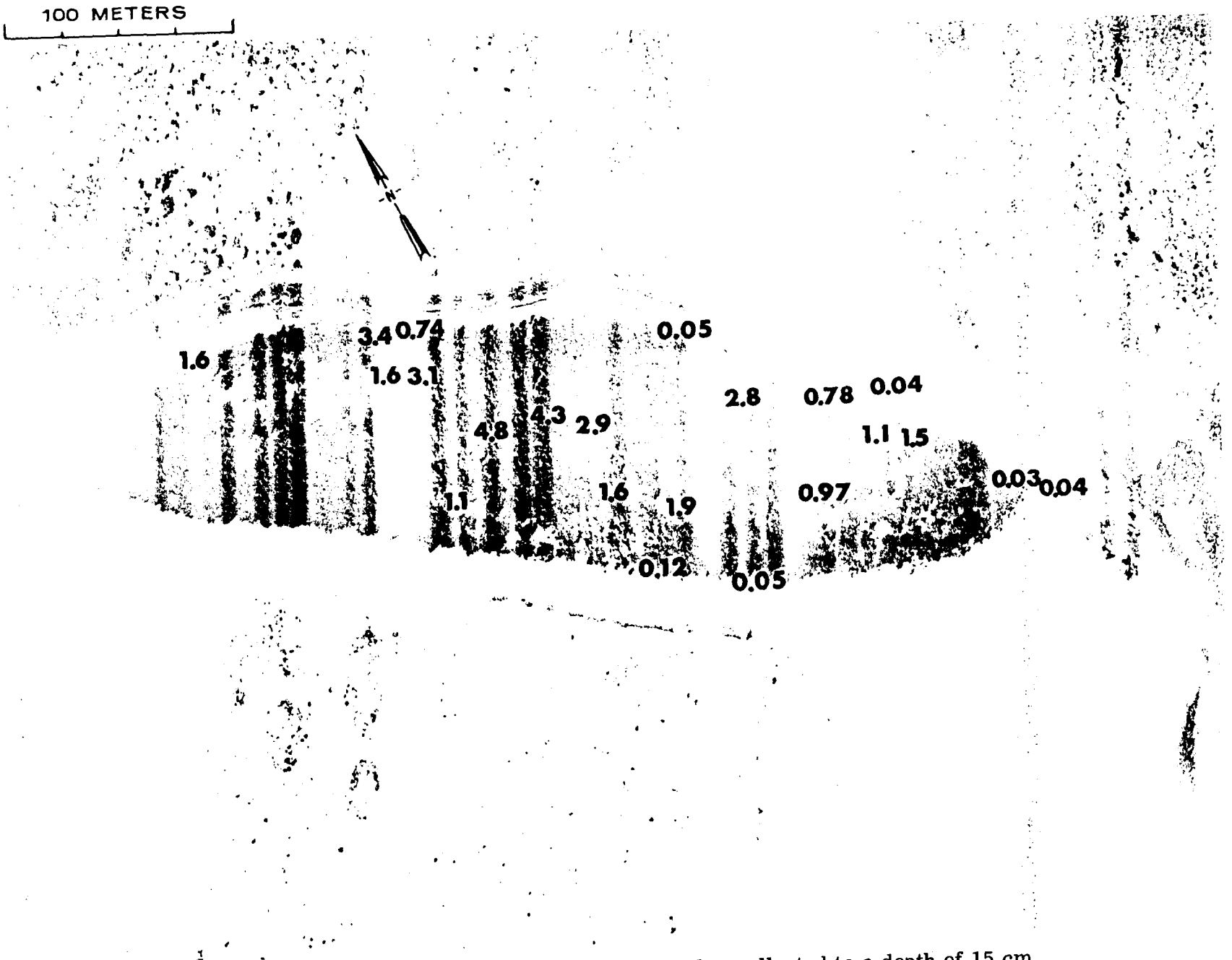

Fig. B.12.1.n. The average ^{60}Co activities (pCi/g) in soil samples collected to a depth of 15 cm.

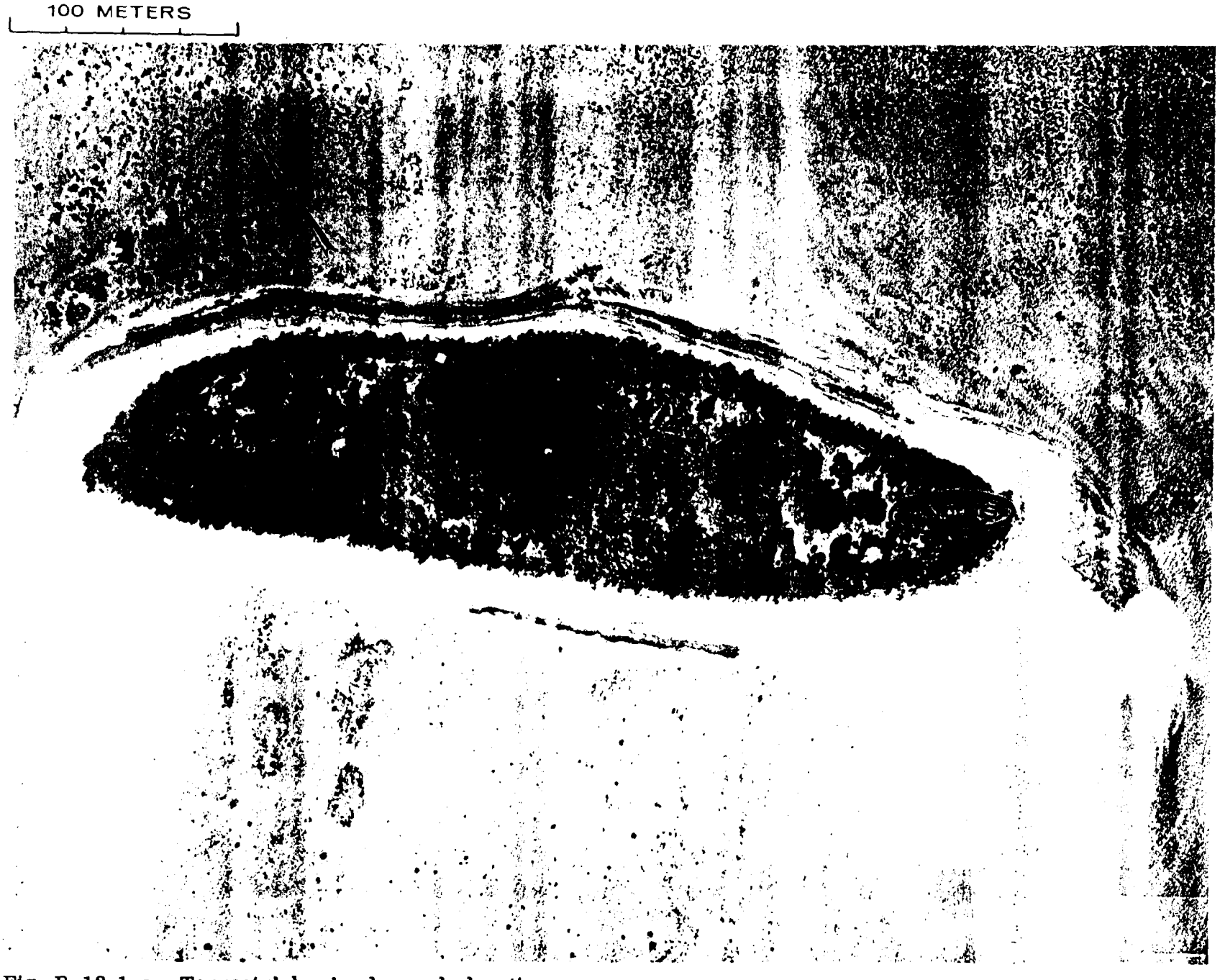

Fig. B.12.1.o. Terrestrial animal sample locations.

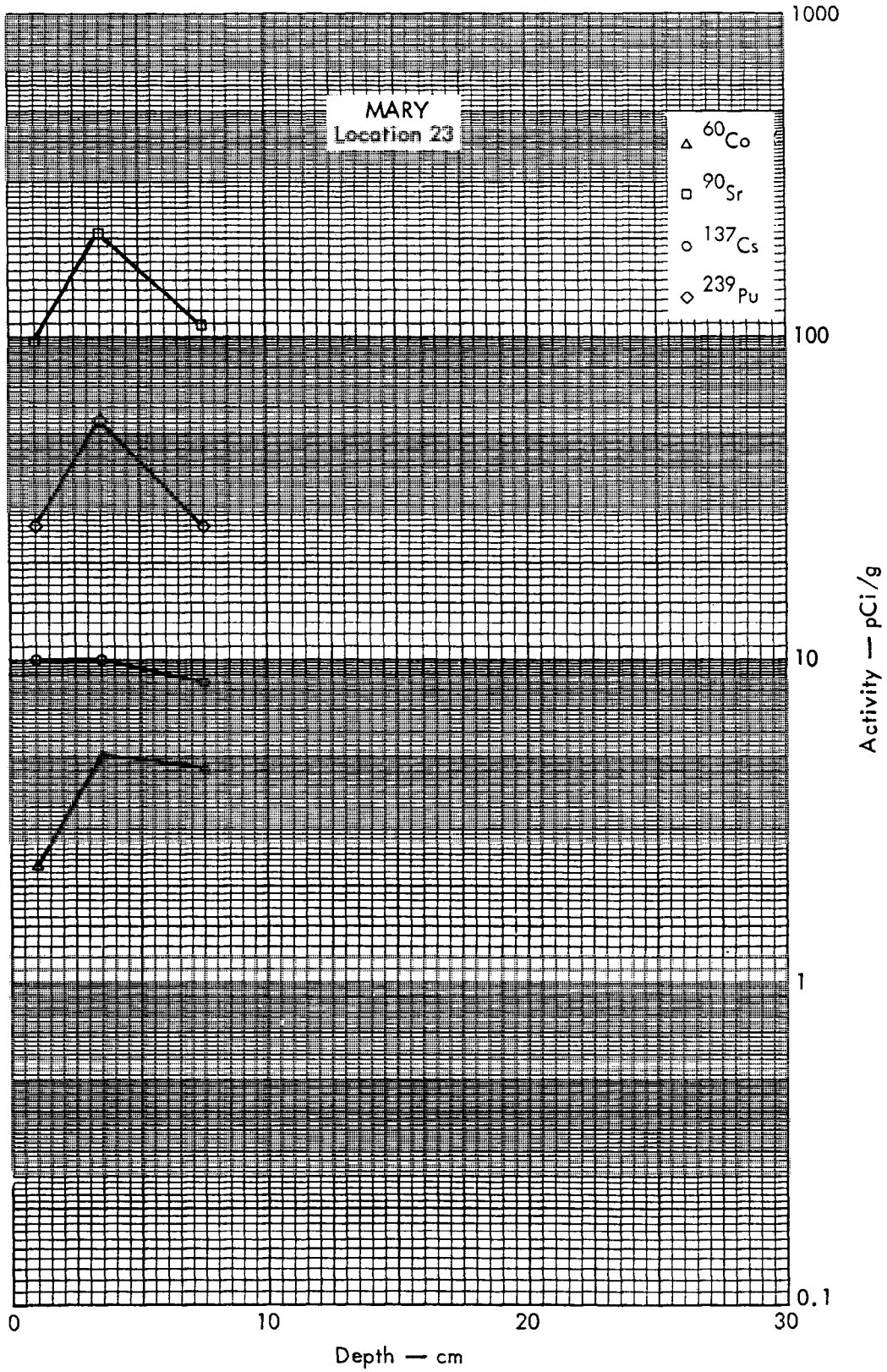

Fig. B. 12. 2a. Activities of selected radionuclides as a function of soil depth.

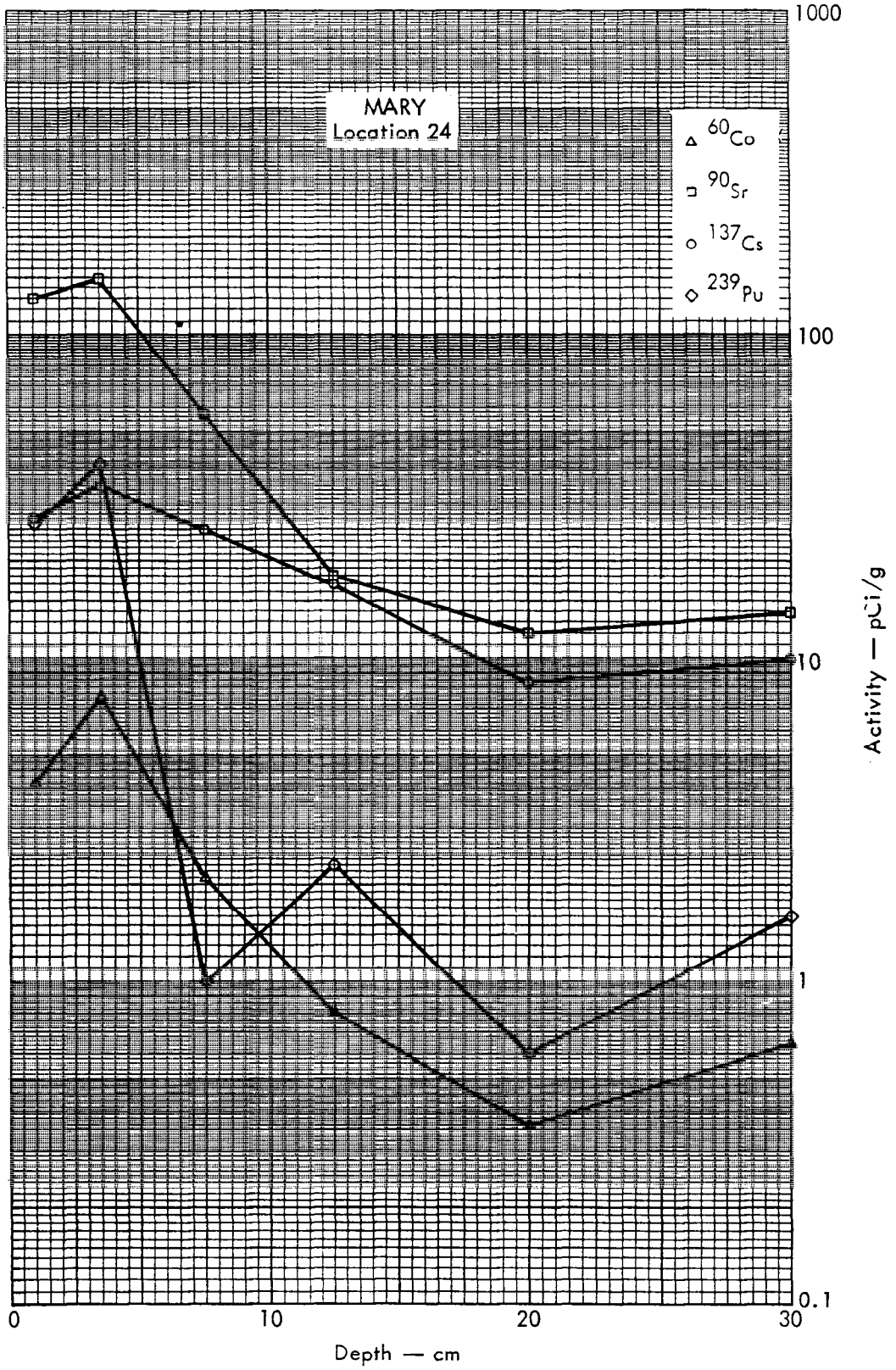

Fig. B. 12. 2b. Activities of selected radionuclides as a function of soil depth.

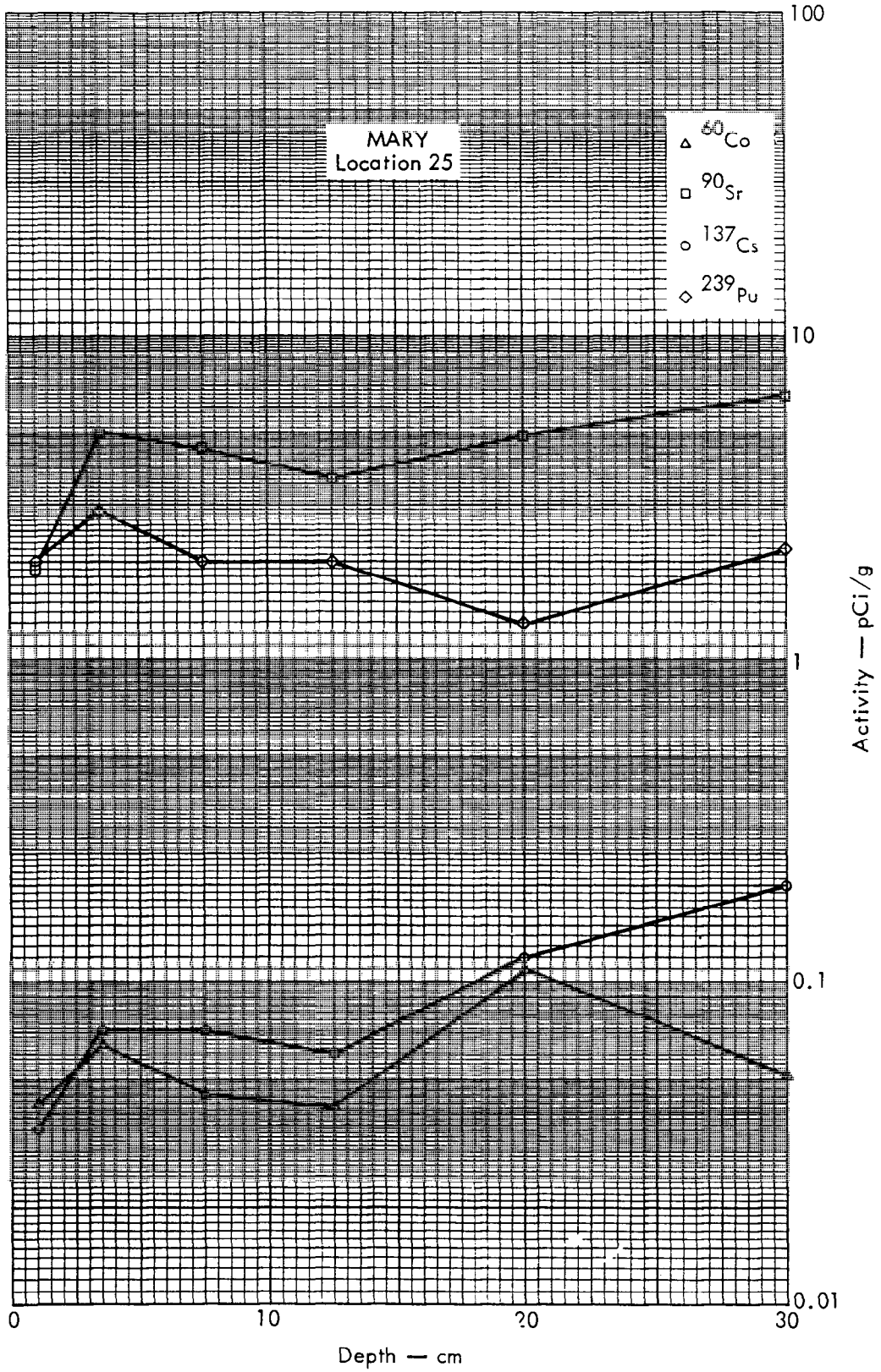

Fig. B. 12. 2c. Activities of selected radionuclides as a function of soil depth.

Fig. B.13.1.a.

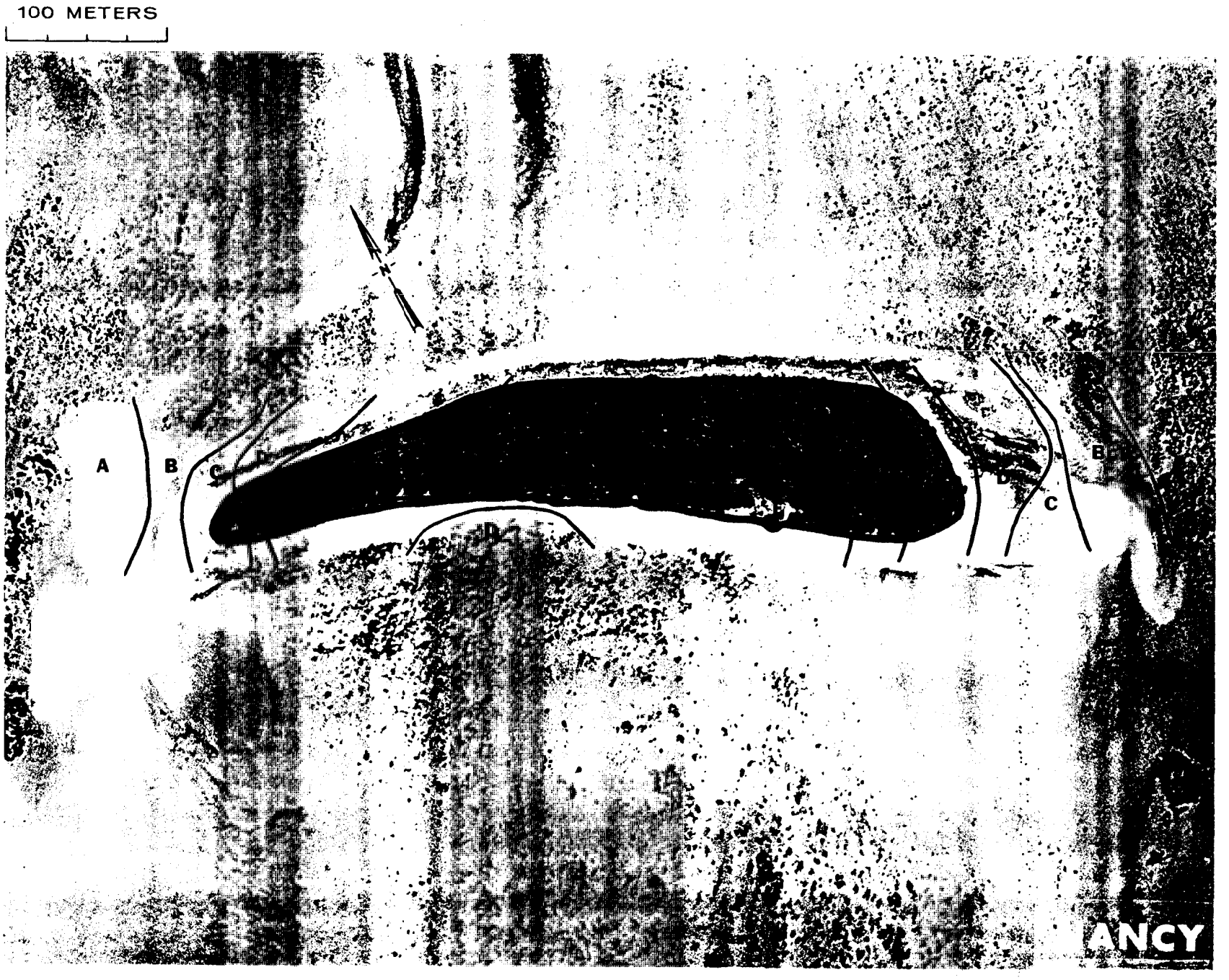

Fig. B.13.1.b. Gross count isoexposure contours. (Refer to alphabetic symbol key in this appendix.)

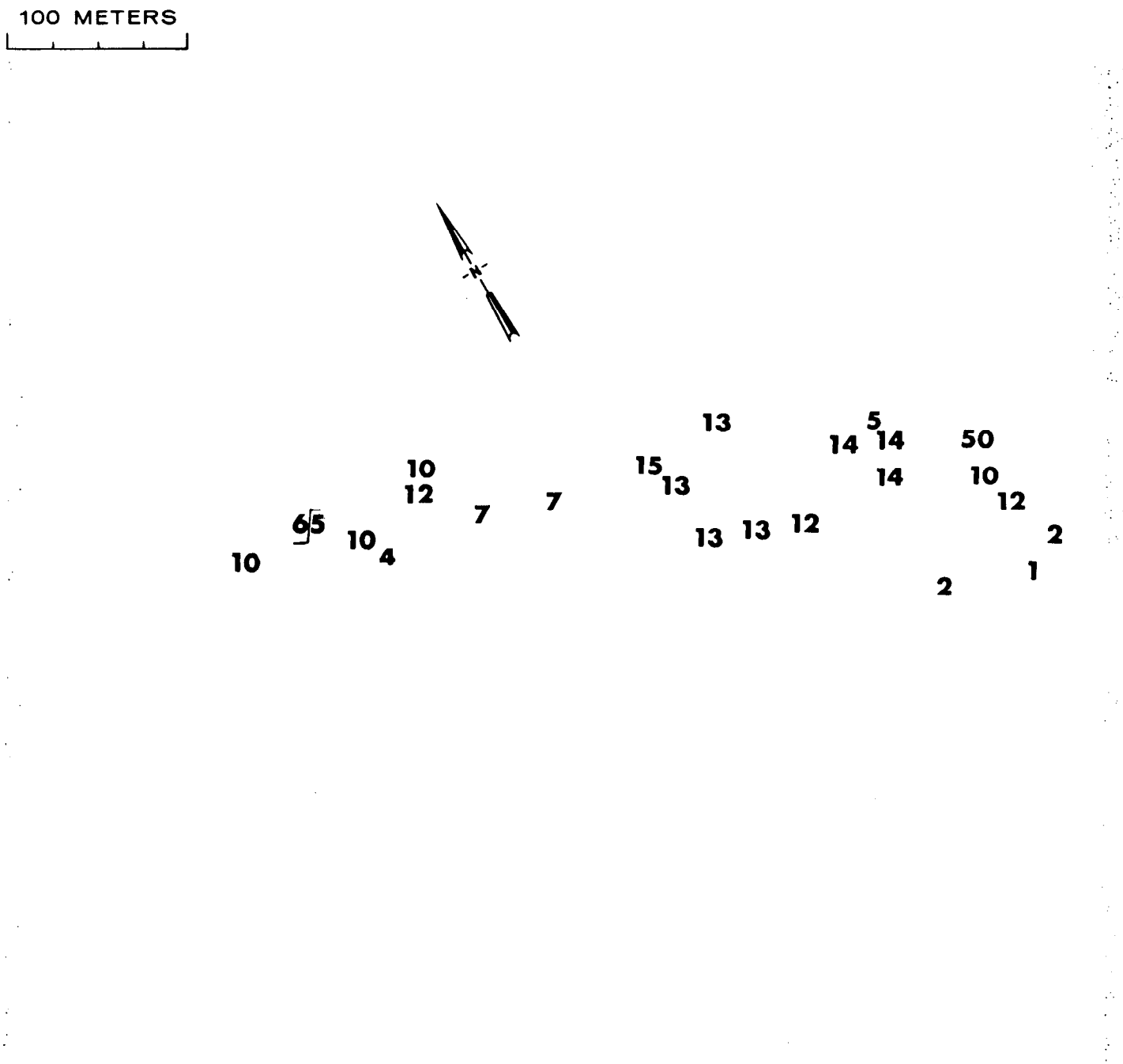

Fig. B.13.1.d. The gamma background exposure rate (μR/hr) at 1 m above the ground, measured with a portable NaI scintillation counter.

Fig. B.13.1.f. Soil-sample locations.

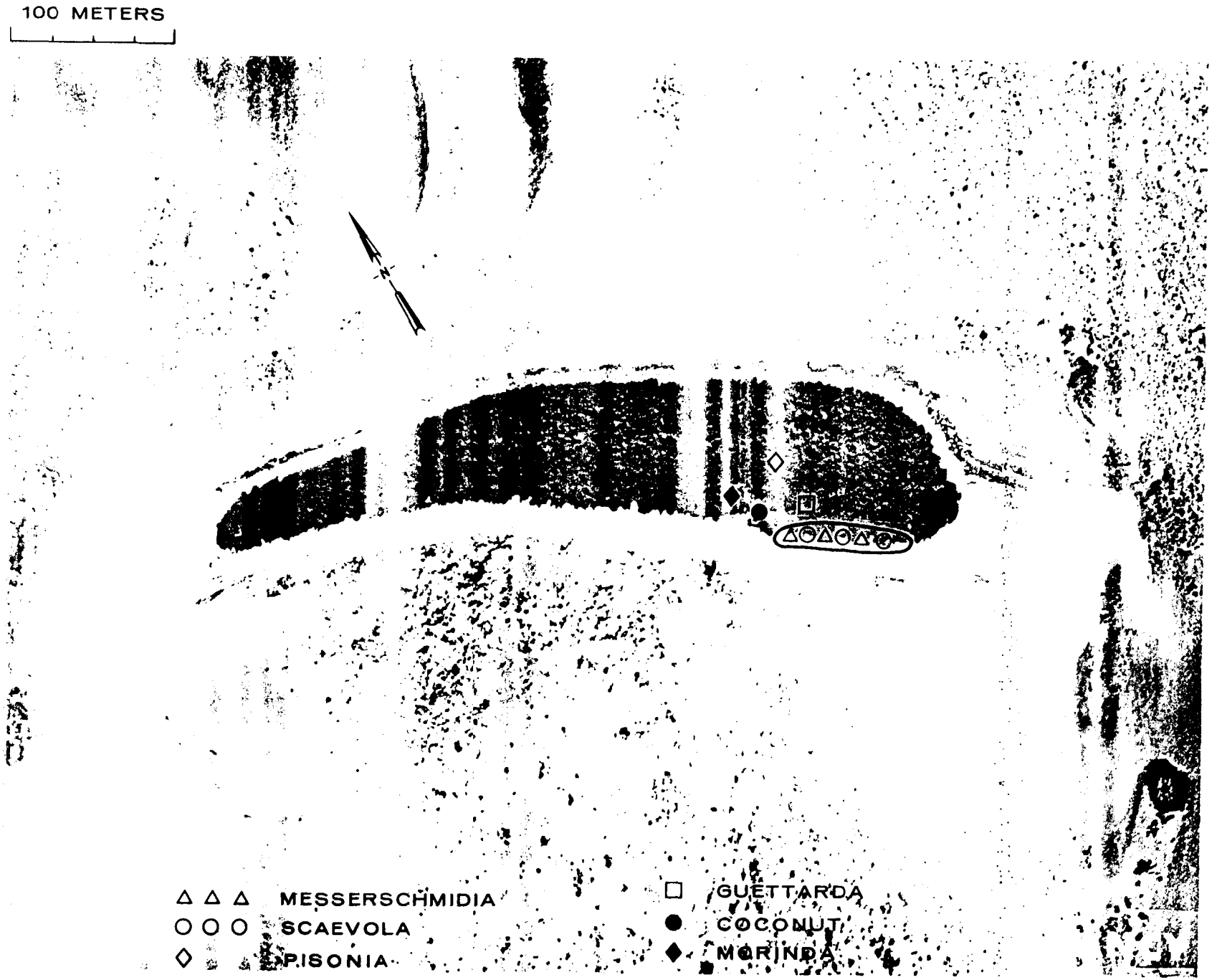

Fig. B.13.1.g. Vegetation sample locations.

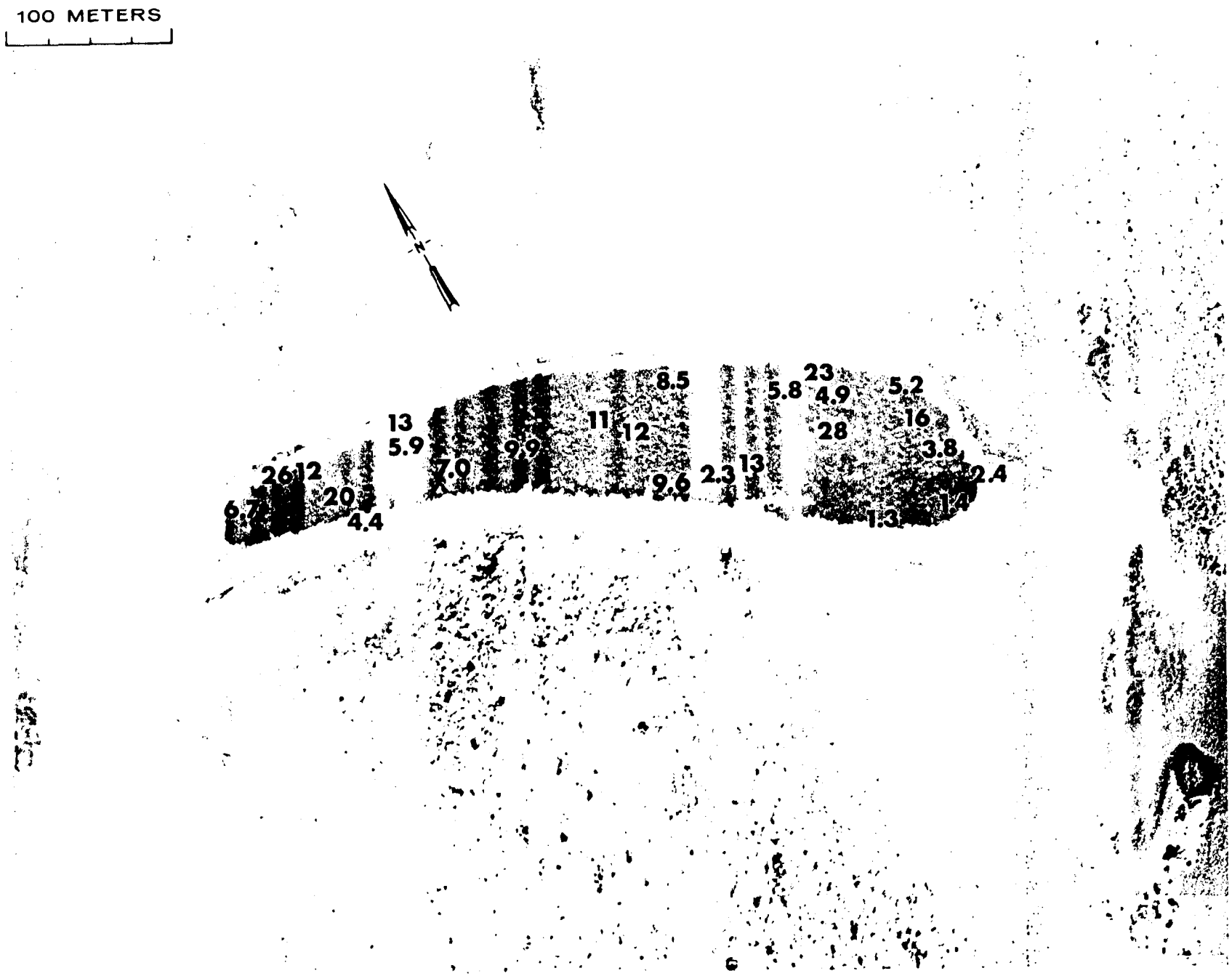

Fig. B.13.1.i. The average ^{239}Pu activities (pCi/g) in soil samples collected to a depth of 15 cm.

Fig. B.13.1.j. The average ^{90}Sr activities (pCi/g) in soil samples collected to a depth of 15 cm.

Fig. B.13.1.k. ^{137}Cs isoexposure and isoconcentration contours. (Refer to alphabetic symbol key in this appendix.)